Ε Θ Ν Ι Κ Ο   Μ Ε Τ Σ Ο Β Ι Ο   Π Ο Λ Υ Τ Ε Χ Ν Ε Ι Ο
ΣΧΟΛΗ ΠΟΛΙΤΙΚΩΝ ΜΗΧΑΝΙΚΩΝ - ΤΟΜΕΑΣ ΓΕΩΤΕΧΝΙΚΗΣ
Ηρώων Πολυτεχνείου 9, Πολυτεχνειούπολη Ζωγράφου 157 80
Τηλ: 210 772 3780, Fax: 210 772 3428, e-mail: gbouck@central.ntua.gr
www.georgebouckovalas.com

ΠΡΑΞΗ:

«ΘΑΛΗΣ- ΕΜΠ: ΠΡΩΤΟΤΥΠΟΣ ΣΧΕΔΙΑΣΜΟΣ ΒΑΘΡΩΝ ΓΕΦΥΡΩΝ ΣΕ ΡΕΥΣΤΟΠΟΙΗΣΙΜΟ ΕΔΑΦΟΣ ΜΕ ΧΡΗΣΗ ΦΥΣΙΚΗΣ ΣΕΙΣΜΙΚΗΣ ΜΟΝΩΣΗΣ»

MIS 380043

Επιστημονικός Υπεύθυνος: Καθ. Γ. ΜΠΟΥΚΟΒΑΛΑΣ

ΔΡΑΣΗ 6

Εφαρμογή σε Στατικώς Ορισμένη Γέφυρα Ο.Σ.

ΠΑΡΑΔΟΤΕΑ:

Συγκριτική μελέτη Συμβατικού και Πρωτότυπου Σχεδιασμού για Στατικώς Ορισμένη Γέφυρα Ο.Σ. (Π6β)

Ιούλιος 2015

European Union
European Social Fund
OPERATIONAL PROGRAMME
EDUCATION AND LIFELONG LEARNING
investing in knowledge society
MINISTRY OF EDUCATION & RELIGIOUS AFFAIRS, CULTURE & SPORTS
MANAGING AUTHORITY
Co-financed by Greece and the European Union
NSRF 2007-2013
programme for development
EUROPEAN SOCIAL FUND

ΕΙΣΑΓΩΓΗ

Η παρούσα Τεχνική Έκθεση αποτελεί το **Παραδοτέο (Π6β)** του Ερευνητικού Προγράμματος με τίτλο:

ΘΑΛΗΣ-ΕΜΠ (MIS 380043)

Πρωτότυπος Σχεδιασμός Βάθρων Γεφυρών σε Ρευστοποιήσιμο Έδαφος με Φυσική Σεισμική Μόνωση

με Συντονιστή (Ερευνητικό Υπεύθυνο) τον Γεώργιο Μπουκοβάλα, Καθηγητή ΕΜΠ και με Συντονιστή της Ομάδας Εργασίας και Επιστημονικό Υπεύθυνο της Δράσης Δ6 τον Ιωάννη Ψυχάρη, Καθηγητή ΕΜΠ.

Συγκεκριμένα, παρουσιάζονται τα αποτελέσματα της Δράσης Δ6, με τίτλο:

"Εφαρμογή σε στατικώς Ορισμένη Γέφυρα από *Ο.Σ.*"

Το αντικείμενο του εν λόγω παραδοτέου περιγράφεται στην εγκεκριμένη ερευνητική πρόταση και αφορά τα σημεία (2) και (3) του Π.Ε.6, ως ακολούθως:

(2) Θα επιλεγεί μια τυπική οδική ή σιδηροδρομική γέφυρα Ο.Σ. με ισοστατικό φορέα, σε διασταύρωση με ποταμό από τις πολλές που κατασκευάζονται ή έχουν ήδη κατασκευαστεί στη χώρα μας, με άνοιγμα 40-60μ. μεταξύ των βάθρων και θα γίνει ο στατικός και ο αντισεισμικός σχεδιασμός των βάθρων με τη συμβατική μεθοδολογία θεμελίωσης (πάσσαλοι και καθολική βελτίωση του ρευστοποιήσιμου εδάφους). Βασική προϋπόθεση αποτελεί η ύπαρξη πλήρους γεωτεχνικής έρευνας στη θέση του έργου και η ύπαρξη εκτενούς ρευστοποίησης του εδάφους στις θέσεις των βάθρων.

(3) Θα επαναληφθεί ο στατικός και ο αντισεισμικός σχεδιασμός της γέφυρας, αλλά με τη νέα μεθοδολογία «φυσικής» σεισμικής μόνωσης της θεμελίωσης (επιφανειακή θεμελίωση και δημιουργία επιφανειακής μόνον κρούστας βελτιωμένου εδάφους), σε συνδυασμό με τις ανεκτές μετατοπίσεις του βάθρου που προέκυψαν από την δραστηριότητα (1) του ιδίου Π.Ε. Θα ακολουθήσει αξιολόγηση της νέας μεθοδολογίας, σε σύγκριση με τη συμβατική, τόσο με τεχνικά όσο και με οικονομικά κριτήρια.

ΜΕΘΟΔΟΛΟΓΙΑ ΚΑΙ ΑΠΟΤΕΛΕΣΜΑΤΑ

Μελετάται μία τυπική οδική, στατικώς ορισμένη, γέφυρα Ο.Σ. σε διασταύρωση με ποταμό, που θεμελιώνεται σε έδαφος ρευστοποιήσιμο σε μεγάλο βάθος. Το γεωτεχνικό προφίλ του εδάφους έχει επιλεγεί από μία υπαρκτή γέφυρα στην περιοχή του ποταμού Στρυμώνα και συνεπώς διατίθεται μια πλήρης γεωτεχνική έρευνα στη θέση του έργου. Επίσης προβλέπεται εκτενής ρευστοποίηση του εδάφους στη θέση του μεσοβάθρου. Θεωρείται ότι τα ακρόβαθρα θεμελιώνονται στο βραχώδες αναδυόμενο υπόβαθρο το οποίο, φυσικά, δεν διατρέχει κίνδυνο ρευστοποίησης.

Η γέφυρα που μελετάται αποτελείται από δύο αμφιέρειστα ανοίγματα θεωρητικού μήκους 42.00m το καθένα, τα οποία συνδέονται μεταξύ τους με πλάκα συνέχειας. Το πλάτος του καταστρώματος ισούται με 11.25m, με πεζοδρόμια πλάτους 1.25 m εκατέρωθεν. Αποτελείται από 14 (=2x7) προκατασκευασμένες, προεντεταμένες δοκούς μήκους 40.50m η κάθε μια, που στηρίζονται στα ακρόβαθρα και το μεσόβαθρο μέσω ελαστομεταλλικών εφεδράνων. Το μεσόβαθρο αποτελείται από τη δοκό έδρασης και ένα στύλο τοιχοειδούς διατομής μήκους 8.35m και πάχους 1.5m από οπλισμένο σκυρόδεμα, έχει δε ύψος 10.0m συμπεριλαμβανομένης της δοκού έδρασης (8.0+2.0m).

Στο πρώτο μέρος της εργασίας αυτής επιχειρείται ο σχεδιασμός της γέφυρας με βάση τη συμβατική μεθοδολογία θεμελίωσης, που συνίσταται στη χρήση βαθιάς θεμελίωσης με πασσάλους και καθολική βελτίωση του ρευστοποιήσιμου εδάφους. Για το σκοπό αυτό μορφώθηκαν χωρικά προσομοιώματα από πεπερασμένα γραμμικά και επιφανειακά στοιχεία που αντιπροσωπεύουν τα μέλη της κατασκευής. Η αλληλεπίδραση εδάφους – κατασκευής ελήφθη υπόψη με τη χρήση κατάλληλων οριζόντιων και κατακόρυφων ελατηρίων. Εκτελέστηκαν γραμμικές ελαστικές αναλύσεις έναντι στατικών και σεισμικών δράσεων (δυναμική φασματική ανάλυση). Για τον προσδιορισμό της σεισμικής δράσης χρησιμοποιήθηκε κατάλληλο φάσμα που διατέθηκε από τη Γεωτεχνική Ομάδα για το βελτιωμένο έδαφος στην περιοχή του μεσοβάθρου, για σεισμό με περίοδο επαναφοράς 1000 χρόνια. Η γέφυρα εξετάστηκε για τις Οριακές Καταστάσεις Λειτουργικότητας και Αστοχίας σύμφωνα με τους Ευρωκώδικες, απ' όπου προέκυψαν οι τελικές διαστάσεις και όπλιση των επιμέρους μελών (τοιχοειδές βάθρο, κεφαλόδεσμος πασσάλων, πάσσαλοι, προεντεταμένες δοκοί και πλάκα καταστρώματος, εφέδρανα, αρμοί).

Στο δεύτερο μέρος της εργασίας, η γέφυρα επανασχεδιάζεται με μια νέα φιλοσοφία σύμφωνα με την οποία το έδαφος κάτω από τη θεμελίωση αφήνεται να ρευστοποιηθεί προσφέροντας μια *«φυσική» σεισμική μόνωση* στην κατασκευή. Τώρα, γίνεται χρήση επιφανειακής θεμελίωσης επί μιας επιφανειακής, μικρού πάχους, κρούστας βελτιωμένου εδάφους επί του ρευστοποιήσιμου εδάφους. Για τις ανάγκες του νέου σχεδιασμού συντάσσεται μια μεθοδολογία σύμφωνα με την οποία:

- Γίνεται αρχικά μια προδιαστασιολόγηση της γέφυρας έναντι στατικών και σεισμικών δράσεων για σεισμούς με περίοδο επαναφοράς 225 και 1000 χρόνια με χρήση των ανάλογων φασμάτων όπως διατέθηκαν από τη Γεωτεχνική Ομάδα. Υπενθυμίζεται ότι σύμφωνα με τη γεωτεχνική μελέτη για τον σεισμό των 225 χρόνων το έδαφος δεν ρευστοποιείται, ενώ για το σεισμό των 1000 χρόνων το έδαφος ρευστοποιείται. Στην περίπτωσή μας, για όλα τα μέλη πλην της θεμελίωσης χρησιμοποιήθηκαν αρχικά οι διαστάσεις και η όπλιση που προέκυψαν από τη συμβατική λύση.
- Γίνεται έλεγχος ευαισθησίας του βάθρου (το οποίο, σε ισοστατικούς φορείς αποτελεί το κρισιμότερο στοιχείο για το σχεδιασμό έναντι σεισμικών δράσεων) για τις εισαγόμενες καθιζήσεις και στροφές στη θεμελίωση του, λόγω ρευστοποίησης, με απαίτηση την πρακτικά ελαστική λειτουργία του. Το βήμα αυτό έχει ήδη εκτελεστεί

και παρουσιαστεί στο Παραδοτέο Π6α, όπου η μέγιστη επιτρεπτή καθίζηση υπολογίστηκε ίση με 23cm.

- Γίνεται η διαστασιολόγηση της νέας θεμελίωσης (θεμέλιο και επιφανειακή κρούστα). Αρχικά διαστασιολογείται το θεμέλιο έναντι εκκεντρότητας σε σεισμικές δράσεις. Στη συνέχεια καθορίζονται οι τελικές διαστάσεις του θεμελίου και της κρούστας έναντι δύο κριτηρίων:
    - Η παραγόμενη καθίζηση λόγω ρευστοποίησης να είναι μικρότερη της μέγιστης επιτρεπόμενης όπως καθορίστηκε στο προηγούμενο βήμα.
    - Ο απομένων συντελεστής ασφάλειας μετά τη ρευστοποίηση να είναι μεγαλύτερος του 1.10.

  Για το σκοπό αυτό γίνεται χρήση κατάλληλου λογισμικού που ετοιμάστηκε από τη γεωτεχνική ομάδα. Στην περίπτωσή μας η παραγόμενη καθίζηση βρέθηκε ίση με 6.8cm πολύ μικρότερη της μέγιστης καθίζησης των 23cm και συνεπώς αποδείχτηκε κρίσιμος για το σχεδιασμό ο απομένων συντελεστής ασφάλειας. Τελικά, προέκυψε θεμέλιο διαστάσεων 8x15m^2 επί βελτιωμένης εδαφικής κρούστας πάχους 4m. Με βάση τις διαστάσεις αυτές υπολογίστηκαν στη συνέχεια από τη γεωτεχνική ομάδα, για στατικές και δυναμικές συνθήκες, κατάλληλες σταθερές ελατηρίων και αποσβεστήρων για την ανάλυση, για τις περιπτώσεις ρευστοποίησης ή μη του εδάφους.

- Γίνεται η τελική διαστασιολόγηση της γέφυρας έναντι των σεισμικών δράσεων με χρήση δυναμικής φασματικής ανάλυσης. Εξετάζονται οι σεισμοί των 225 χρόνων (περίπτωση μη ρευστοποίησης) και των 1000 χρόνων (περίπτωση ρευστοποίησης). Στην περίπτωση ρευστοποίησης εξετάζονται δύο καταστάσεις:
    (α) Κατά τη διάρκεια του σεισμού, όπου εφαρμόζονται με κατάλληλο συνδυασμό, αδρανειακές δράσεις σεισμού σύμφωνα με το φάσμα της περιοχής του μεσοβάθρου καθώς και πρόσθετοι εδαφικοί καταναγκασμοί (οριζόντια επιβαλλόμενες μετακινήσεις) στη βάση του μεσοβάθρου ώστε να ληφθεί υπόψη η ασύγχρονη κίνηση ακροβάθρου-μεσοβάθρου λόγω διαφορετικών συνθηκών θεμελίωσης. Στην περίπτωσή μας επιβλήθηκαν οριζόντιες μετακινήσεις της τάξης των 12 εκ.
    (β) Αμέσως μετά το τέλος του σεισμού, όπου εφαρμόζονται οι συσσωρευμένες καθιζήσεις και στροφές λόγω ρευστοποίησης στη βάση του μεσοβάθρου (στην περίπτωσή μας 6.8 cm).

  Από την ανάλυση αποδείχτηκε ότι ο πιο κρίσιμος συνδυασμός ήταν αυτός για την περίπτωση της μη ρευστοποίησης του εδάφους με βάση τον οποίο προέκυψαν οι τελικές διαστάσεις και όπλιση των μελών της γέφυρας (τοιχοειδές βάθρο, θεμέλιο, κατάστρωμα, εφέδρανα, αρμοί).

- Σε περίπτωση διαφοροποίησης των διαστάσεων ή της όπλισης του μεσοβάθρου η διαδικασία επαναλαμβάνεται από το δεύτερο βήμα. Δεδομένου ότι στην περίπτωσή μας προέκυψε μείωση του απαιτούμενου οπλισμού σε σχέση με εκείνον της συμβατικής λύσης επανελέχθηκε η ευαισθησία του μεσοβάθρου έναντι των εισαγόμενων, λόγω ρευστοποίησης, καθιζήσεων και στροφών στη θεμελίωση του. Διαπιστώθηκε ότι η τελικά μέγιστη επιτρεπόμενη καθίζηση ήταν ίση με 20cm και παρέμενε σημαντικά μεγαλύτερη της παραγόμενης λόγω ρευστοποίησης (6.8cm). Συνεπώς η διαδικασία σχεδιασμού είχε ολοκληρωθεί.

Κατά τη συγκριτική διερεύνηση των δύο λύσεων διαπιστώθηκε ότι κατά τον πρωτότυπο σχεδιασμό οι εισαγόμενες σεισμικές εντάσεις είναι σημαντικά μικρότερες εκείνων του συμβατικού, ακόμα και για την περίπτωση της μη ρευστοποίησης. Ειδικότερα για την περίπτωση ρευστοποίησης η μέγιστη αναπτυσσόμενη επιτάχυνση είναι κατά 50% περίπου μικρότερη από εκείνην της συμβατικής λύσης και πράγματι η ρευστοποίηση λειτουργεί ως μια *«φυσική» σεισμική μόνωση* για την κατασκευή. Εντούτοις σε περίπτωση ρευστοποίησης, κατά τη διάρκεια του σεισμού εισάγονται πρόσθετοι εδαφικοί καταναγκασμοί στη θεμελίωση λόγω ασύγχρονης κίνησης ακροβάθρου-μεσοβάθρου. Σε τέτοιου είδους καταναγκασμούς (οριζόντια επιβαλλόμενες μετατοπίσεις) το μεσόβαθρο αποδείχτηκε ιδιαίτερα ευαίσθητο. Εντούτοις, για την τάξη μεγέθους των καταναγκασμών που επιβλήθηκαν (περίπου 12cm οριζόντια μετατόπιση) ο συνδυασμός αυτός δεν αποδείχτηκε κρίσιμος. Επιπλέον, οι εισαγόμενες καθιζήσεις (στην περίπτωσή μας 6.8 cm) και στροφές αμέσως μετά το πέρας της δόνησης δεν αποδείχτηκαν κρίσιμες για το σχεδιασμό, αφού παρέμειναν σημαντικά μικρότερες της μέγιστης επιτρεπόμενης καθίζησης για την ελαστική λειτουργία του βάθρου. Κρίσιμη για τον πρωτότυπο σχεδιασμό αποδείχτηκε τελικά η περίπτωση μη ρευστοποίησης, η οποία επέφερε μείωση της έντασης του τοιχοειδούς βάθρου κατά 15% έναντι αυτής του συμβατικού σχεδιασμού. Πρέπει πάντως να επισημανθεί ότι, λόγω της ευαισθησίας που παρουσιάζει το βάθρο στην εισαγωγή εδαφικών καταναγκασμών λόγω ρευστοποίησης, τόσο κατά τη διάρκεια όσο και μετά το πέρας της σεισμικής δόνησης, πρέπει να δίνεται ιδιαίτερη προσοχή στην σωστή εκτίμηση του μεγέθους τους. Τα λοιπά μέλη της κατασκευής (κατάστρωμα, εφέδρανα, κλπ), στην περίπτωση του ισοστατικού φορέα που εξετάστηκε, δεν αποδείχτηκαν κρίσιμα για το σχεδιασμό.

Επιχειρώντας μια οικονομική σύγκριση των δύο λύσεων διαπιστώθηκε ότι κατά τον πρωτότυπο σχεδιασμό επιτεύχθηκε σημαντική μείωση των απαιτούμενων ποσοτήτων σκυροδέματος και χάλυβα έναντι αυτών της συμβατικής. Η μεγαλύτερη εξοικονόμηση οφειλόταν στην μείωση του όγκου του βελτιωμένου εδάφους και την απουσία πασσάλων θεμελίωσης. Συγκεκριμένα, ο όγκος των χαλικοπασσάλων βελτίωσης του εδάφους μειώθηκε κατά 80%, το σκυρόδεμα και ο χάλυβας της νέας θεμελίωσης κατά 60% περίπου, και ο οπλισμός του βάθρου κατά 12%. Επήλθε επίσης μείωση των ποσοτήτων των εφεδράνων και των αρμών (κατά 16% και 20% αντίστοιχα). Οι μειώσεις αυτές οδήγησαν σε μια σημαντική μείωση του κόστους θεμελίωσης της γέφυρας κατά 67% και του συνολικού κόστους της γέφυρας κατά 12% περίπου.

NATIONAL TECHNICAL UNIVERSITY OF ATHENS
SCHOOL OF CIVIL ENGINEERING – LABORATORY FOR EARTHQUAKE ENGINEERING
9 Iroon Polytechniou str., 15780, Zografou Campus, Zografou, Greece
Tel: +30 210 772 1154, Fax: +30 210 772 1182, e-mail: ipsych@central.ntua.gr

PROJECT:

«THALIS-NTUA: INNOVATIVE DESIGN OF BRIDGE PIERS ON LIQUEFIABLE SOILS WITH THE USE OF NATURAL SEISMIC ISOLATION»

MIS: 380043

Coordinator: PROF. G. BOUCKOVALAS

WORK PACKAGE 6

Statically determinate concrete bridge

DELIVERABLES

Comparative study of Conventional and Innovative design for Statically Determinate R.C. Bridges (D6b)

July 2015

European Union
European Social Fund
OPERATIONAL PROGRAMME
EDUCATION AND LIFELONG LEARNING
investing in knowledge society
MINISTRY OF EDUCATION & RELIGIOUS AFFAIRS, CULTURE & SPORTS
MANAGING AUTHORITY
Co-financed by Greece and the European Union
NSRF 2007-2013
programme for development
EUROPEAN SOCIAL FUND

Tables of contents

1. INTRODUCTION 5
2. APPLIED CODES 6
3. GEOTECHNICAL AND SEISMOLOGICAL DATA 7
   3.1. Soil profile 7
      3.1.1. Conventional design - Spring constants for the analysis 8
      3.2.2. Conventional design - Bearing capacity of the piles 10
   3.3. Seismic loading 11
      3.3.1. Conventional design (totally improved ground) 11
      3.3.2. Innovative design (natural ground) 11

PART A: CONVENTIONAL DESIGN OF THE BRIDGE

4. BRIDGE DESCRIPTION 15
   4.1. Geometry and cross sections 15
   4.2. Materials 21
5. DESIGN OF THE SUPERSTRUCTURE 22
   5.1. Model 22
   5.2. Load Cases 23
      5.2.1. Self weight of the beams (1st phase – beam section) – LC1 23
      5.2.2. Self weight of the slab (1st phase – beam section) – LC2 23
      5.2.3. Prestress (1st phase – beam section) – LC50 23
      5.2.4. Prestress losses 24
      5.2.5. Additional dead loads – LC3 29
      5.2.6. Live Loads (TS – LC101-141 and LC142-153, UDL – LC170) 29
   5.3. Serviceability Limit State (SLS) 30
      5.3.1. Load Combinations at Serviceability Limit State 30
      5.3.2. Verification of the members at Serviceability Limit State 31
   5.4. Ultimate Limit State (ULS) 35
   5.5. Required reinforcement 36
6. DESIGN OF SUBSTRUCTURE 37
   6.1. Model 37
   6.2. Loads 40
      6.2.1. Self-weight – LC1 40

6.2.2. Additional dead loads – LC2 40
6.2.3. Shrinkage and creep – LC3 40
6.2.4. Live Loads – LC4-LC7 40
6.2.5. Uniform road traffic loads – LC10 40
6.2.6. Braking load (+/- LC11-LC12) 41
6.2.7. Uniform difference of temperature on deck 41
6.2.8. Earthquake loads 41
6.3. Vibration modes and natural frequencies 41
6.4. Load Combinations at Ultimate Limit State (ULS) 43
6.5 Results 44
6.5.1. Piles' internal forces due to "Persistent design situation" 44
6.5.2. Piles' internal forces due to "Seismic design situation" (q=1.0) 45
6.5.3. Pier's internal forces due to "Persistent design situation" 46
6.5.4. Pier's internal forces due to "Seismic design situation" 47
6.6. Design of piles 48
6.6.1. Bearing capacity 48
6.6.2. Required reinforcements 48
6.7. Design of the pier 49
6.8. Design of the pilecap 50
7. DESIGN OF BEARINGS AND EXPANSION JOINTS 51
7.1. Abutment's bearings 51
7.2. Pier's bearings 55
7.3. Expansion joints 59

PART B: INNOVATIVE DESIGN OF THE BRIDGE

8. INTRODUCTION 61
8.1. Generally 61
9. BRIDGE DESCRIPTION 63
9.1. Geometry and cross sections 63
9.2. Materials 63
10. DESIGN OF THE FOUNDATION 64
10.1. Check of eccentricity against seismic actions (Step 1) 64
10.1.1. Model 64
10.1.2. Loads 64
10.1.2.1. Self weight 64

10.1.2.2. Additional dead loads 64
10.1.2.3. Shrinkage and creep 65
10.1.2.4. Uniform road traffic loads 65
10.1.2.5. Uniform difference of temperature on deck 65
10.1.2.6. Earthquake loads 65
10.1.3. Load Combinations 65
10.1.4. Results 65
10.2. Estimation of max allowable foundation settlement ρ_{all} (step 2) 66
10.3. Estimation of footing and curst dimensions (step 3) 66
10.4. Estimation of the stiffness characteristics of the support springs for the analysis (step 4) 68
11. FINAL DESIGN OF THE INNOVATIVE BRIDGE (step 5) 71
11.1. Introduction 71
11.2. Model 71
11.3. Loads 71
11.3.2. Self weight 71
11.3.3. Additional dead loads 71
11.3.4. Shrinkage and creep 71
11.3.5. Uniform road traffic loads 71
11.3.6. Uniform difference of temperature on deck 71
11.3.7. Earthquake loads 71
11.4. Load combinations 73
11.5. Vibration modes and natural frequencies 74
11.6. Results 76
11.6.1. No liquefaction - Pier's internal forces 76
11.6.2. Liquefaction - Pier's internal forces 77
11.6.3. Design of the pier 81
11.6.4. Design of the footing 81
11.7 DESIGN OF THE OTHER MEMBERS OF THE BRIDGE 83
11.7.1. Design of the superstructure 83
11.7.2. Design of bearings and expansion joints 84
11.7.2.1. Abutments's bearings 84
11.7.2.2. Pier's bearings 88
11.7.2.3. Expansion joints 92
12. VERIFICATION (step 6) 93

13. COMPARISON OF THE RESULTS 97
13.1 Technical Comparison 97
13.1 Economical Comparison 99

APPENDICES

1. INTRODUCTION

This Technical Report presents the actions taken and the associated results of Work Package WP6, entitled: *"Application to statically determinate concrete bridges"*

The Scope of **Work Package WP6** has been described in the approved Research Proposal as follows:

"The aim of this WP is to explore the feasibility of the proposed new design methodology, and the resulting advantages over conventional design methods, in the case of statically determinate concrete bridges, which probably consist the most common type of bridge in our country.

The main work tasks presented in this deliverable are extensively described at the approved proposal as points (2) and (3) of W.P.6, as follows:

(2) Next, a typical statically determinate concrete bridge with spans of 40-60 m, will be designed using the conventional foundation approach, i.e. pile groups with ground improvement between and around the piles. It is our intention to select an actual (existing or in the design stage) river bridge site, where the subsoil conditions are well established by geotechnical surveys, while extensive liquefaction is expected underneath one or more of the bridge piers.

(3) Finally, the static and seismic design of this bridge will be repeated with the new methodology of "natural" seismic isolation (i.e. shallow foundation and partial improvement, of the top part only of the liquefiable soil), in connection with the allowable foundation movements which were established in work task (1) above. The comparative advantages and limitations of the new design methodology, relative to the conventional ones, will be consequently evaluated on the basis of technical, as well as cost criteria.

2. APPLIED CODES

The following codes are used for the design of the bridge:

- Eurocode 0: Basis of structural design;
- Eurocode 1-1.5: Actions on structures – General actions, Thermal actions;
- Eurocode 1-2: Actions on structures – Traffic loads on bridges;
- Eurocode 2-1.1: Design of concrete structures – General rules and rules for buildings;
- Eurocode 2-2: Design of concrete structures – Concrete Bridges – Design and detailing rules;
- Eurocode 7-1: Geotechnical design - General rules;
- Eurocode 8-1: Design of structures for earthquake resistance – General rules, seismic actions and rules for buildings;
- Eurocode 8-2: Design of structures for earthquake resistance – Bridges;
- DIN 4141-14: Structural bearings, laminated elastomeric bearings – design and construction;
- EN1337-1: Structural bearings – Elastomeric bearings;
- DIN 4014: Bored Cast-in-place Piles - Formation, Design and Bearing Capacity;
- DIN Fachbericht 101 & 102;
- Οδηγίες για την Αντισεισμική Μελέτη Γεφυρών σε συνδυασμό με DIN-FB 102, 103, 104 (ΟΑΜΓ-FB), Ιούνιος 2007.

3. GEOTECHNICAL AND SEISMOLOGICAL DATA

3.1. Soil profile

The selected site is located within the riverbed of Strymonas River in Serres, Greece. The results of the geotechnical investigation of the foundation of "Strymonas river" bridge of "Egnatia Odos" Highway were processed by the geotechnical team of this project (as part of the actions of Work Package 4, see Deliverable D4) and are used in the present design. The soil profile at the site has been created from river deposits and consists of loose liquefiable silty sands and soft clays, while the ground water table is located on the ground surface, a fact that is further enhancing the liquefaction susceptibility. More specifically, the following soil layers were identified:

Layer 1 (0-28m): Silty sand (SM) and locally non-plastic silt (ML)
Layer 2 (28-31m): Low plasticity clay (CL)
Layer 3 (31-34m): Silty sand (SM) and locally low plasticity clayey sand (SM-SC)
Layer 4 (34-43m): Low plasticity clay (CL)
Layer 5 (43-50m): Non-plastic silt (ML) and locally well graded silty sand (SW-SM).

In more detail, the soil profile that is used for the numerical analyses is plotted in Figure 3.1, along with the factor of safety against liquefaction (according to the Geotechnical Report, see Deliverable D4).

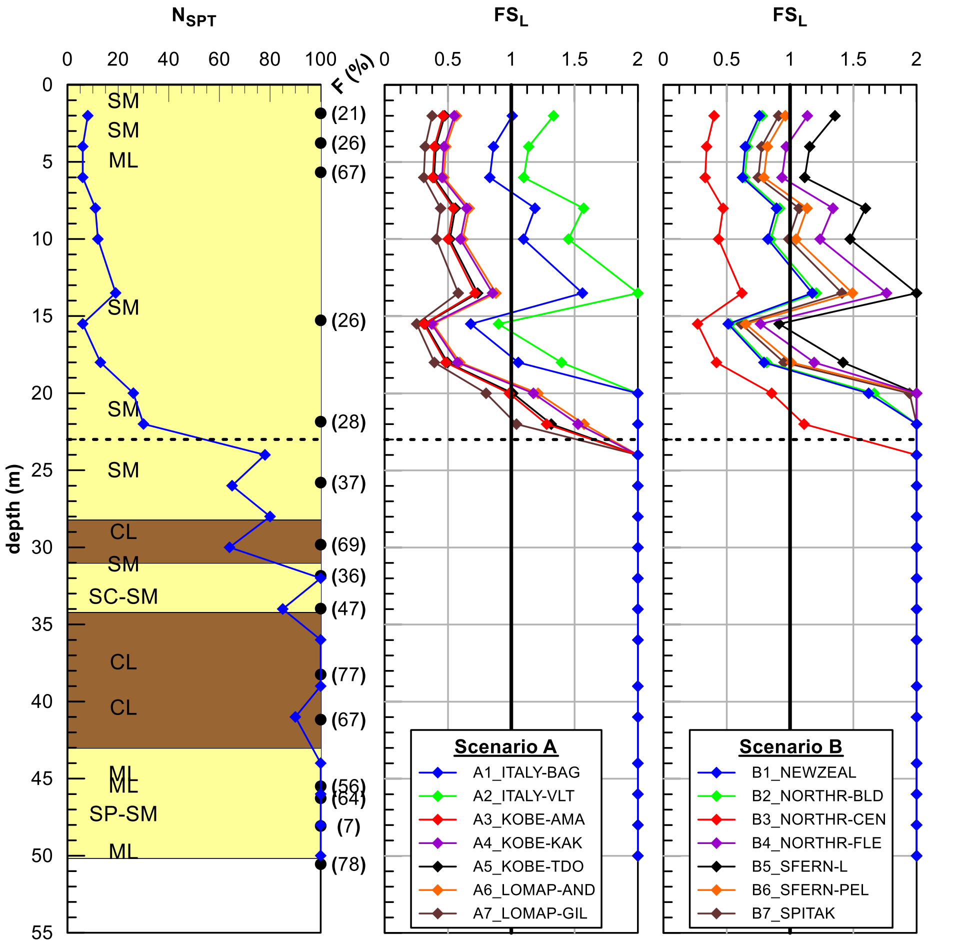

Figure 3.1: Examined soil profile and factor of safety against liquefaction with depth

Σχήμα 3.1: Εδαφικό προφίλ και έλεγχος ρευστοποίησης

3.1.1. Conventional design - Spring constants for the analysis

The Young's Modulus of the soil's layers is given in Table 3.1 together with the coefficient of the horizontal subgrade reaction to be used for the calculation of the equivalent soil springs along the piles. The horizontal coefficient of the subgrade reaction was calculated using the formula K_h=E/D, where D is the pile's diameter; however, for D>1.0m, D is taken equal to 1.00 m.

Table 3.1: Young Modulus E of the soil's layers and horizontal coefficient of subgrade reaction for piles of diameter D=1.00 m

Πίνακας 3.1: Μέτρο ελαστικότητας Ε του εδάφους και οριζόντιος συντελεστής εδάφους για πάσσαλο διαμέτρου D=1.00 m

Depth (m)	E (MPa)	K_h (MN/m³)
0 – 24	20	20
24 – 28	25	25
28 – 31	30	30
31 – 34	30	30
34 – 43	55	55
43 - 50	38	38

These values of K_h given in Table 3.1 correspond to a single pile and have to be reduced according to the methodology described in DIN1054 to take into account the effect of group of piles.

The reduced values $K_{h,i}$ are calculated as follows:

$K_{h,i}=\alpha_i \cdot k_h$ for $\ell/L < 4.00$

$K_{h,i}=\alpha_i^{1.33} \cdot k_h$ for $\ell/L > 4.00$

where ℓ is the pile's length and L the elastic length of the pile which is given by:

$$L=\left(\frac{E \cdot I}{k_s D}\right)^{0.2}$$

The reduction coefficient α_i is calculated as: $\alpha_i = \alpha_L \cdot \alpha_Q$, where α_L is the coefficient in the direction in which the force is applied and α_Q is the coefficient in the normal to the force direction. The factors α_L and α_Q are calculated from Figures 3.2 and 3.3.

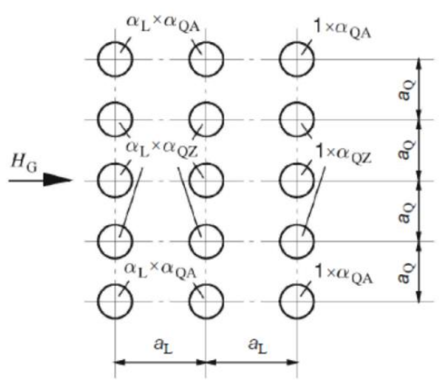

Figure 3.2: Definition of coefficients α_L and α_Q

Σχήμα 3.2: Ορισμός συντελεστών α_L και α_Q

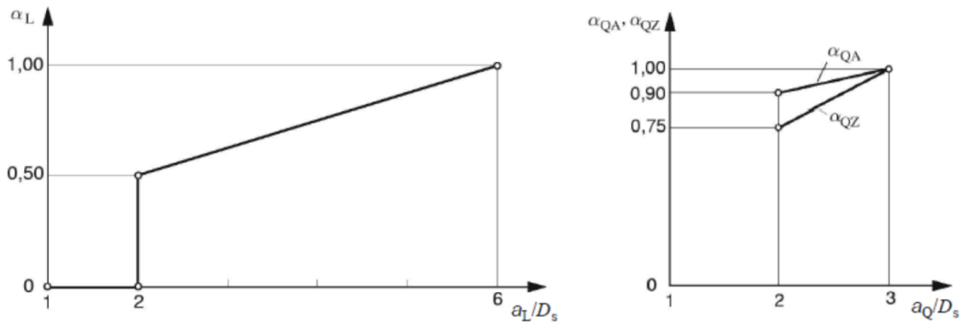

Figure 3.3: Coefficients α_L και α_Q for the calculation of the reduction of horizontal pile stiffness according to DIN1054

Σχήμα 3.3: Υπολογισμός συντελεστών α_L και α_Q για την απομείωση της οριζόντιας ελατηριακής σταθεράς κατά DIN1054

In Table 3.2, the vertical springs for pile's diameter D=1.00 m and piles of various lengths are given. These values have also to be reduced to take under consideration the group effect. The corresponding reduction factors R_s calculated according to Poulos and Davis (1974) are given to Table 3.3.

Table 3.2: Vertical spring's constant for pile's diameter D=1.00m

Πίνακας 3.2: Κατακόρυφα ελατήρια για πάσσαλο διαμέτρου D=1.00m

L (m)	**K_v (MN/m) for D=1.00m**
15	124
20	150
25	178
30	210
35	251

Table 3.3: Reduction factor R_s for the vertical springs of a group of piles

Πίνακας 3.3: Μειωτικός συντελεστής R_s για τα κατακόρυφα ελατήρια ομάδας πασσάλων αιχμής

Length / Diameter	Distance / Diameter	Number of piles in the group															
(L/B)	(e/B)	4				9				16				25			
		Pile's Stiffness K															
		10	100	1000	∞	10	100	1000	∞	10	100	1000	∞	10	100	1000	∞
	2	1.52	1.14	1.00	2.02	1.31	1.31	1.00	1.00	2.39	1.49	1.00	1.00	2.70	1.63	1.00	1.00
10	5	1.15	1.08	1.00	1.23	1.23	1.12	1.02	1.00	1.30	1.14	1.02	1.00	1.33	1.15	1.03	1.00
	10	1.02	1.01	1.00	1.04	1.04	1.02	1.00	1.00	1.04	1.02	1.00	1.00	1.03	1.02	1.00	1.00
	2	1.88	1.62	1.05	1.00	2.84	2.57	1.16	1.00	3.70	3.28	1.33	1.00	4.48	4.13	1.50	1.00
25	5	1.36	1.36	1.08	1.00	1.67	1.70	1.16	1.00	1.94	2.00	1.23	1.00	2.15	2.23	1.28	1.00
	10	1.14	1.15	1.04	1.00	1.23	1.26	1.06	1.00	1.30	1.33	1.07	1.00	1.33	1.38	1.08	1.00
	2	2.54	2.26	1.81	1.00	4.40	3.95	3.04	1.00	6.24	5.89	4.61	1.00	8.18	7.93	6.40	1.00
100	5	1.85	1.84	1.67	1.00	2.71	2.77	2.52	1.00	3.54	3.74	3.47	1.00	4.33	4.68	4.45	1.00
	10	1.44	1.49	1.46	1.00	1.84	1.99	1.98	1.00	2.21	2.48	2.53	1.00	2.53	2.98	3.10	1.00

3.2.2. Conventional design - Bearing capacity of the piles

For the given soil profile of Figure 3.1, the bearing capacity of the piles is calculated in the Geotechnical Report (see Deliverable D4), for three pile diameters, Φ100, Φ120 and Φ150 (Figure 3.4).

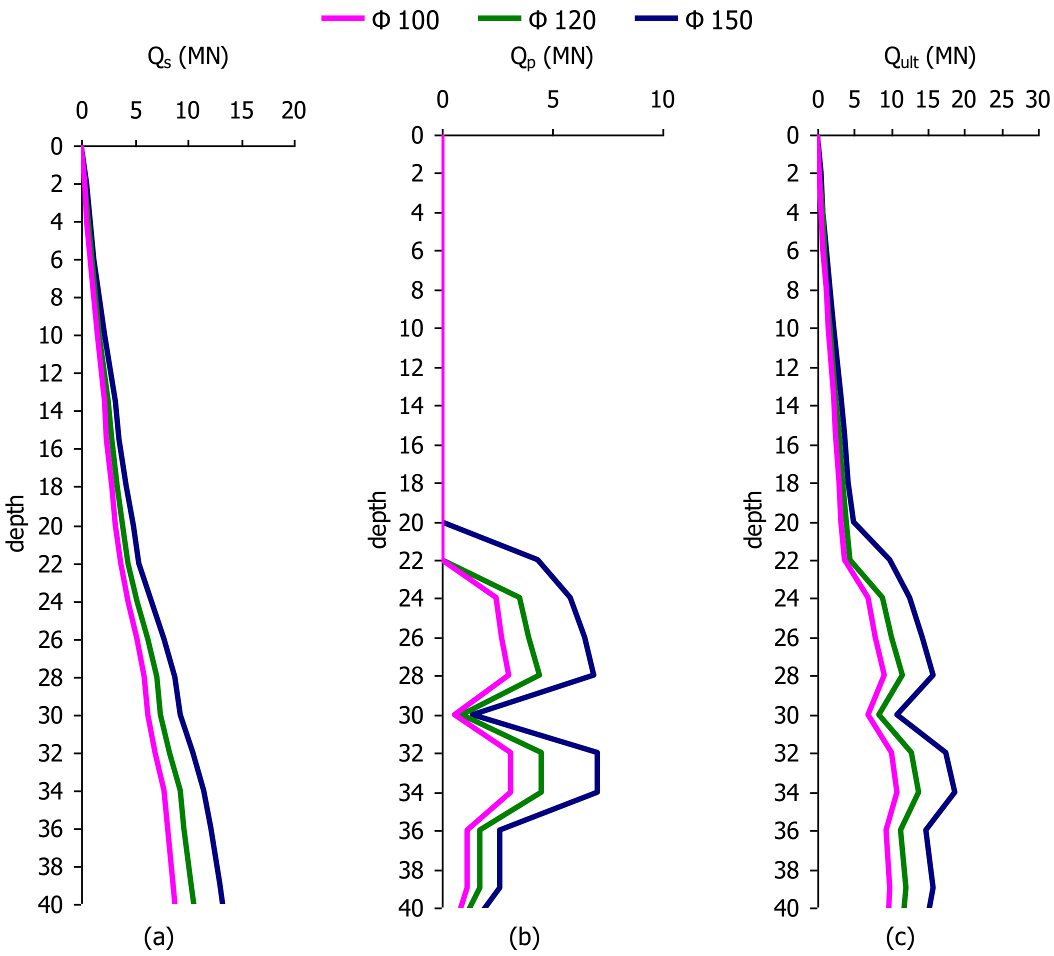

Figure 3.4: Bearing capacity of piles: (a) Ultimate load due to lateral friction; (b) Tip ultimate load; (c) Total ultimate load

Σχήμα 3.4: Φέρουσα ικανότητα πασσάλων: (a) Οριακό φορτίο τριβής, (b) Οριακό φορτίο αιχμής, (c) Συνολικό οριακό φορτίο

For the calculation of the design bearing capacity, safety factors 2.00 and 1.30 were considered for the static combinations and seismic ones, respectively. Thus, the bearing capacity of a pile with a diameter 1.00m and depth of 28.00m (25.00+3.00m) is 8.50MN/ 2.00=4.25MN for static loads and 8.50MN/1.30=6.54MN for seismic loads.

3.3. Seismic loading

3.3.1. Conventional design (totally improved ground)

According to the Geotechnical Report (see Deliverable D4), the seismic actions are calculated from the design spectrum of Eurocode 8 for soil type D with soil factor S=0.80 and peak ground acceleration a_g=0.32g accounting for the Seismic Scenario A described in the report, with the following characteristics:

- return period T_{ret} = 1000 years
- earthquake magnitude M_w = 7.0
- peak ground acceleration at outcropping bedrock PGA_b = 0.32 g

The following parameters were considered:

- Behavior factor q_h=1.50
  q_v=1.00 (§4.1.6(12)P of EC8-2)
- Damping correction factor η=1.0
- Peak ground acceleration $a_{g,h}$=0.32g, $a_{g,v}$=0.90×0.32 g=0.288 g
- Soil factor S=0.80
- Characteristic periods for horizontal component (T_B=0.20s, T_C=0.80s, T_D=2.00s)
- Characteristic periods for vertical component (T_B=0.05s, T_C=0.15s , T_D=1.00s)

The horizontal elastic response spectrum is illustrated in Figure 3.5(a), while Figure 3.5(b) shows the vertical one.

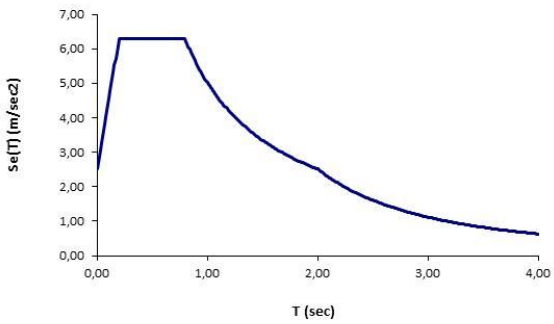

(a)

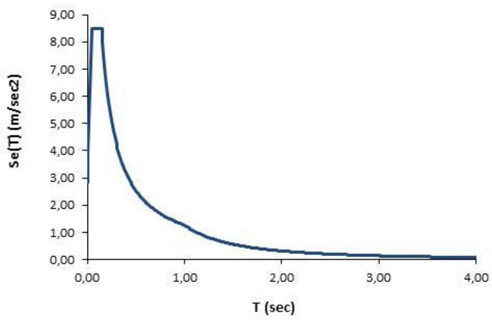

(b)

Figure 3.5: (a) Elastic response spectrum in the horizontal direction; (b) Elastic response spectrum in the vertical direction – improved ground

Σχήμα 3.5: (a) Ελαστικό φάσμα απόκρισης στην οριζόντια διεύθυνση, (b) Ελαστικό φάσμα απόκρισης στην κατακόρυφη διεύθυνση – βελτιωμένο έδαφος

3.3.2. Innovative design (natural ground)

According to the Geotechnical Report (see Deliverable D4), the seismic actions were calculated for the following two Seismic Scenarios (A and B):

<u>Scenario A</u>

In this case the ground is not liquefied. The seismic actions are calculated from the design spectrum of Eurocode 8 for soil type D with soil factor S=0.96 and peak ground acceleration a_g=0.22g, as follows:

- return period Tret = 225 years
- earthquake magnitude M_w = 6.2
- peak ground acceleration at outcropping bedrock PGA_b = 0.22 g

The following parameters were considered:

- Behavior factor q_h=1.50
  q_v=1.00 (§4.1.6(12)P of EC8-2)
- Damping correction factor η=1.0
- Peak ground acceleration $a_{g,h}$=0.22g, $a_{g,v}$=0.90×0.22 g=0.198 g
- Soil factor S=0.80
- Characteristic periods for horizontal component (T_B=0.20s, T_C=0.80s, T_D=2.00s)
- Characteristic periods for vertical component (T_B=0.05s, T_C=0.15s, T_D=1.00s)

The horizontal elastic response spectrum is illustrated in Figure 3.5(a), while Figure 3.5(b) shows the vertical one.

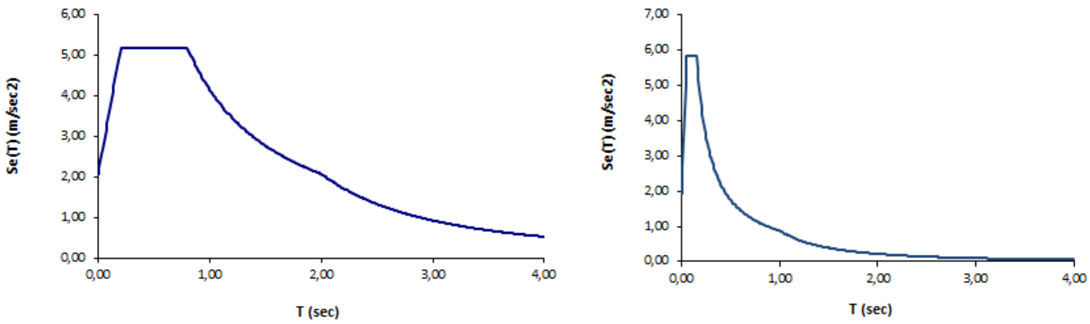

(a) (b)

Figure 3.6: (a) Elastic response spectrum in the horizontal direction; (b) Elastic response spectrum in the vertical direction – Natural ground – Scenario A

Σχήμα 3.6: (a) Ελαστικό φάσμα απόκρισης στην οριζόντια διεύθυνση, (b) Ελαστικό φάσμα απόκρισης στην κατακόρυφη διεύθυνση – Φυσικό έδαφος – Σενάριο Α

<u>Scenario B</u>

In this case the ground is liquefied. The seismic actions are calculated from the design spectrum of Eurocode 8 for soil type C with soil factor S=0.50 and peak ground acceleration a_g=0.32g, as follows:

- return period T_{ret} = 1000 years
- earthquake magnitude M_w = 7.0
- peak ground acceleration at outcropping bedrock PGA_b = 0.32 g

The following parameters were considered:

- Behavior factor q_h=1.50
  q_v=1.00 (§4.1.6(12)P of EC8-2)
- Damping correction factor η=1.0
- Peak ground acceleration $a_{g,h}$=0.32g, $a_{g,v}$=0.90×0.32 g=0.288 g
- Soil factor S=0.50

- Characteristic periods for horizontal component (T$_B$=0.20s, T$_C$=0.60s, T$_D$=2.00s)
- Characteristic periods for vertical component (T$_B$=0.05s, T$_C$=0.15s, T$_D$=1.00s)

The horizontal elastic response spectrum is illustrated in Figure 3.5(a), while Figure 3.5(b) shows the vertical one.

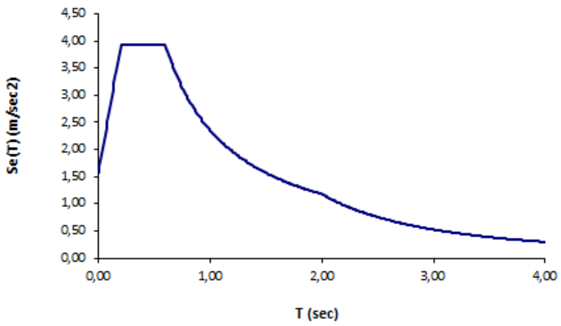

(a)

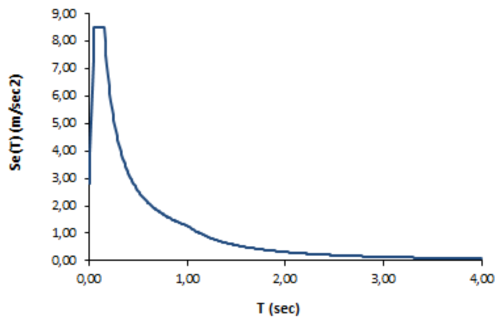

(b)

Figure 3.7: (a) Elastic response spectrum in the horizontal direction; (b) Elastic response spectrum in the vertical direction– Natural ground – Scenario B

Σχήμα 3.7: (a) Ελαστικό φάσμα απόκρισης στην οριζόντια διεύθυνση, (b) Ελαστικό φάσμα απόκρισης στην κατακόρυφη διεύθυνση – Φυσικό έδαφος – Σενάριο B

PART A:
CONVENTIONAL DESIGN OF THE BRIDGE

4. BRIDGE DESCRIPTION

4.1. Geometry and cross sections

The bridge under investigation is a statically determinate, two-span (2×42.00 m) concrete bridge crossing a river. The deck is 11.25 m wide, plus 1.25 m wide pavements at each side. It is composed of 2×7 precast, prestressed concrete beams of length 40.50 m. A cast in-situ slab of 0.25 m min thickness is constructed. The concrete beams are resting upon the abutments and the mid-pier via elastomeric anchored bearings with dimensions 400×500mm^2 (t_{el}=121mm) for the abutments and 350×450mm^2 (t_{el}=99 mm) for the pier. Bearings with external striped plates can also be used. The pier is a wall-type column of cross section 1.50 m × 8.35 m founded on a soil prone to liquefaction under seismic action. The conventional design of the deep foundation on liquefiable soil involves 3×4 ∅100 concrete piles of 25.00 m length, combined with improvement of the liquefiable soil layers.

The plan view of the bridge is illustrated in Figure 4.1 and the plan arrangement of the precast prestressed beams of the deck in Figure 4.2. The longitudinal section of the bridge is shown in Figure 4.3, while in Figure 4.4 the plan view of the foundation of the bridge is depicted. The geometry of the midpier is illustrated in

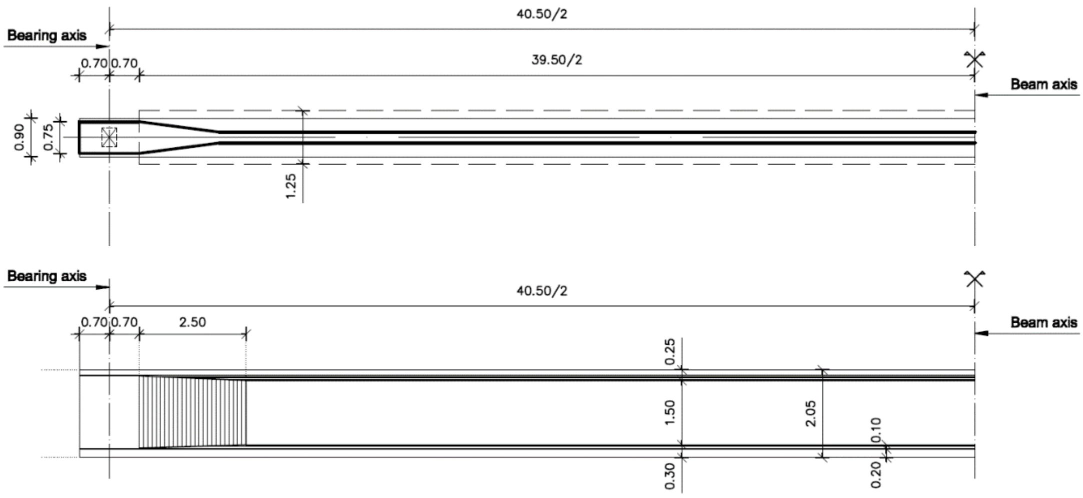

(a)

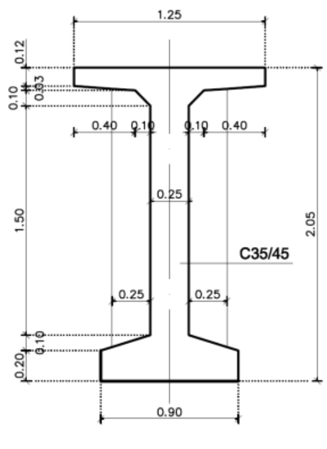

(b)

Figure 4.5. The cross section of the bridge at the midspan is given in Figure 4.6. The plan, elevation and cross section of the precast, prestressed beam are illustrated in Figure 4.7.

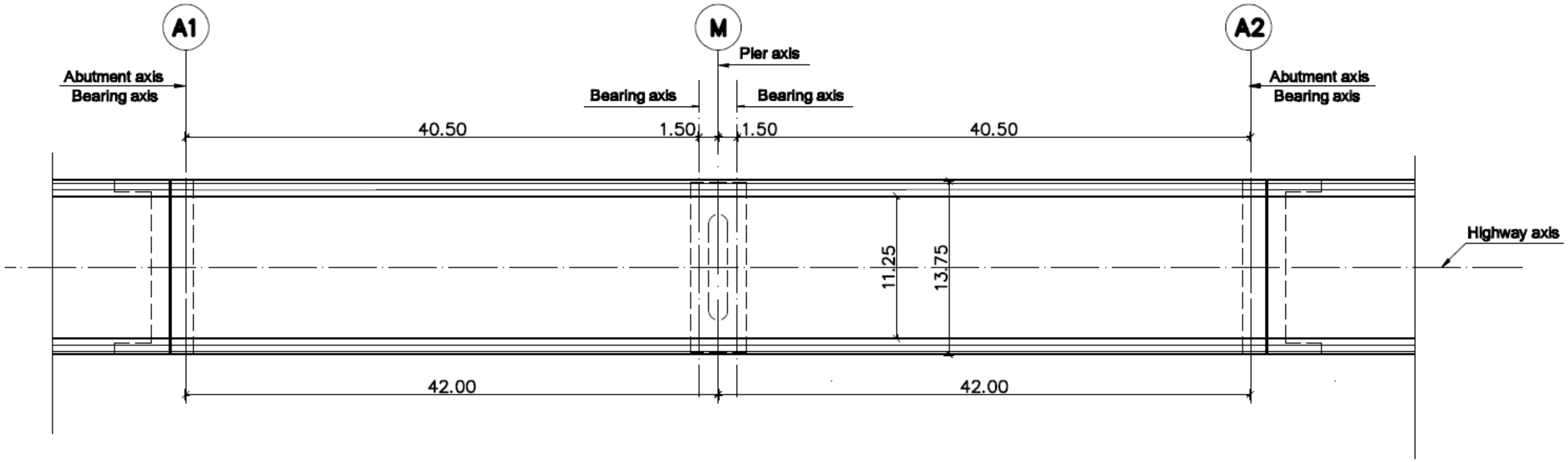

Figure 4.1: Plan view of the bridge

Σχήμα 4.1: Κάτοψη γέφυρας

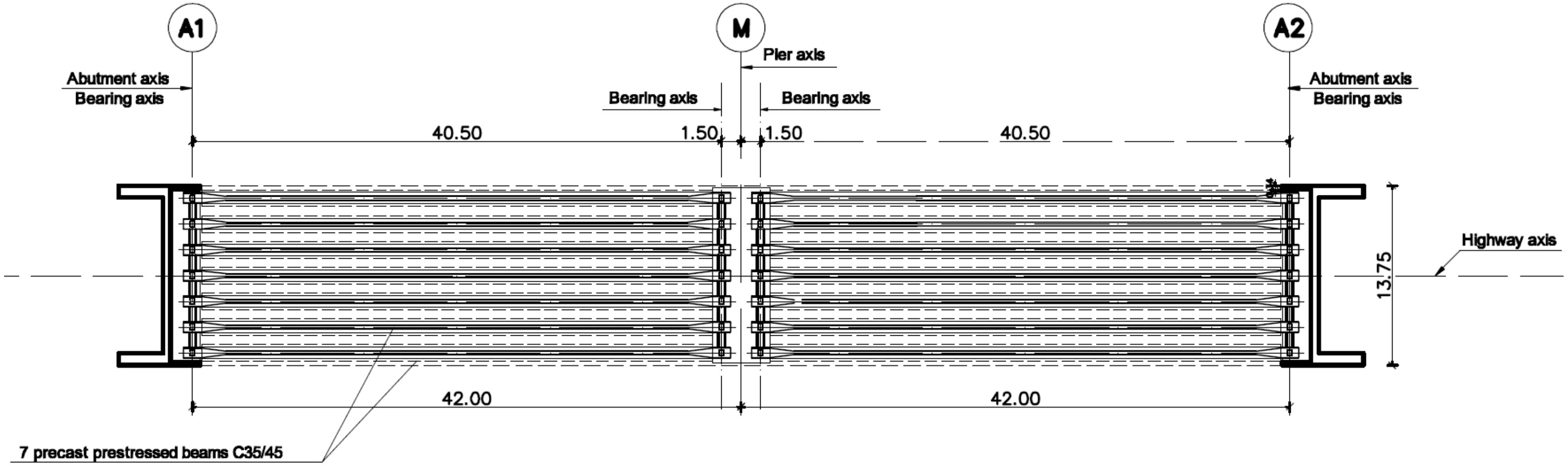

Figure 4.2: Arrangement in plan view of the prestressed beams of the deck

Σχήμα 4.2: Διάταξη προεντεταμένων δοκών καταστρώματος γέφυρας

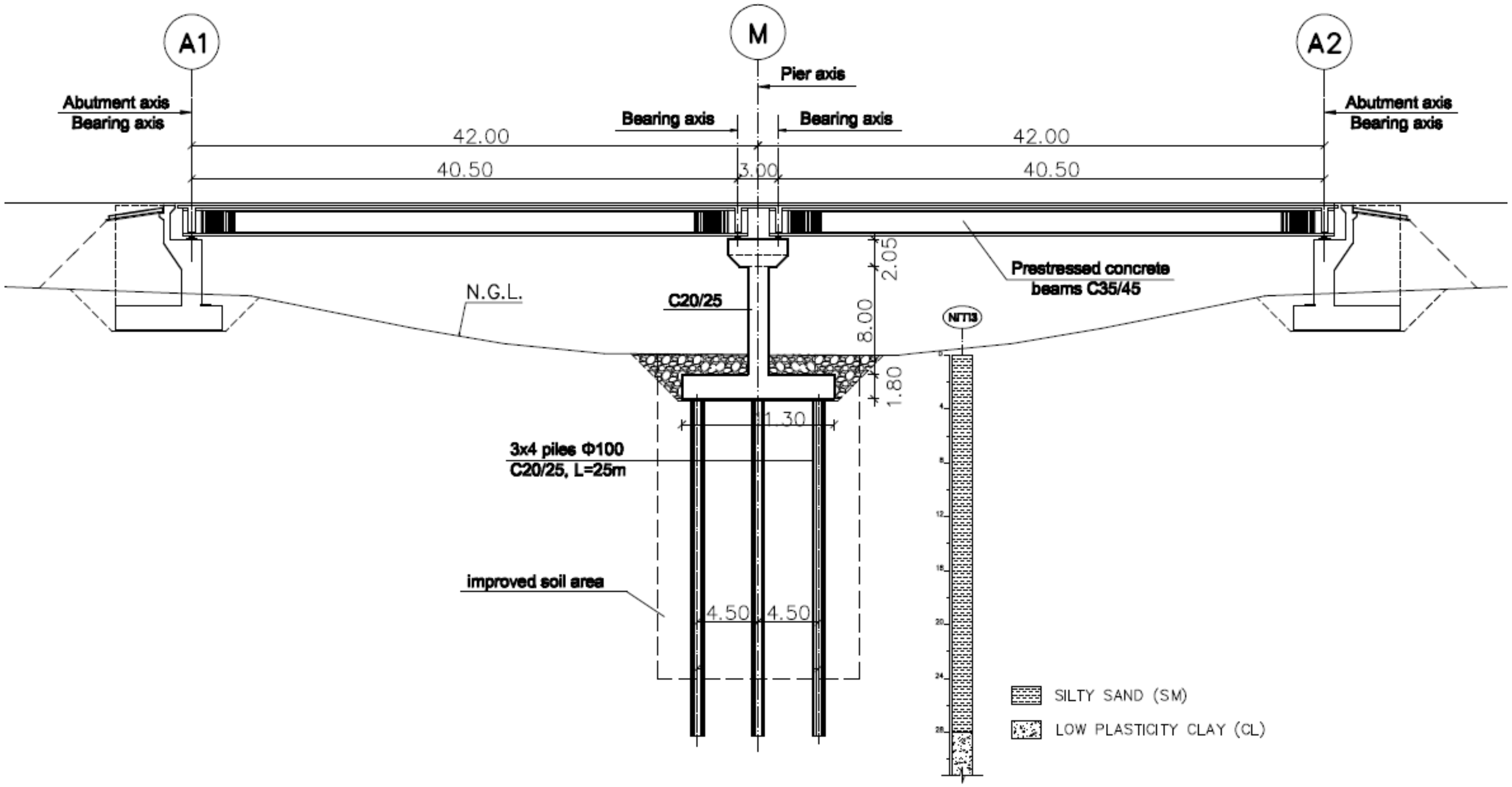

Figure 4.3: Londitudinal section of the bridge

Σχήμα 4.3: Κατά μήκος τομή γέφυρας

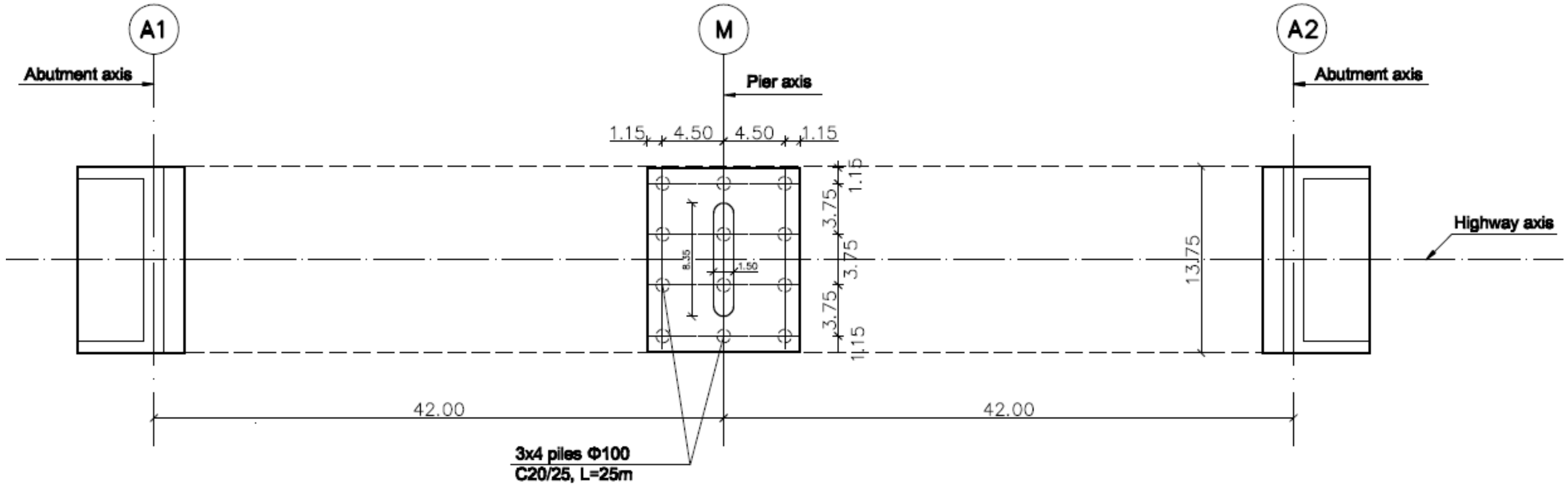

Figure 4.4: Foundation of the bridge in plan

Σχήμα 4.4: Κάτοψη θεμελίωσης της γέφυρας

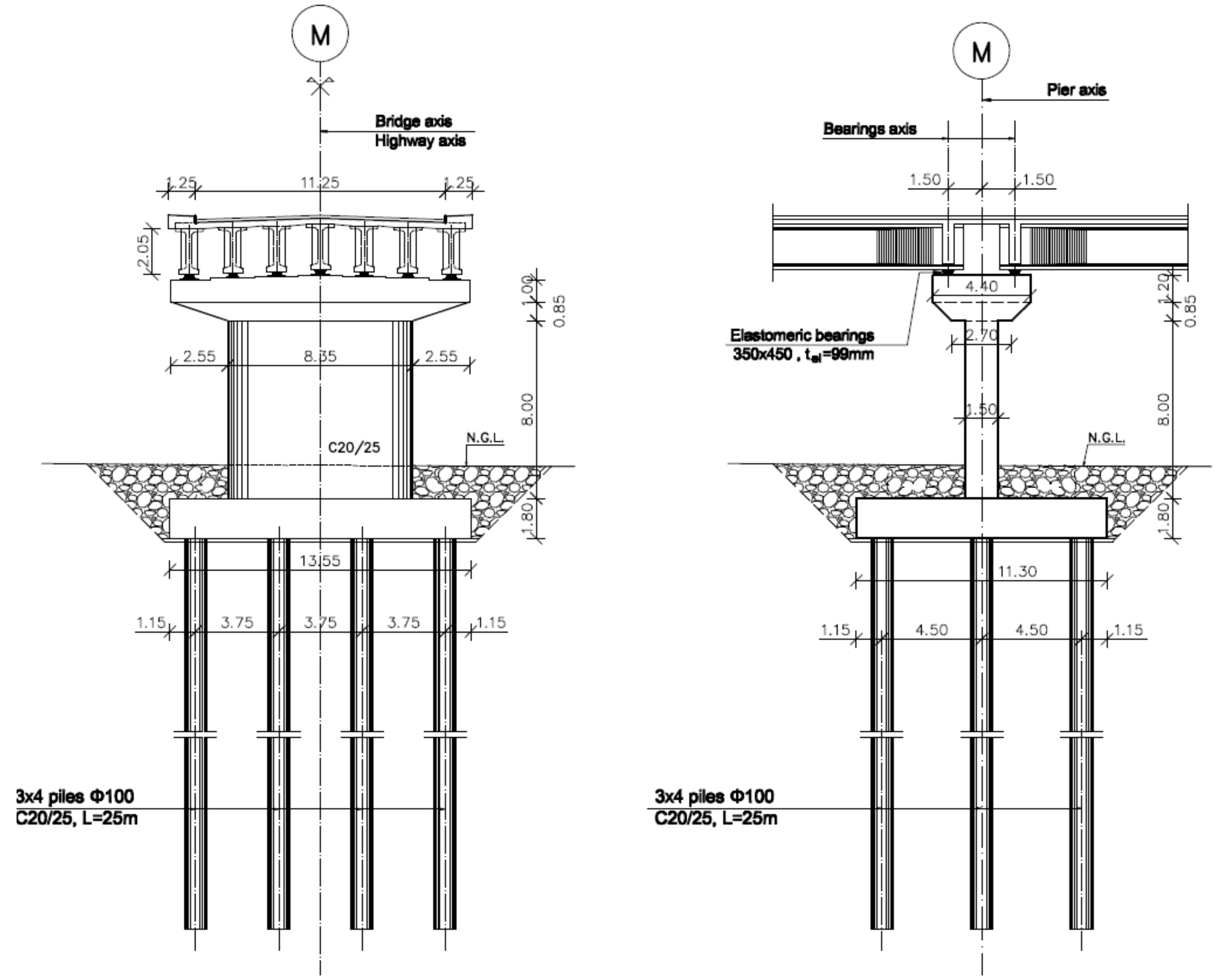

(a) (b)

Figure 4.5: Geometry of the pier : (a) in longitudinal direction , (b) in lateral direction of the bridge

Σχήμα 4.5: Γεωμετρία μεσοβάθρου: (a) στη διαμήκη διεύθυνση, (b) στην εγκάρσια διεύθυνση της γέφυρας

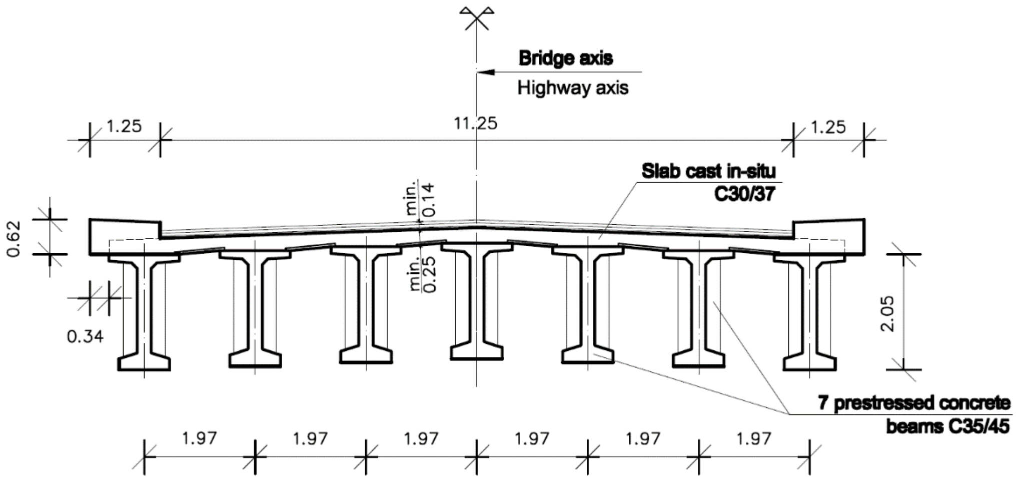

Figure 4.6: Cross section of the bridge at midspan

Σχήμα 4.6: Εγκάρσια τομή ανωδομής γέφυρας στο μέσον του ανοίγματος

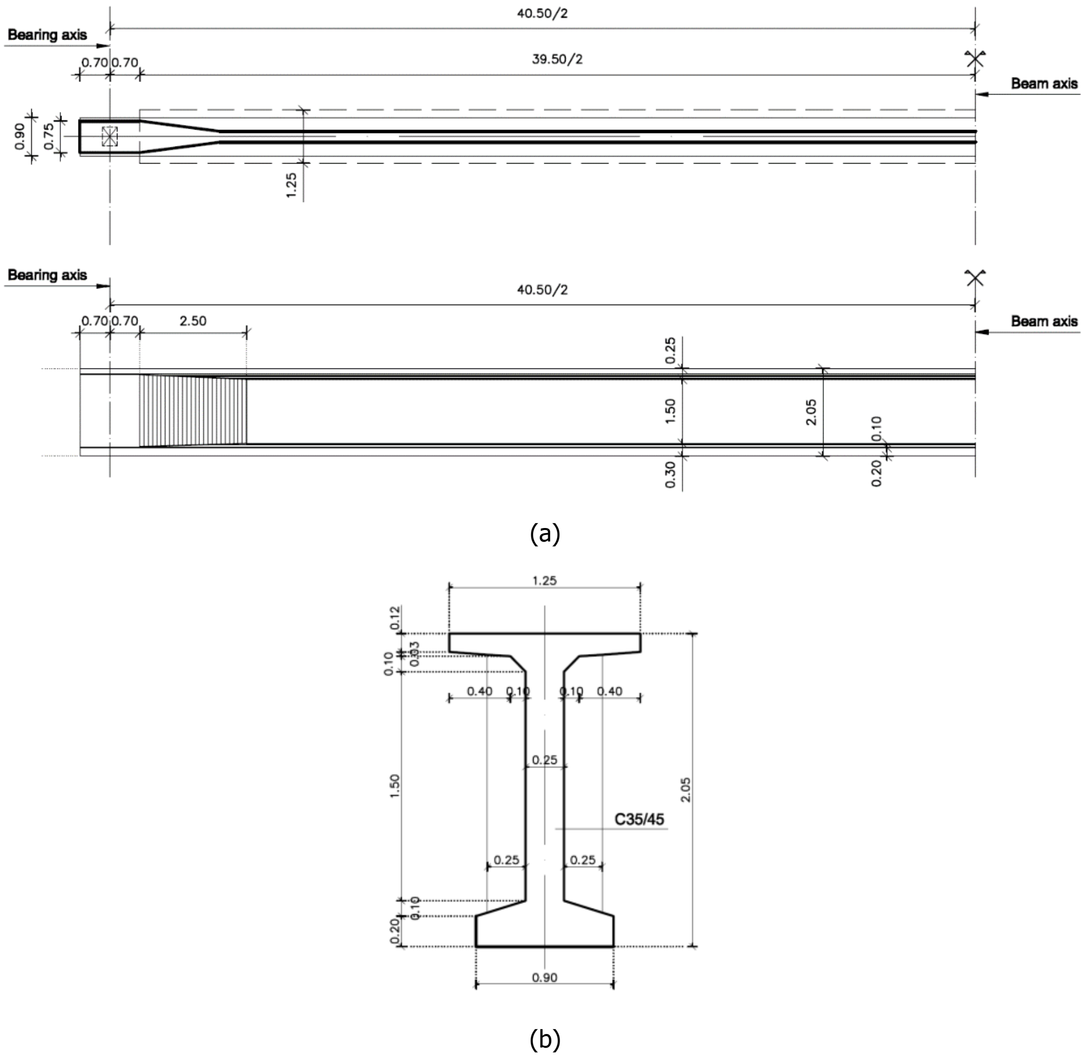

Figure 4.7: Precast, prestressed beam: (a) Semi-plan, semi-elevation view, (b) cross section view

Σχήμα 4.7: Προκατασκευασμένη, προεντεταμένη δοκός: (a) ημικάτοψη, ημιόψη (b) διατομή

4.2. Materials

The prestressed precast beams are made of concrete of grade C35/45, the cast in-situ reinforced concrete slabs of concrete C30/37, the pilecap, the columns and the beam of the pier of concrete C20/25 and the piles of concrete C20/25. The reinforcing steel grade is B500C while the prestressing tendons are of steel 1600/1860.

5. DESIGN OF THE SUPERSTRUCTURE

5.1. Model

For the design of the superstructure against static loads and the determination of the internal stresses and forces as well as of the displacements of the prestressed beams and the slab, a grid of beams representing a single span was analyzed. The main prestressed beams were modeled with beam elements with appropriate geometry and stiffness characteristics. Transverse beam elements were used for the modeling of the stiffness of the slab at the transverse direction. Construction phases were also taken into account.

The bearings at the abutments and the pier were modeled with equivalent elastic springs, with appropriate stiffness for static combinations. The considered horizontal and vertical stiffness of the springs for static load combinations was:

Abutment (400x500x121-mm) : $K_{b,st,hor}$=1454 kN/m, $K_{b,st,vert}$=603400 kN/m

Pier (350x450x99-mm) : $K_{b,st,hor}$=1396 kN/m, $K_{b,st,vert}$=473500 kN/m

The abutments were modelled with springs connected in series with the springs modelling the bearings. The 'abutment' springs were determined from a separate finite element analysis of the abutment-soil system, thus the flexibility of the soil was also considered. More specifically, the horizontal and vertical stiffness of these springs were:

K_h=30000 kN/m

K_v=900000 kN/m

All the analyses were performed using the code Sofistik. The model of the structure and the sections of the members are shown hereafter.

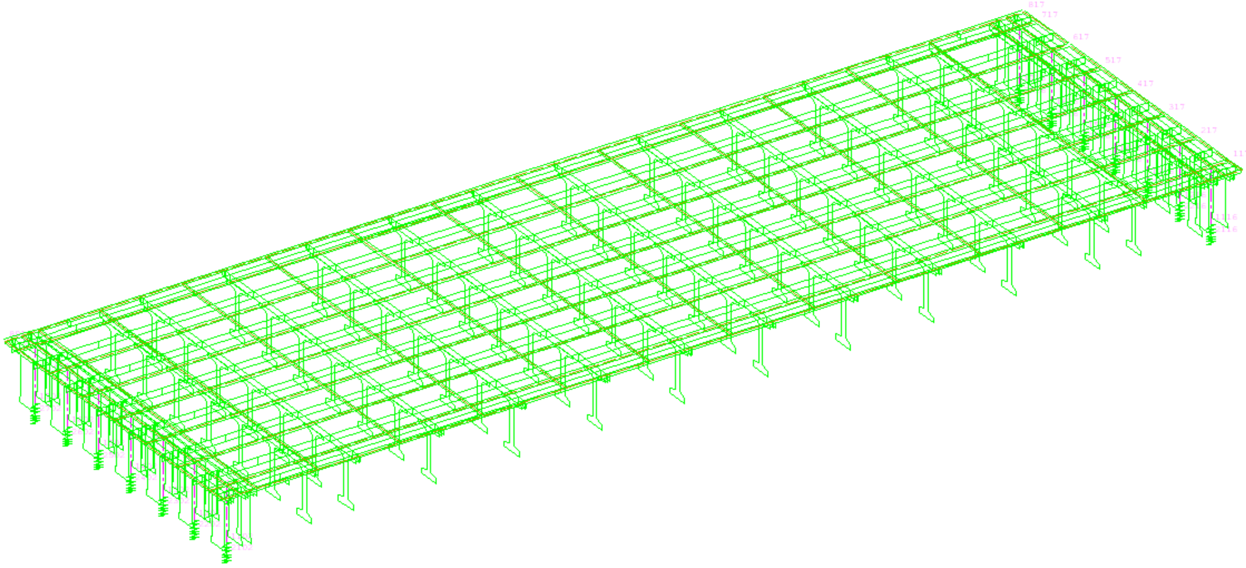

Figure 5.1: Model of the superstructure and sections of the members

Σχήμα 5.1: Προσομοίωμα ανωδομής και διατομές μελών

5.2. Load Cases

The load cases considered are the following:

5.2.1. <u>Self weight of the beams</u> (1st phase – beam section) – LC1

It is automatically calculated by the program for specific weight of the RC: g_{con}=25 kN/m^3.

5.2.2. <u>Self weight of the slab</u> (1st phase – beam section) – LC2

$$0.27 \text{ m} \times 25.0 \text{ kN/m}^3 = 6.75 \text{ KN/m}^2$$

5.2.3. <u>Prestress</u> (1st phase – beam section) – LC50

4 tendons of type Preco 12T15 per beam (12 strands per tendon), with the following characteristics:

Tensile strength f_{ptk}	:	1860 MPa
Yield stress (proof load 0.1%) f_{pok}	:	1670 MPa
Nominal diameter of strands	:	0.60″ = 15.70 mm
Nominal area of strands	:	A_p = 150 mm^2
Slip at prestressing anchor	:	s = 6mm

Prestress load:

max σ_p = min (0.65f_{ptk}, 0.75f_{pok}) = min (0.65x1860, 0.75x1600) = 1200 MPa

F_p = 1200×150 = 180.00 kN per strand, F_p = 12×180 = 2160 kN per tendon

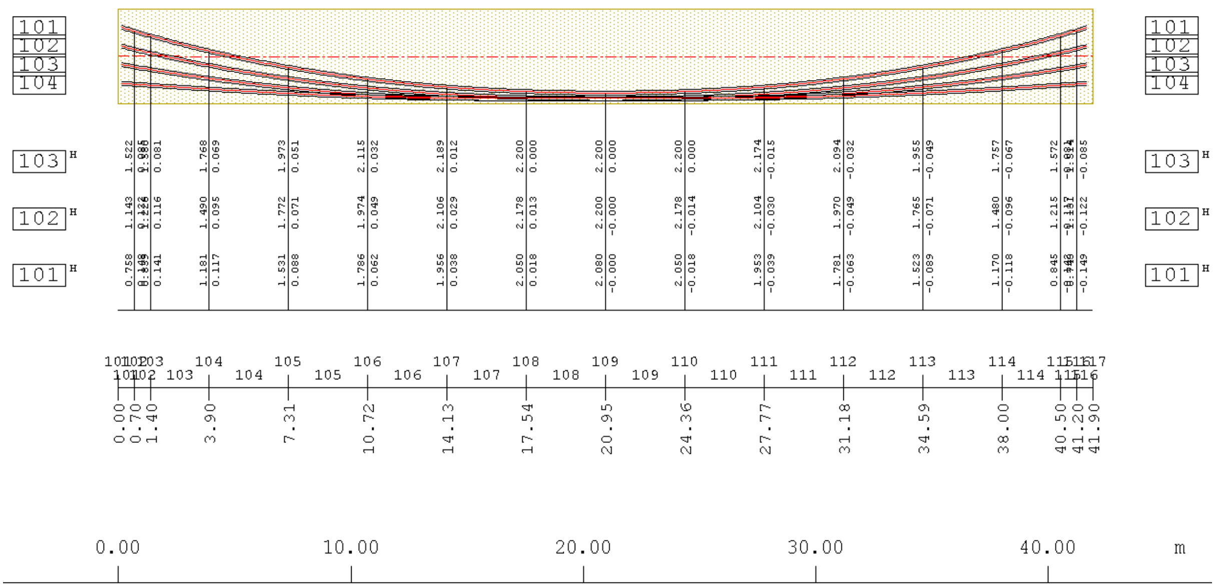

Figure 5.2: Arrangement of the prestressing tendons (elevation view of the beam)

Σχήμα 5.2: Διάταξη τενόντων προέντασης σε όψη

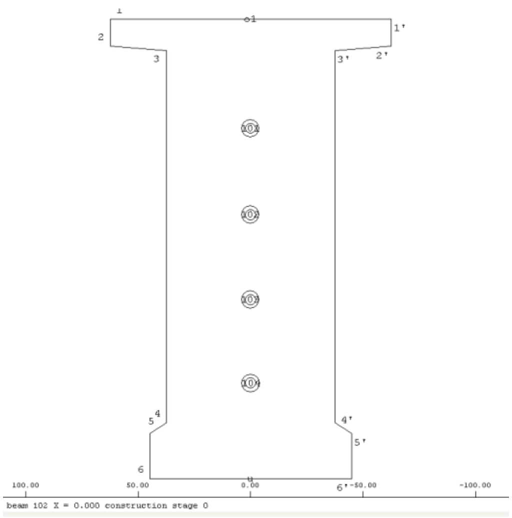

(a)

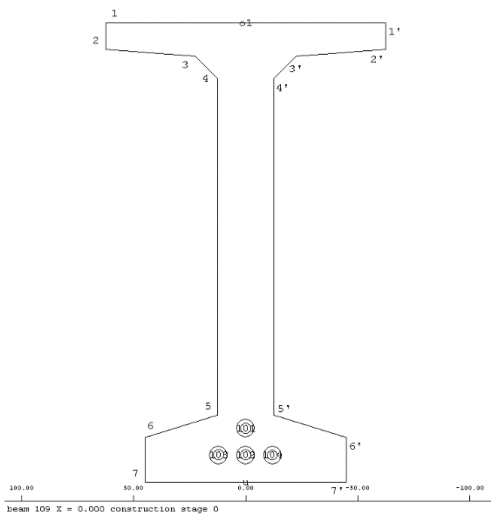

(b)

Figure 5.3: Section of the beam (a) at the support, (b) at the mid-span

Σχήμα 5.3: Διατομή δοκού (a) στη στήριξη, (b) στο μέσον του ανοίγματος

5.2.4. Prestress losses

(a) Friction losses (1st phase – beam section)

They are automatically calculated by the program (see Figures 5.4 to 5.7) according to the following relationship:

$P_x = P_o\ e^{-(\mu\ \alpha + k\ x)}$

where $\mu = 0.20\ rad^{-1}$ and $k = 0.01$ rad/m

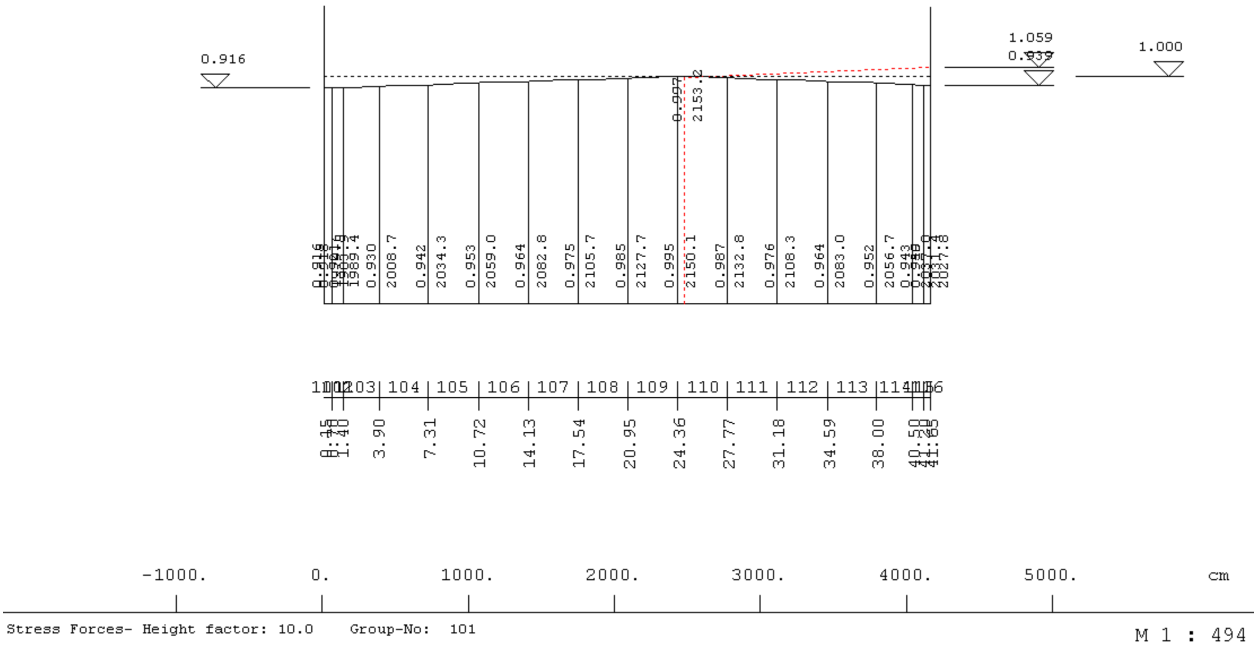

Figure 5.4: Diagram of friction losses for tendon 101

Σχήμα 5.4: Διάγραμμα απωλειών τριβής τένοντα no. 101

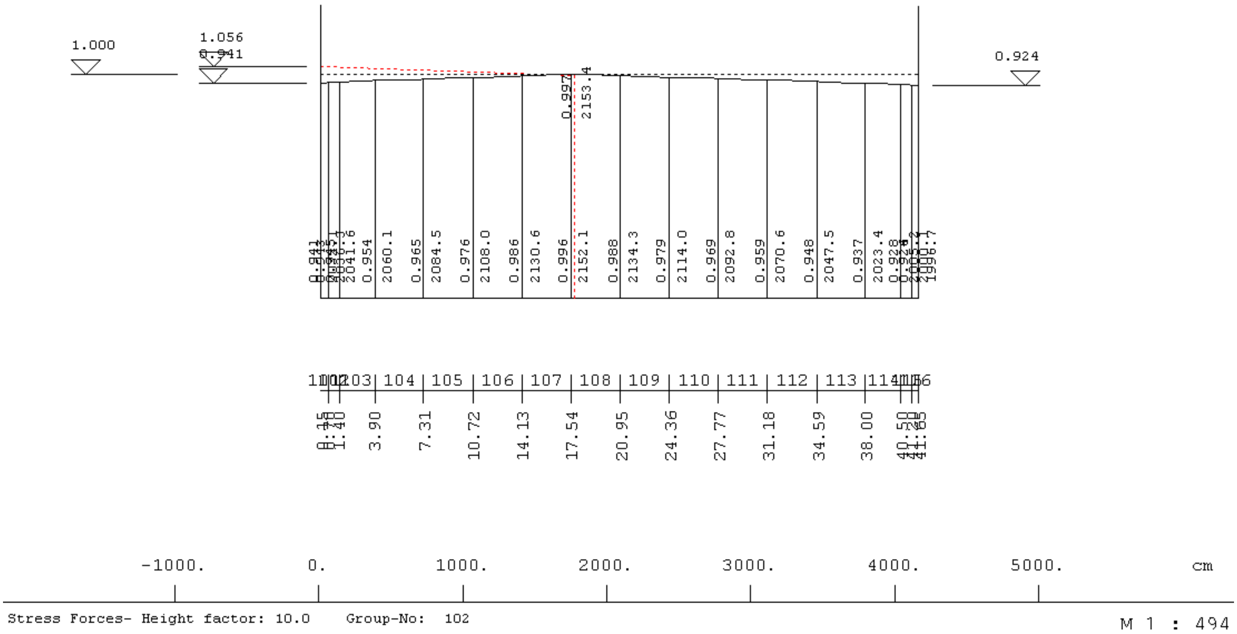

Figure 5.5: Diagram of friction losses for tendon 102

Σχήμα 5.5: Διάγραμμα απωλειών τριβής τένοντα no. 102

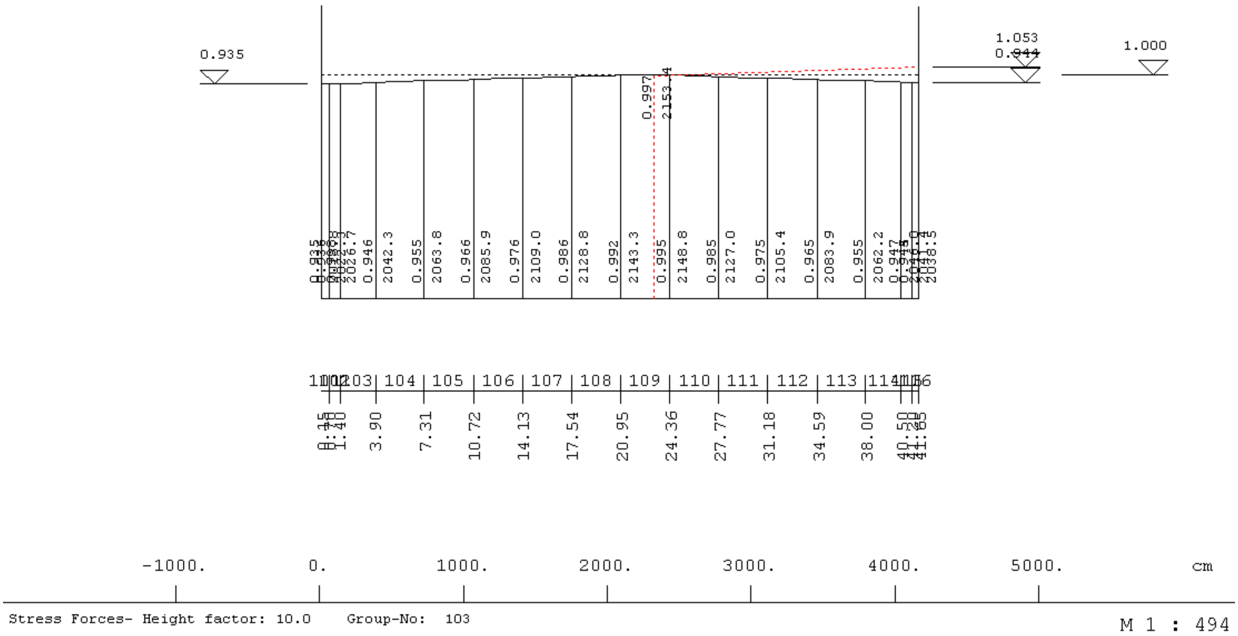

Figure 5.6: Diagram of friction losses for tendon 103

Σχήμα 5.6: Διάγραμμα απωλειών τριβής τένοντα no. 103

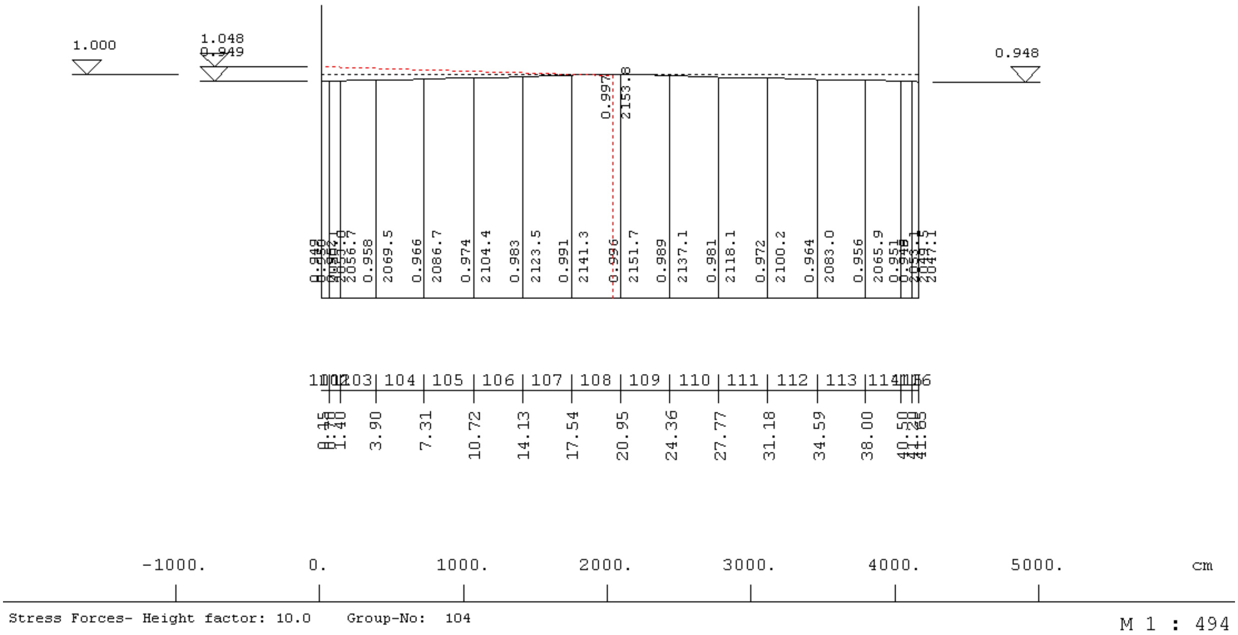

Figure 5.7: Diagram of friction losses for tendon 104

Σχήμα 5.7: Διάγραμμα απωλειών τριβής τένοντα no. 104

(b) Creep and shrinkage (1st phase – **LC9**, 2nd phase – **LC11**)

The relevant coefficients are calculated according to EC2.

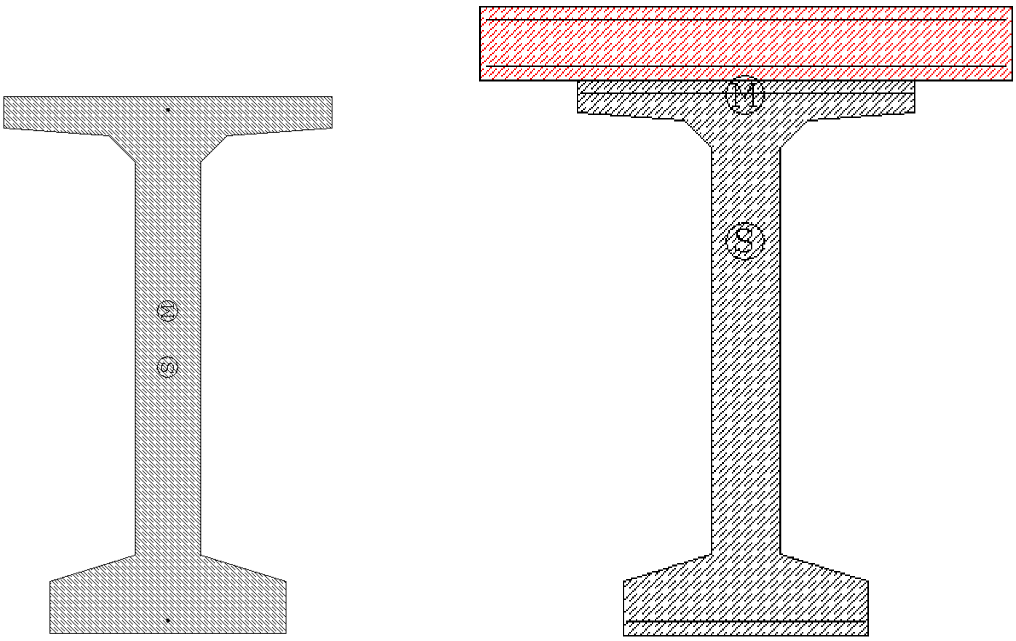

(a) (b)

Figure 5.8: (a) Cross section of the 1st phase (beam), (b) Cross section of the 2nd phase (beam+slab)

Σχήμα 5.8: (a) Διατομή 1ης φάσης (δοκός), (b) Διατομή 2ης φάσης (δοκός +πλάκα)

Table 5.1: Characteristics of the cross section of the beam (A_c is the cross-sectional area, u the perimeter of the member in contact with the atmosphere and h_0 the notional size of the member)

Πίνακας 5.1: Χαρακτηριστικά διατομής δοκού

	A_c (m^2)	u (m)	$h_0=2A_c/u$ (mm)
1st phase (beam)	0.823	7.41	222
2nd phase (beam+slab)	1.31	9.57	270

According to EC2 – Annex B, the creep coefficient $\varphi(t,t_0)$ may be calculated from:

$\varphi(t,t_0) = \varphi_0\, \beta_c(t,t_0)$

where:

φ_0 is the notional creep coefficient and may be estimated from:

$\varphi_0=\varphi_{RH}\, \beta(f_{cm})\, \beta(t_0)$ and f_{cm}=43 MPa (C35/45)

φ_{RH} is a factor to allow for the effect of relative humidity on the notional creep coefficient and for f_{cm}=43MPa is:

$$\varphi_{RH}=\left[1+\frac{1-RH/100}{0.1\sqrt[3]{h_0}}\cdot a_1\right]\cdot a_2$$

RH is the relative humidity of the ambient environment in %. In our case RH=80

a_1 , a_2 are coefficients to consider the influence of the concrete strength:

$a_1=\left[\frac{35}{f_{mc}}\right]^{0.7}=0.87$ and $a_2=\left[\frac{35}{f_{mc}}\right]^{0.2}=0.96$

Thus $\varphi_{RH}=1.24$

$\beta(f_{cm})$ is a factor to allow for the effect of concrete strength on the notional creep coefficient:

$$\beta(f_{cm})=\frac{16.8}{\sqrt{f_{cm}}}=2.56$$

$\beta(t_0)$ is a factor to allow for the effect of concrete age at loading on the notional creep coefficient. For t_0=15 days (the age of concrete at loading) is:

$$\beta(t_0)=\frac{1}{(0.1+t_0^{0.20})}=0.55$$

Then

$\varphi_0=1.24\times2.56\times0.55=1.75$

It is also:

$$\beta_c(t,t_0)=\left[\frac{(t-t_0)}{(\beta_H+t-t_0)}\right]^{0.3}$$

$\beta_H=1.5\,(1+(0.012\,RH)^{18})\,h_0+250\,a_3$ and $a_3=\left[\frac{35}{f_{mc}}\right]^{0.5}=0.90$

Thus, β_H =718 and for t=90 days (the age of concrete at the moment considered)

$\beta_c(t,t_0)$ = 0.49

Finally:

$\varphi\ (90, 15)$ = 1.75×0.49 = <u>0.86</u>

The final creep coefficient can be calculated as previously or taken directly from Figure 3.1 of EC2 for RH=80 (outside conditions) and quality of concrete C35/45, as equal to:

$\varphi\ (\infty, 15)$ = <u>1.75</u>

The total shrinkage strain ε_{cs} may be calculated from:

$\varepsilon_{cs} = \varepsilon_{cd} + \varepsilon_{ca}$

where ε_{cd} is the drying shrinkage strain and ε_{ca} the autogenic shrinkage strain.

It is:

$\varepsilon_{cd}(t) = \beta_{ds}(t,t_s)\ k_h\ \varepsilon_{cd,0}$

where, $\varepsilon_{cd,0}$ the basic drying shrinkage strain equal to $0{,}30 \mathrm{x} 10^{-3}$

$$\beta_{ds}(t,ts) = \frac{t-t_s}{(t-t_s)+0.04\cdot\sqrt{h_0^3}}$$

For the 1st phase t=90 days, t_s=15 days and h_0=222 mm, then $\beta_{ds}(t,t_s)$=0.36

From Table 3.3 of EC2 for h_0=222 mm, k_h=0.83 and

$\varepsilon_{cd}(90) = 0.36\times0.83\times0.30\times10^{-3} = 8.96\times10^{-3}$

It is also:

$\varepsilon_{ca}(t) = \beta_{as}(t)\ \varepsilon_{ca}(\infty)$

where $\varepsilon_{ca}(\infty) = 2.5\ (f_{ck} - 10)\times10^{-6}$ and in our case f_{ck}=35 MPa and $\varepsilon_{ca}(\infty) = 6.25\times10^{-5}$

$\beta_{as}(t) = 1 - \exp(-0.2t^{0.5})$ resulting to $\beta_{as}(90) = 0.85$ and then for the 1st phase to:

$\varepsilon_{ca}(90) = 0.85\times6.25\times10^{-5} = 5.31\times10^{-5}$

For the 1st phase the total shrinkage strain ε_{cs} (90) is then calculated as:

$\varepsilon_{cs}(90) = \varepsilon_{cd}(90) + \varepsilon_{ca}(90) = 8.96\times10^{-5} + 5.31\times10^{-5} = \underline{14.27\times10^{-5}}$

Accordingly for the 2nd phase:

$\varepsilon_{cs}(\infty) = \varepsilon_{cd}(\infty) + \varepsilon_{ca}(\infty) = 23.4\times10^{-5} + 6.25\times10^{-5} = \underline{29.65\times10^{-5}}$

Finally for the 1st phase (beams only) the following values were taken into account for the analysis:

φ (90, 15) = <u>0.86</u>

$\varepsilon_{cs}(90) = \underline{14.27\times10^{-5}}$

and for the 2nd phase (beams and deck):

for the deck: φ (∞, 90) = <u>1.75</u> , $\varepsilon_{cs}(\infty) = \underline{29.65\times10^{-5}}$ and

for the beams: φ (∞, 90) = 1.75 -0.86 = <u>0.89</u> and

$\varepsilon_{cs}(\infty) = 29.65\times10^{-5} - 14.27\times10^{-5} = \underline{15.38\times10^{-5}}$

5.2.5. Additional dead loads – LC3

Pavement layer and lining concrete

$$0.09\times22.0 + 0.06\times25.0 = 1.98 + 1.50 = 3.48 \quad \sim \underline{3.50\ \text{KN/m}^2}$$

5.2.6. Live Loads (TS – LC101-141 and LC142-153, UDL – LC170)

<u>Tandem System of Traffic Load Model 1</u>

The carriageway width is 11.25 m, thus, three lanes are considered with width 3.00 m and a tandem system is applied at varied positions on the bridge, as:

Lane 1: 0.9×150 kN = 135 KN/wheel (four wheels)

Lane2: 0.9×100 kN = 90 KN/wheel (four wheels)

Lane3: 0.9×50 kN = 45 KN/wheel (four wheels)

<u>UDL System of Traffic Load Model 1</u>

A distributed load is applied on the deck equal to 2.5 KN/m^2. At Lane 1 an additional distributed load was applied, equal to 6.5 KN/m^2.

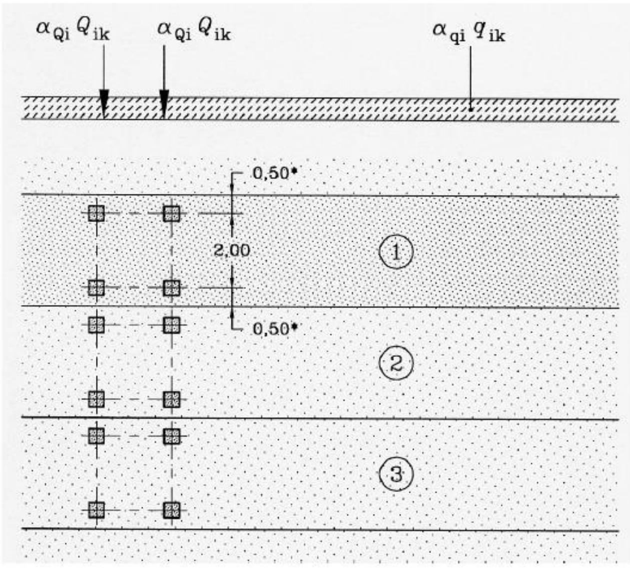

Key

(1) Lane Nr. 1 : $Q_{1k} = 300$ kN ; $q_{1k} = 9$ kN/m^2

(2) Lane Nr. 2 : $Q_{2k} = 200$ kN ; $q_{2k} = 2{,}5$ kN/m^2

(3) Lane Nr. 3 : $Q_{3k} = 100$ kN ; $q_{3k} = 2{,}5$ kN/m^2

* For $w_l = 3{,}00$ m

Figure 5.9: Details of Traffic Load_Model 1

Σχήμα 5.9: Πρότυπη φόρτιση 1

To obtain the most adverse results, Lane 1 was placed near the sidewalk. The tandem system was moving along the bridge with a step of about 1.0 m, which represents the 1/40 of the span length (LC 101-141). In the design, the envelope of the internal forces was taken into account (LC 142-153).

5.3. Serviceability Limit State (SLS)

5.3.1. Load Combinations at Serviceability Limit State

The load combinations at the SLS are:

Characteristic combination: $\sum_{j\geq1} G_{kj}"+"P_k"+"Q_{k1}"+"\sum_{i\geq1}\psi_0\cdot Q_{ki}$

Frequent combination: $\sum_{j\geq1} G_{kj}"+"P_k"+"\psi_{1,1}\cdot Q_{k1}"+"\sum_{i\geq1}\psi_{2i}\cdot Q_{ki}$

Quasi-permanent combination: $\sum_{j\geq1} G_{kj}"+"P_k"+"\sum_{i\geq1}\psi_{2i}\cdot Q_{ki}$

For characteristic and frequent combinations, where prestress P_k is critical, it is set: $P_{k,inf}=0.9\cdot P_k$ and $P_{k,sup}=1.1\cdot P_k$.

The load factors ψ for road bridges are given in Table 5.2:

Table 5.2: Factors ψ for road bridges
Πίνακας 5.2: Συντελεστές ψ για οδογέφυρες

Actions	Symbol		ψ_0	ψ_1	ψ_2
Traffic load	Gr1 (LM1)	TS	0.75	0.75	0.00
		UDL	0.40	0.40	0.00

The following SLS load combinations were considered:

LC80 : LC1+LC50 (Combination: G_0+P_0)

LC81 : LC1+LC50+ LC2+LC9 (Combination: $G_0+P_0+G_1+Creep_1$)

<u>Characteristic combinations</u>

LC82 (& LC91): LC1+0.9*LC50+ LC2+LC3+0.9*LC9+0.9*LC11+maxLC(142-153)+LC170
(Combination: $G_t+0.9*P_\infty+TS+UDL$)

LC83 (& LC92): LC1+1.1*LC50+ LC2+LC3+1.1*LC9+1.1*LC11+maxLC(142-153)+LC170
(Combination: $G_t+1.1*P_\infty+ TS+UDL$)

<u>Quasi-permanent combinations</u>

LC84 : LC1+0.9*LC50+ LC2+LC3+0.9*LC9+0.9*LC11
(Combination: $G_t+0.9*P_\infty$)

LC85 : LC1+1.1*LC50+ LC2+LC3+1.1*LC9+1.1*LC11
(Combination: Gt+1.1*P∞)

<u>Frequent combinations</u>

LC90 (& LC95): LC1+LC50+ LC2+LC3+LC9+LC11+0.75*maxLC(142-153)+0.4*LC170
(Combination: $G_t+1.1*P_\infty+0.75*TS+0.4*UDL$)

5.3.2. Verification of the members at Serviceability Limit State

Table 5.3: Checks per SLS combination (according to FB102 and EC2)

Πίνακας 5.3: Έλεγχοι ανά συνδυασμό λειτουργικότητας (κατά FB102 και EC2)

SLS combination	**Check**	**LC**
1. Characteristic	a) $\sigma_c<0.60f_{ck}$	82, 83
	b) Limitation of concrete tensile stresses $\sigma_t<f_{ctm}$	82, 83
	c) Limitation of crack width – Indirect calculation of min reinforcement (w_k=0.2mm)	91, 92
2. Frequent	a) - If $\max\sigma_c<-1$ MPa => min reinforcement for crack control - If $-1<\max\sigma_c<f_{ctm}$ => go to 1c, - Otherwise direct calculation of crack width	90
	b) Main oblique tensile stresses $\sigma_I<f_{ctk,0.05}$	95
3. Quasi-permanent	a) $\sigma_c<0$	84, 85
	b) $\sigma_c<0.45f_{ck}$	84, 85
	c) $\sigma_s<0.65f_{pk}$ (for prestressed steel)	84, 85

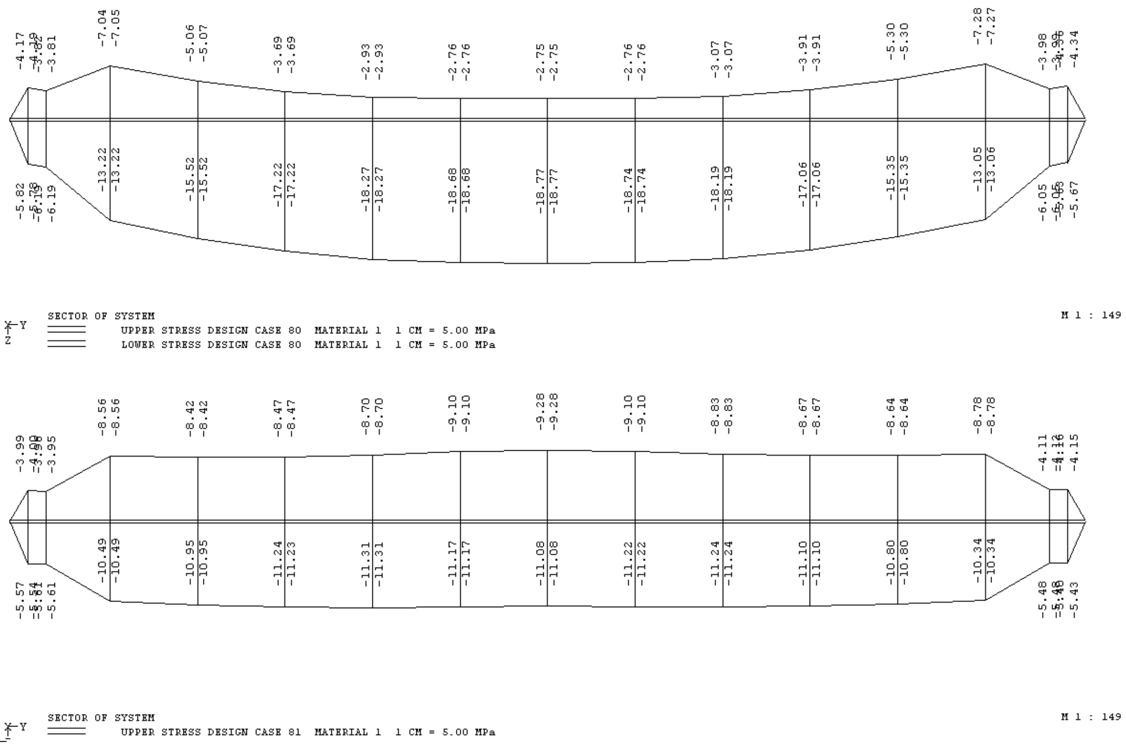

Figure 5.10: Chart of beam stresses for load combinations 80 (G_0+P_0) and 81 (G_0+P_0+G_1+$Creep_1$)

Σχήμα 5.10: Διάγραμμα τάσεων της δοκού για τους συνδυασμούς φορτίσεων 80 και 81

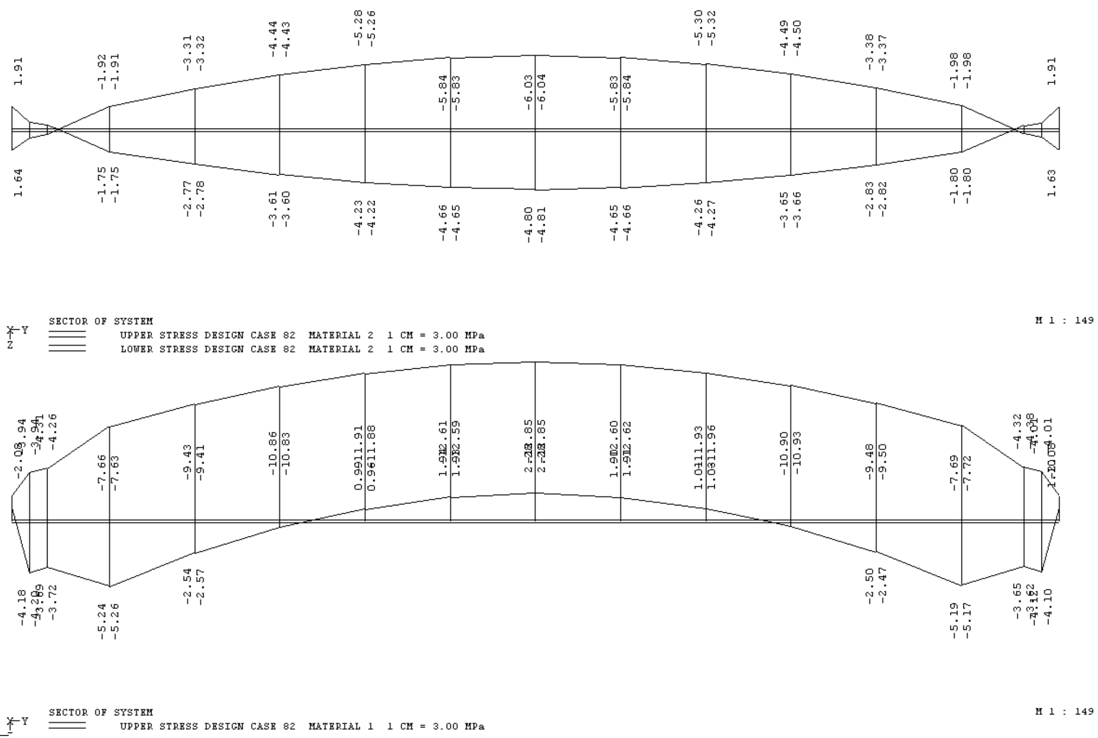

Figure 5.11: Plot of stresses for load combination 82 (G_t+0.9*P_∞+TS+UDL): top: slab; bottom: beam

Σχήμα 5.11: Διάγραμμα τάσεων για το συνδυασμό φορτίσεως 82 (πάνω για την πλάκα, κάτω για τη δοκό)

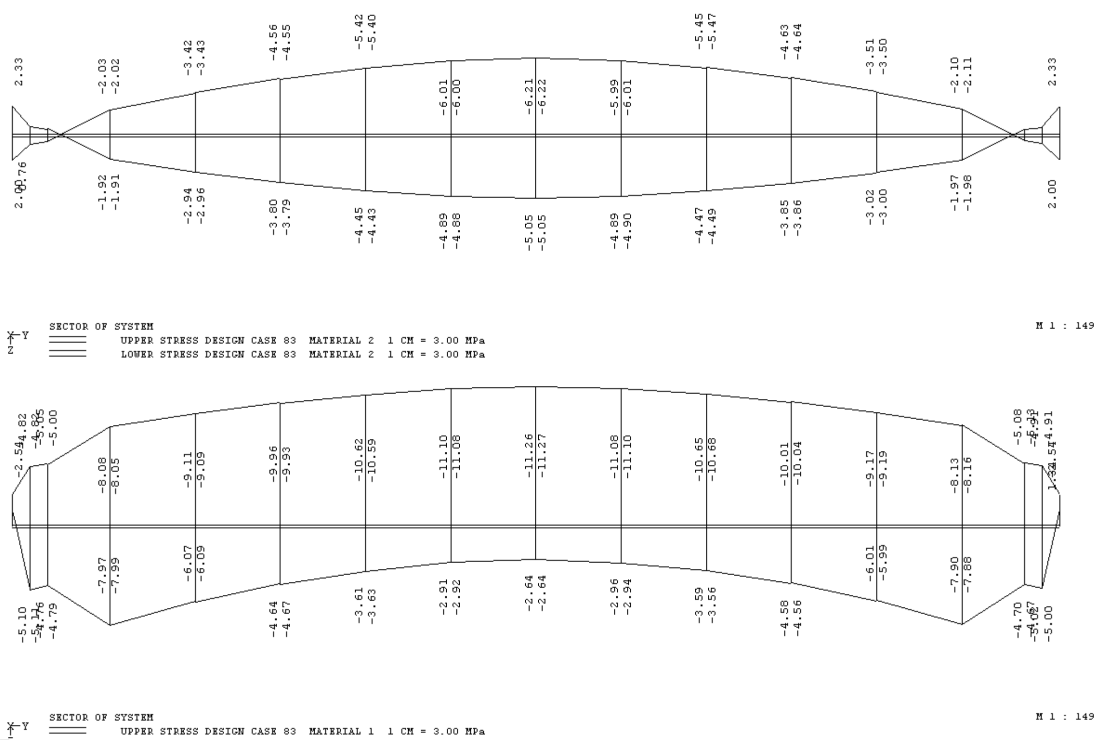

Figure 5.12: Plot of stresses for load combination 83 (G_t+1.1*P_∞+ TS+UDL): top: slab; bottom: beam

Σχήμα 5.12: Διάγραμμα τάσεων για το συνδυασμό φορτίσεως 83 (πάνω για την πλάκα, κάτω για τη δοκό)

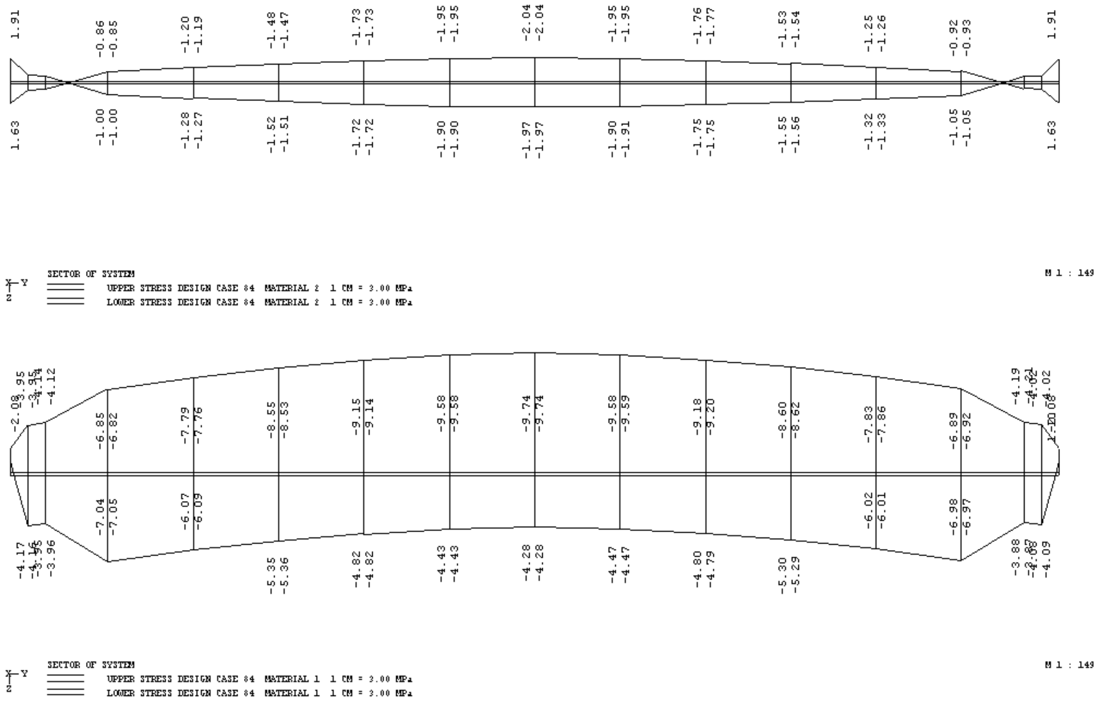

Figure 5.13: Plot of stresses for load combination 84 (G_t+0.9*P_∞): top: slab; bottom: beam

Σχήμα 5.13: Διάγραμμα τάσεων για το συνδυασμό φορτίσεως 84 (πάνω για την πλάκα, κάτω για τη δοκό)

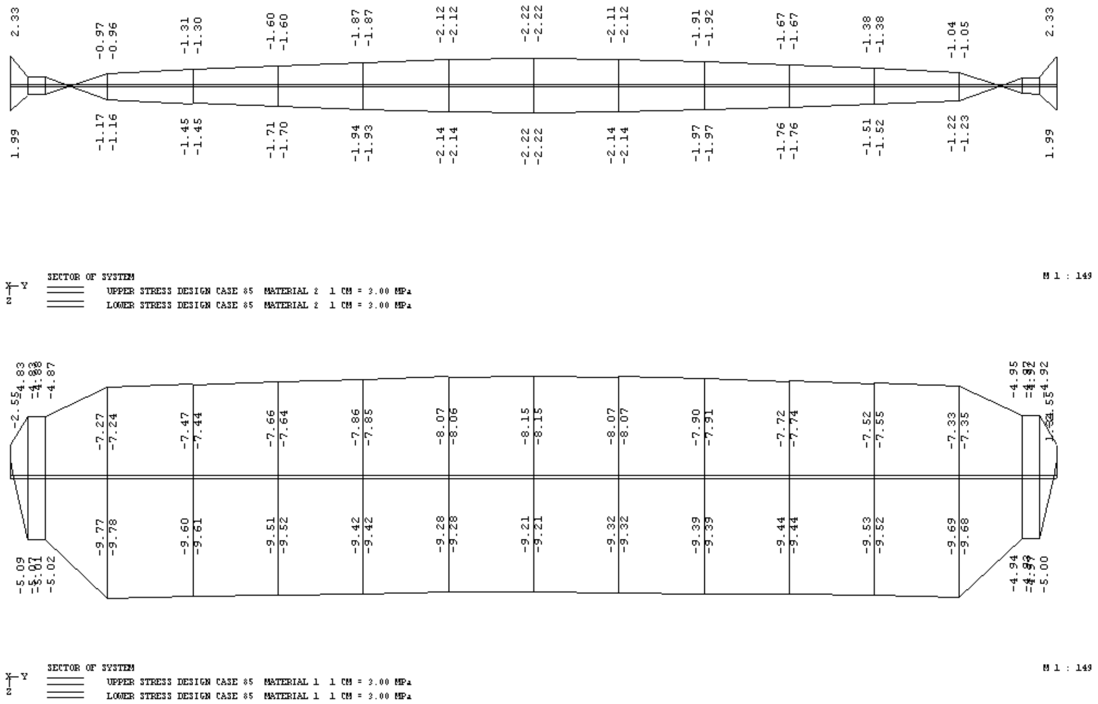

Figure 5.14: Plot of stresses for load combination 85 (G_t+1.1*P_∞): top: slab; bottom: beam

Σχήμα 5.14: Διάγραμμα τάσεων για το συνδυασμό φορτίσεως 85 (πάνω για την πλάκα, κάτω για τη δοκό)

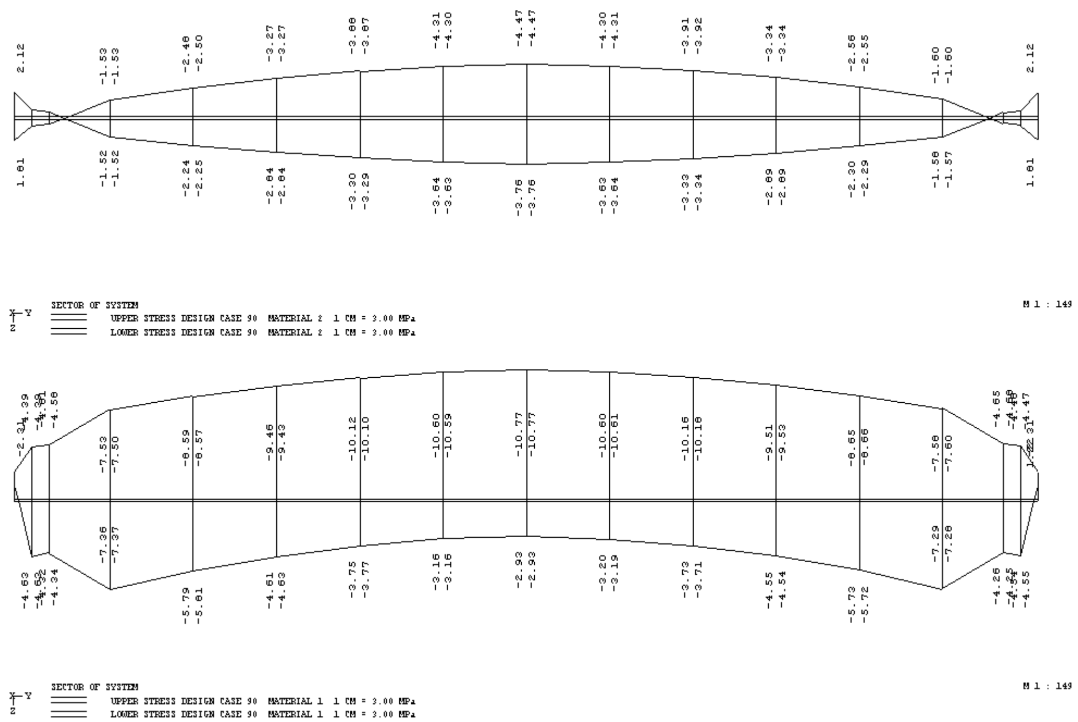

Figure 5.15: Plot of stresses of external beam for load combination 90 (G_t+1.1*P_∞+0.75*TS+0.4*UDL): top: slab; bottom: beam

Σχήμα 5.15: Διάγραμμα τάσεων της ακραίας δοκού για το συνδυασμό φορτίσεως 90 (πάνω για την πλάκα, κάτω για τη δοκό)

Materials

Material 1 (beam) : C35/45 with f_{ctm}=3.2 MPa, $f_{ctk,0.05}$=2.2 MPa, f_{ck}=35 MPa.
Material 2 (slab) : C30/37 with f_{ctm}=2.9 MPa, $f_{ctk,0.05}$=2.0 MPa, f_{ck}=30 MPa.
Also, f_{pk}=1860 MPa.

The max values of concrete and steel stresses for material 1 (beam) and material 2 (slab) for various combinations are presented below.

Characteristic combinations

CHECKS: $\min\sigma_c = -12.85 > 0.60\times(-35) = -21.0$ MPa
$\max\sigma_t = 2.3 < 3.2$ MPa

Frequent combinations

CHECKS: $\max\sigma_c = -2.93 < -1.0$ MPa $\rightarrow$ min reinforcement
$\max\sigma_I = 0.1 < 2.0$ MPa

Quasi-permanent combinations

CHECKS: Only compressive stresses: $\max\sigma_c < 0$
$\min\sigma_c = -9.78 < 0.45\times(-35) = -15.75$ MPa
$\max\sigma_s = 1108.7 < 0.65\times1800 = 1170$ MPa

5.4. Ultimate Limit State (ULS)

The load combination at ULS is:

$$\sum_{j\geq 1}\gamma_{Gj}\cdot G_{kj}"+"\gamma_P\cdot P_k"+"\gamma_{Q1}\cdot Q_{k1}"+"\sum_{i\geq 1}\gamma_{Qi}\cdot\psi_{0\iota}\cdot Q_{ki}$$

where the partial factors γ_G and γ_Q are listed in

Table **5.**4:

Table 5.4: Partial factors for actions in ULS

Πίνακας 5.4: Επιμέρους συντελεστές για δράσεις σε ΟΚΑ

Action	Contribution	Factor	S/V
Permanent actions	unfavourable	γ_{Gsup}	1.35
	favourable	γ_{Ginf}	1.00
Prestress	unfavourable	γ_P	1.00
	favourable	γ_P	1.00
Traffic loads	unfavourable	γ_Q	1.35
	favourable	γ_Q	0.00
Other variable actions	unfavourable	γ_Q	1.50
	favourable	γ_Q	0.00

S: Persistent design situation, V: Transient design situation

The following ULS load combinations were considered:

Design against flexure

LC100 : 1.35×LC1+0.9×LC50+ 1.35×LC2+1.35×LC3+0.9×LC9+0.9×LC11
+1.35×maxLC(142-153)+1.35×LC170
(1.35×G_t+0.9×P_∞+1.35×TS+1.35×UDL)

Design against shear and torsion

LC110 : 1.35×LC1+0.9×LC50+ 1.35×LC2+1.35×LC3+0.9×LC9+0.9×LC11
+1.35×maxLC(142-153)+1.35×LC170
(1.35×G_t+0.9×P_∞+1.35×TS+1.35×UDL)

5.5. Required reinforcement

The required reinforcement was calculated from the results of the analysis taking under consideration the minimum reinforcement specified in the Codes. In Figures 5.16 and 5.17, the prestressing tendons and the reinforcing steel of the beam and the slab respectively are presented.

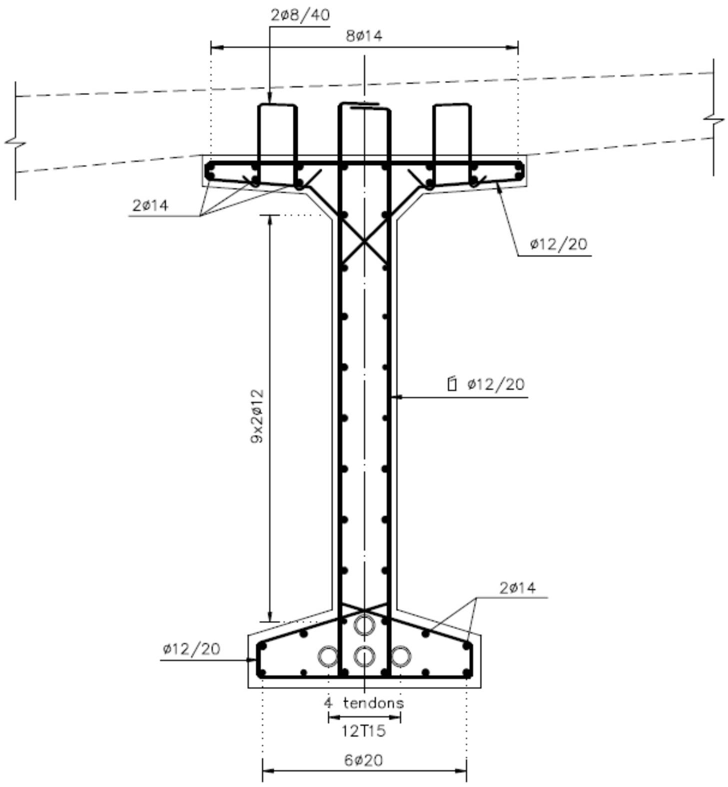

Figure 5.16: Beam reinforcement at midspan

Σχήμα 5.16: Οπλισμός δοκού στο μέσον του ανοίγματος

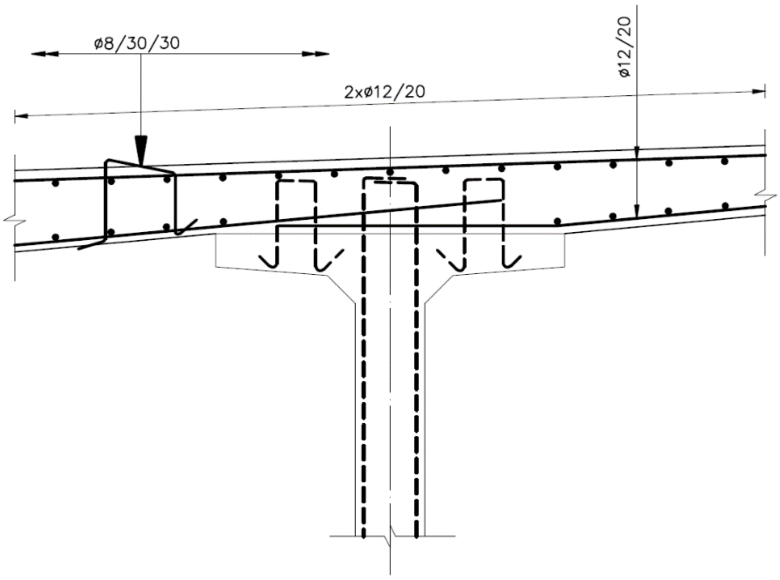

Figure 5.17: Slab reinforcement

Σχήμα 5.17: Οπλισμός πλάκας

6. DESIGN OF SUBSTRUCTURE

6.1. Model

For the design of the substructure (pier and its foundation) against static and seismic loads and the determination of the internal forces and displacements of the structure, the model illustrated in Figure 6.1 was considered. The superstructure, the pier column-cap, the pier column and the foundation piles were modeled with beam elements representing in detail the geometry and stiffness characteristics of the various members. The concrete pile-cap with a thickness of 1.80m, was simulated using shell elements.

The bearings at the abutments and the pier were modeled with equivalent elastic springs, with different stiffness for static and seismic combinations. The following values were considered:

- For static load combinations, shear modulus G= 0.90 MPα

  Abutment (400x500x121-mm) : $K_{b,st,hor}$=1454 kN/m, $K_{b,st,vert}$=603400 kN/m

  Pier (350x450x99-mm) : $K_{b,st,hor}$=1396 kN/m, $K_{b,st,vert}$=473500 kN/m

- For displacements under seismic load combinations, G=1.25x0.90=1.125 MPα:

  Abutment (400x500x121-mm) : $K_{b,st,hor}$=1820 kN/m, $K_{b,st,vert}$=720615 kN/m

  Pier (350x450x99-mm) : $K_{b,st,hor}$=1745 kN/m, $K_{b,st,vert}$=570145 kN/m

- For internal forces under seismic load combinations, G=1.20x1.25x0.90=1,35 MPα:

  Abutment (400x500x121-mm) : $K_{b,st,hor}$=2180 kN/m, $K_{b,st,vert}$=827820 kN/m

  Pier (350x450x99-mm) : $K_{b,st,hor}$=2095 kN/m, $K_{b,st,vert}$=659900 kN/m

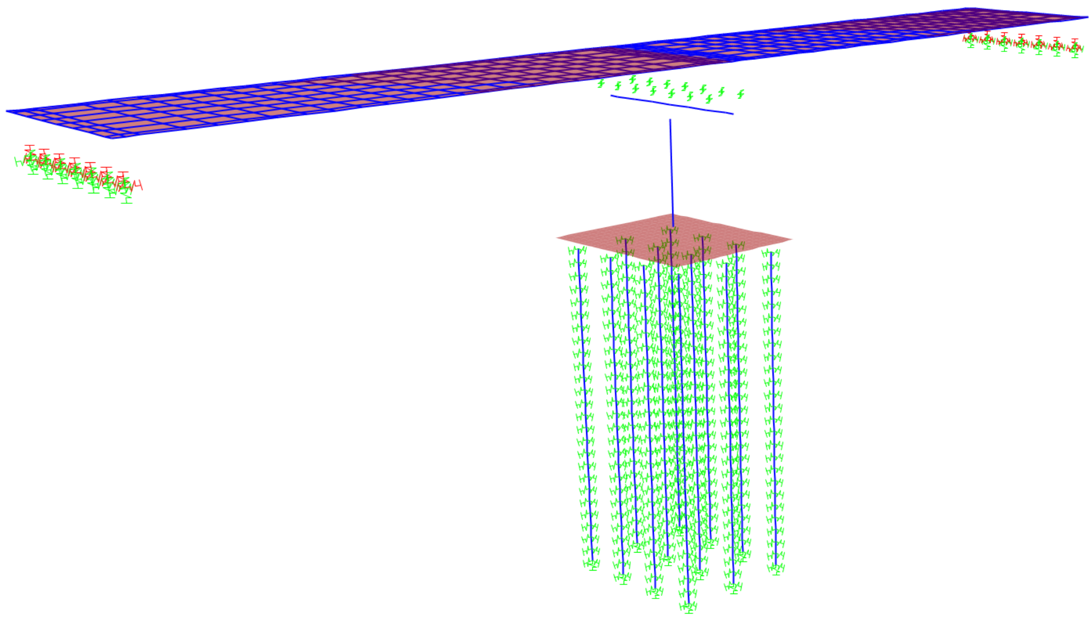

Figure 6.1: Finite element model of the bridge

Σχήμα 6.1: Προσομοίωμα πεπερασμένων στοιχείων της γέφυρας

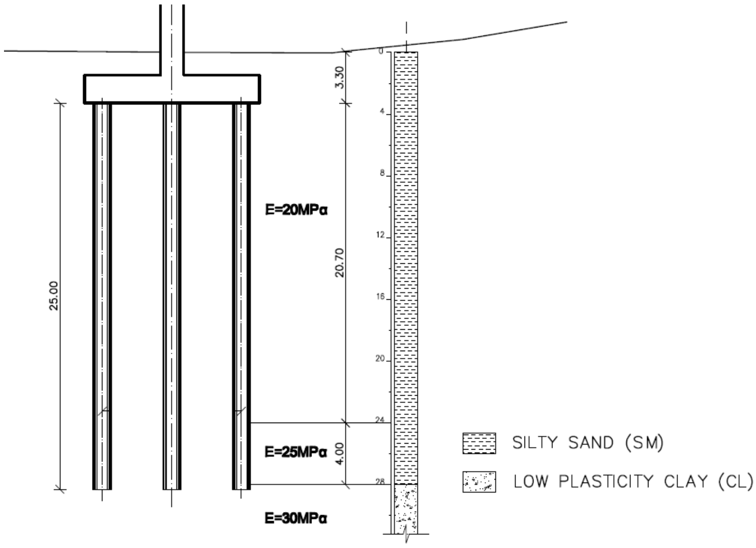

Figure 6.2: Young's modulus E of soil with respect to the piles' length

Σχήμα 6.2: Μέτρο ελαστικότητας εδάφους E σε σχέση με το μήκος πασσάλων

The soil-structure interaction was taken into account with equivalent springs acting on the piles. More specifically, first the spring constant of a single pile was calculated based on the values of Table 3.1 and the values of soil's Young's modulus shown in Figure 6.2. Thus,

$K_h = E_h / D$ ➔ $k_h = 20000$ kN/m^3 for the upper 21.00 m of the pile,

$K_h = E_h / D$ ➔ $k_h = 25000$ kN/m^3 for the next 4.00 m of the pile

$K_h = E_h / D$ ➔ $k_h = 30000$ kN/m^3 for the remaining length of the pile

where D is the pile diameter (considered equal to 1.00 m since the pile diameter is larger than 1.00 m).

According to DIN1054, the above calculated values should be reduced to take into account the group effect (see section 4.1). The elastic length of the pile L is:

$$L = \left(\frac{EI}{k_s D}\right)^{0.25} = \left(\frac{30 \cdot 10^6 \cdot \pi \cdot 1.00^4 / 64}{20000 \cdot 1.00}\right)^{0.25} \Rightarrow L = 2.92\text{m}$$

Thus, $\ell/L = 25.00 / 2.92 = 8.56 > 4.00$ (where ℓ is the pile's length).

Also, $K_{h,i} = \alpha_i^{1.33} \cdot k_h$ and $\alpha_i = \alpha_L \, \alpha_Q$

For the specific arrangement of the piles in plan presented in Figure 6.3(b), the resulting reduction factors for the springs' constants are 0.64 in the longitudinal direction of the bridge and to 0.55 in the transverse direction of the bridge. In the analyses, the mean value of 0.60 was taken into account for both directions. Thus:

$K_{h,I} = 0.60 \cdot k_h$

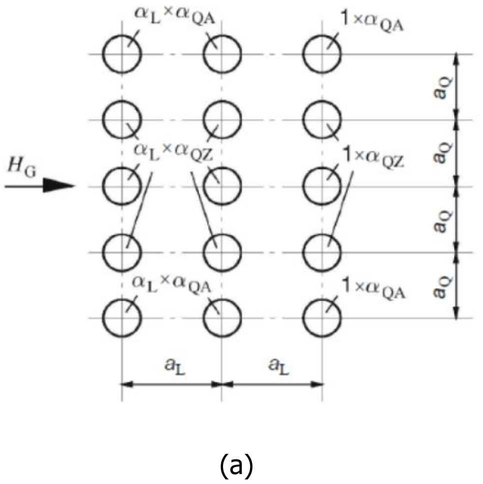

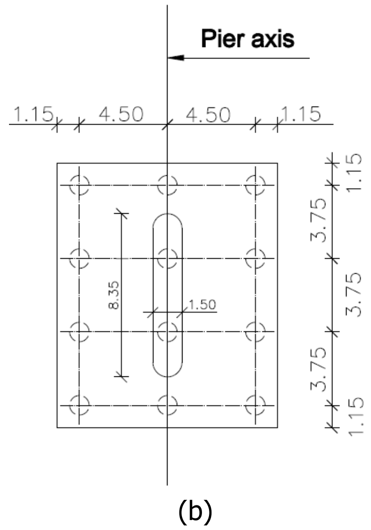

Figure 6.3: (a) Definition of coefficients $α_L$ and $α_Q$ and (b) arrangement of pier piles

Σχήμα 6.3: (a) Ορισμός συντελεστών $α_L$ και $α_Q$ και (b) διάταξη των πασσάλων του μεσοβάθρου

Regarding the vertical springs of the piles, the constant for a pile of L=25.00 m is given in Table 4.2 and it is equal to k_v = 178 MN/m^3, while the reduction factor R_s according to Table 4.3 is equal to 1.05, considering L/B = 25, e/B = 4.50 and K = 2000. Thus, the vertical spring's constant for the piles of diameter 1.00 m is:

k_v = 178000 kN/m / 1.05 = 170000 kN/m

The resistance of the system abutment – backfill is modeled in the analysis with a set of springs, placed below the bearings' springs, with the following characteristics:

K_{hx} = 184000 kN per meter of width of the abutment for the longitudinal direction, and

K_{hy} = 84830 kN per meter of width of the abutment for the lateral direction

Vertically, the abutments are supposed to be practically fixed.

The model of the bridge is shown in Figure 6.1. The analyses were performed using SAP2000.

6.2. Loads

The following load cases were considered:

6.2.1. Self-weight – LC1

It is automatically calculated by the program for g_{con}=25 kN/m^3

6.2.2. Additional dead loads – LC2

Pavement layer and lining concrete:

$$0.09\times22.0 + 0.06\times25.0 = 1.98 + 1.50 = 3.48 \quad \sim 3.50 \text{ KN/m}^2$$

Sidewalk with parapets: g=(0.30 m^2 × 25k N/m^3 + 1.00 kN/m) = 8.50 kN/m

Earth weight on the pilecap: g=1.50 m × 22 kN/m^3 = 33.0 kN/m^2

6.2.3. Shrinkage and creep – LC3

An equivalent uniform decrease of temperature was used to simulate the shrinkage of the concrete beams, calculated as follows:

Elastic movement due to prestress :

$$\delta_{el} = \frac{P_{k,0} \cdot L}{E_c \cdot A_c} = \frac{4 \cdot 12 \cdot 180 \cdot (0.5 \cdot 40.5)}{34 \cdot 10^6 \cdot 1.31} = 3.92\text{mm}$$

Remaining creep coefficient after the placement of the beams: $\varphi(\infty, 90) = 0.89$ (see section 5.2):

Thus, $\delta_{cr} = 0.89\times3.92 = 3.5$ mm which is equivalent to a thermal decrease of:

$$DT' = \frac{\delta_{cr}}{a \cdot \frac{L}{2}} = \frac{3.5 \cdot 10^3}{10^5 \cdot 40.5 \cdot 0.5} = 17.3^0\text{C}$$

Remaining shrinkage coefficient after the placement of the beams: $\varepsilon_{cs}(\infty)=15.38\times10^{-5}$ (see section 5.2), equivalent to DT′ = 15.4° C.

Finally for the beams: DT′ = 17.3+15.4° = 32.7° C

For the continuity slab, DT′ is taken equal to 30° C

6.2.4. Live Loads – LC4-LC7

Tandem System of Traffic Load Model 1 (see also section 5.2)

The carriageway width is 11.25 m, thus, three lanes of width 3.00 m were considered and a tandem system was applied at varying positions of the bridge with the following loads:

Lane 1: 0.9×150 kN = 135 kN/wheel (four wheels)

Lane2: 0.9×100 kN = 90 kN/wheel (four wheels)

Lane3: 0.9×50 kN = 45 kN/wheel (four wheels)

UDL System of Traffic Load Model 1

A distributed load was applied on the deck, equal to 2.5 kN/m^2. At Lane 1 an additional distributed load was applied, equal to 6.5 kN/m^2.

6.2.5. Uniform road traffic loads – LC10

This load case was used for the seismic combinations and was based on Load Model 1.

Q_{ik} =2×0.9× (300+200+100)+84.0× (3.0×9.0+2×3.0×2.5+2.45×2.5) = 5122.5 kN

The distributed uniform load over the bridge's deck is:

Q_{ik} / (11.25 m × 84.00 m) = 5.45 kN/m^2

6.2.6. Braking load (+/- LC11-LC12)

The total braking load is:

$Q_{ik} = 0.6 \cdot \alpha_{Ql} \cdot (2Q_{lk}) + 0.10 \cdot \alpha_{ql} \cdot q_{lk} \cdot w_1 \cdot L$ = 0.6×0.9×2×300+0.10×1.0×9×3×84.00 = 550.8 kN

It is: $180 \times \alpha_{Ql} \leq Q_{ik} \leq 900 \rightarrow 180 \times 0.9 \leq Q_{ik} \leq 900 \rightarrow 162 \leq Q_{ik} \leq 900$.

The distributed uniform horizontal load over the bridge's deck is:

Q_{ik} / (11.25 m × 84.00 m) = 0.58 kN/m^2

6.2.7. Uniform difference of temperature on deck

Considering an initial temperature T_0 = +10° C, a minimum shade air temperature T_{min} = –15° C and a maximum one T_{max} = +45° C, the uniform temperature fluctuations were determined according to EC1-Part.1-5 (for concrete bridges, Type 3) as: $T_{e,min}$ = –7° C and $T_{e,max}$ = +47° C. Thus:

$\Delta T_{N,con} = T_0 - T_{e,min}$ = –17° C (**LC13**)

$\Delta T_{N,exp} = T_{e,max} - T_0$ = +37° C (**LC14**)

The temperature variations were applied to the members of the superstructure.

For the check of bearings and the expansion joints, the uniform difference of temperature was calculated as:

$\Delta T_{N,con}$–20 = –37° C and $\Delta T_{N,exp}$+20 = +57° C.

6.2.8. Earthquake loads

Modal response spectrum analysis was performed to calculate the natural frequencies and vibration modes of the bridge. The spectra presented in section 4.2 were used. For the inertial loads of the design seismic action the masses associated with all gravity loads were considered following the following combination rule:

$\sum_{j\geq 1} G_{kj} "+" \sum_{i\geq 1} \psi_E \cdot Q_{ki}$ where ψ_E=0.20 for road traffic loads.

It was ensured that the sum of the effective modal masses for the modes taken into account was at least 90% of the total mass of the structure without including the piles' mass. The modal maximum displacements, the modal internal loads and the modal stresses were superimposed according to CQC (Complete Quadratic Combination) method. The following load cases were examined:

Earthquake x-x (horizontal longitudinal direction of the bridge) – **LC15**

Earthquake y-y (horizontal lateral direction of the bridge) – **LC16**

Earthquake z-z (vertical direction of the bridge) – **LC17**

6.3. Vibration modes and natural frequencies

The natural frequencies and periods of the first six vibration modes are listed in Table 6.1, while in Figure 6.1 the corresponding modal shapes are depicted.

Table 6.1: First six eigenfrequencies and eigenperiods of the bridge

Πίνακας 6.1: Έξι πρώτες ιδιοσυχνότητες και ιδιοπερίοδοι της γέφυρας

Mode number	Eigenfrequency (rad/sec)	Eigenfrequency (Hz)	Period (sec)
1	4.026	0.641	1.56
2	4.044	0.644	1.55
3	4.907	0.781	1.28
4	14.14	2.250	0.44
5	14.17	2.256	0.44
6	15.78	2.512	0.40

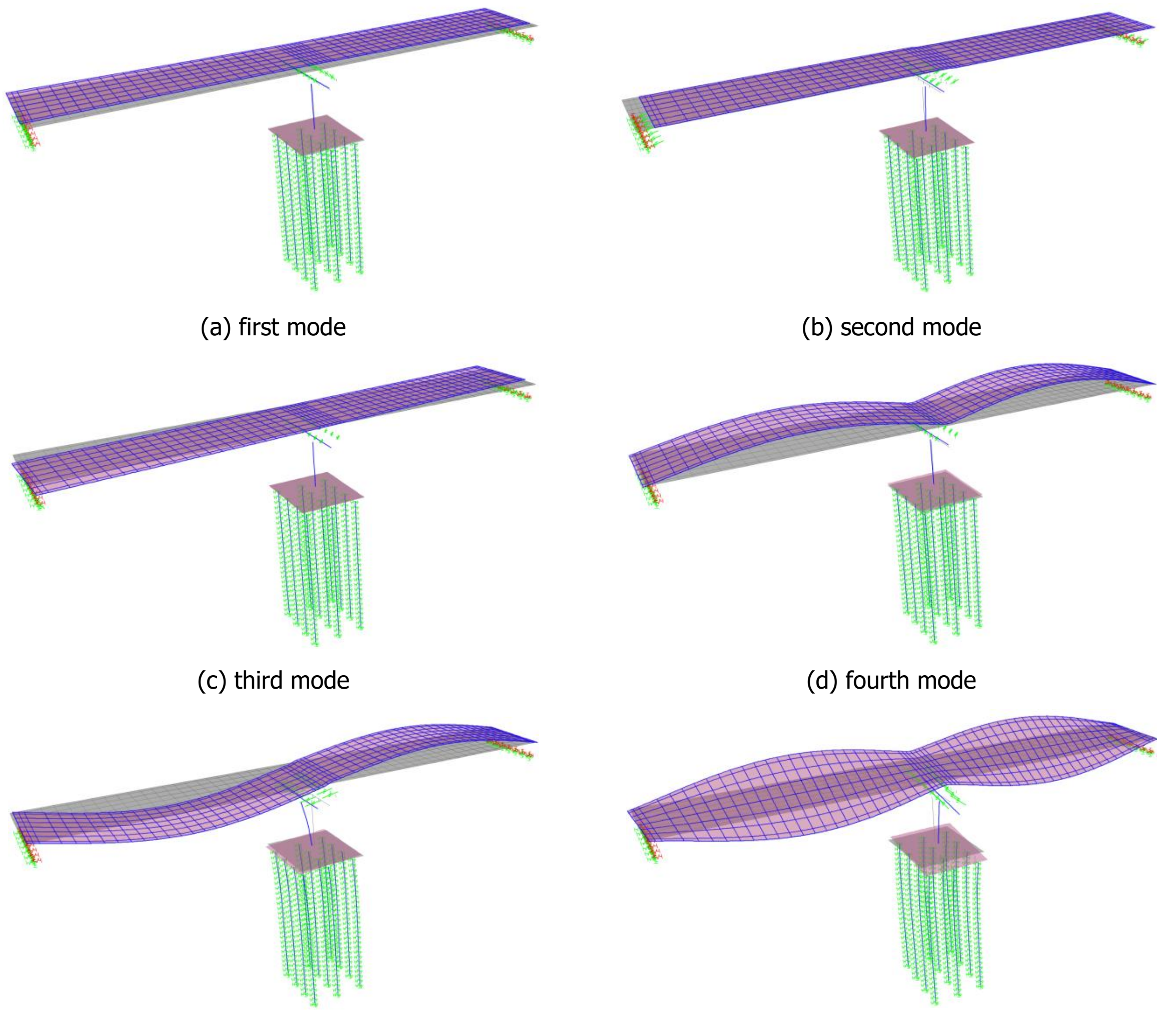

(a) first mode (b) second mode

(c) third mode (d) fourth mode

(e) fifth mode (f) sixth mode

Figure 6.1: Six first eigenmodes of the bridge

Σχήμα 6.1: Έξι πρώτες ιδιομορφές γέφυρας

6.4. Load Combinations at Ultimate Limit State (ULS)

The following load combination was considered at ULS for persistent and transient design situation:

$$\sum_{j\geq1}\gamma_{Gj}\cdot G_{kj}"+"\gamma_P\cdot P_k"+"\gamma_{Q1}\cdot Q_{k1}"+"\sum_{i\geq1}\gamma_{Qi}\cdot\psi_{0\iota}\cdot Q_{ki}$$

where the partial factors γ are listed in

Table **5.**6.2.

Table 6.2: Partial factors for actions in ULS

Πίνακας 6.2: Επιμέρους συντελεστές για δράσεις σε ΟΚΑ

Action	Contribution	Factor	S/V
Permanent actions	unfavourable	γ_{Gsup}	1.35
	favourable	γ_{Ginf}	1.00
Prestress	unfavourable	γ_P	1.00
	favourable	γ_P	1.00
Traffic loads	unfavourable	γ_Q	1.35
	favourable	γ_Q	0.00
Other variable actions	unfavourable	γ_Q	1.50
	favourable	γ_Q	0.00

S: Persistent design situation, V: Transient design situation

For the seismic design situation the following load combination at ULS was considered:

$$\sum_{j\geq1}\gamma_{Gj}\cdot G_{kj}"+"\gamma_P\cdot P_k"+"\psi_{21}\cdot Q_{1k}$$

where the partial factors ψ are listed in

Table **5.**6.3.

Table 6.3: Factors ψ for road bridges

Πίνακας 6.3: Συντελεστές ψ για οδογέφυρες

Actions	Symbol		ψ_0	ψ_2
Traffic load	Gr1 (LM1)	TS	0.75	0.20
		UDL	0.40	0.20
Thermal actions			0.60	0.50

Based on the above, the following ULS load combinations were considered:

<u>Persistent design situation</u>

1.35×LC1+ 1.35×LC2+1.35×LC3+1.35×maxLC(4-7)+1.35×maxLC(11-12) +1.50×0.60×maxLC(13-14)
(1.35×G_t+1.35×TS+1.35×UDL±1.35×Br+1.50×0.60×DT)

<u>Seismic design situation</u>

LC1+LC2+LC3+0.2×LC10±LC15±0.3×LC16±0.3×LC17 (G_t+0.2×Q±Ex±0.3Ey±0.3Ez)

LC1+LC2+LC3+0.2×LC10±0.3×LC15±LC16±0.3×LC17 ($G_t+0.2\times Q\pm 0.3Ex\pm Ey\pm 0.3Ez$)

LC1+LC2+LC3+0.2×LC10±0.3×LC15±0.3×LC16±LC17 ($G_t+0.2\times Q\pm 0.3Ex\pm 0.3Ey\pm Ez$)

6.5 Results

6.5.1. Piles' internal forces due to "Persistent design situation"

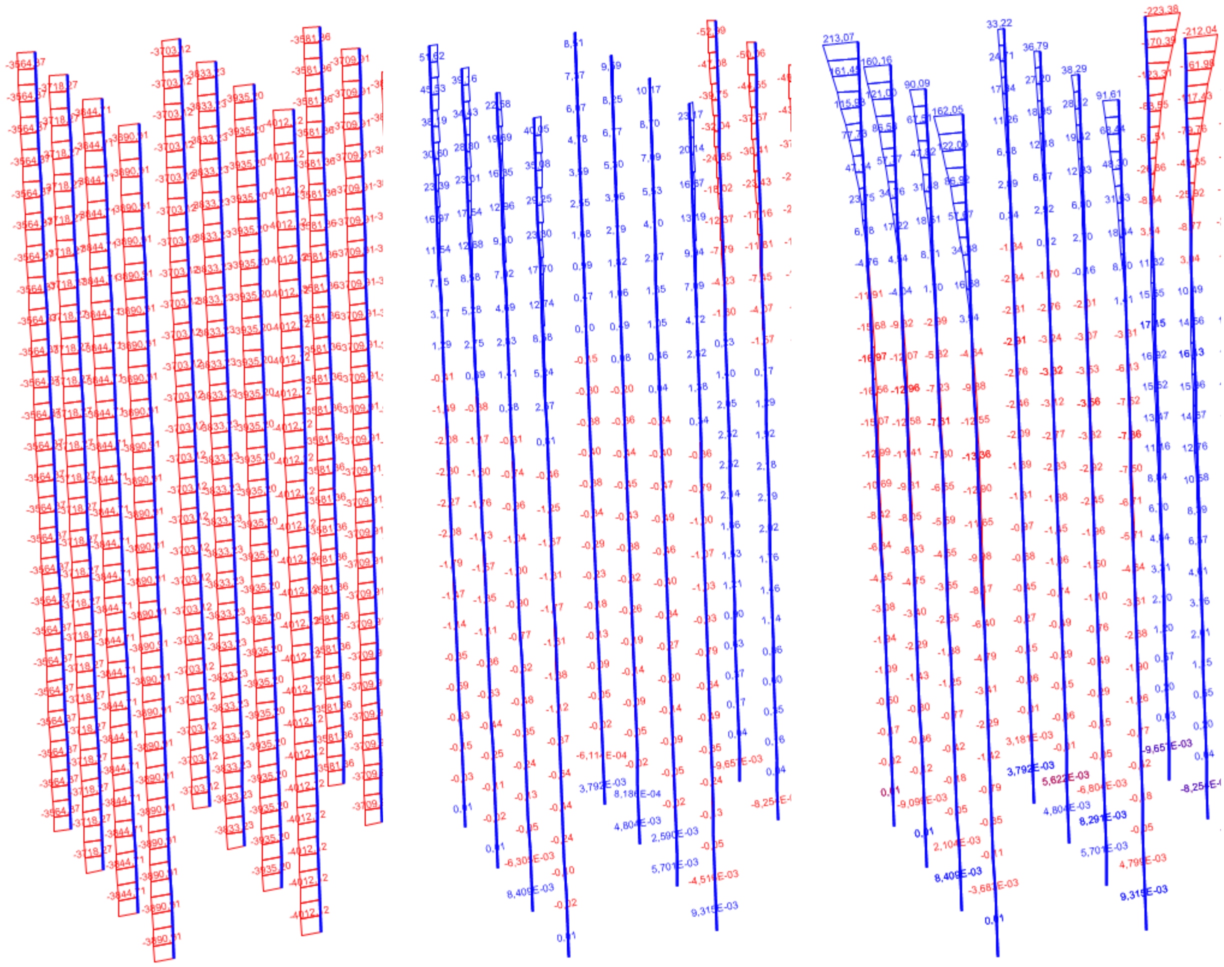

(a) (b) (c)

Figure 6.5: Piles internal forces due to persistent design situation: (a) normal forces N; (b) Shear forces V_x; (c) Moments M_y

Σχήμα 6.5: Εντατικά μεγέθη πασσάλων λόγω καταστάσεων σχεδιασμού με διάρκεια: (a) αξονικές δυνάμεις N, (b) Διατμητικές δυνάμεις V_x, (c) Ροπές M_y

6.5.2. Piles' internal forces due to "Seismic design situation" (q=1.0)

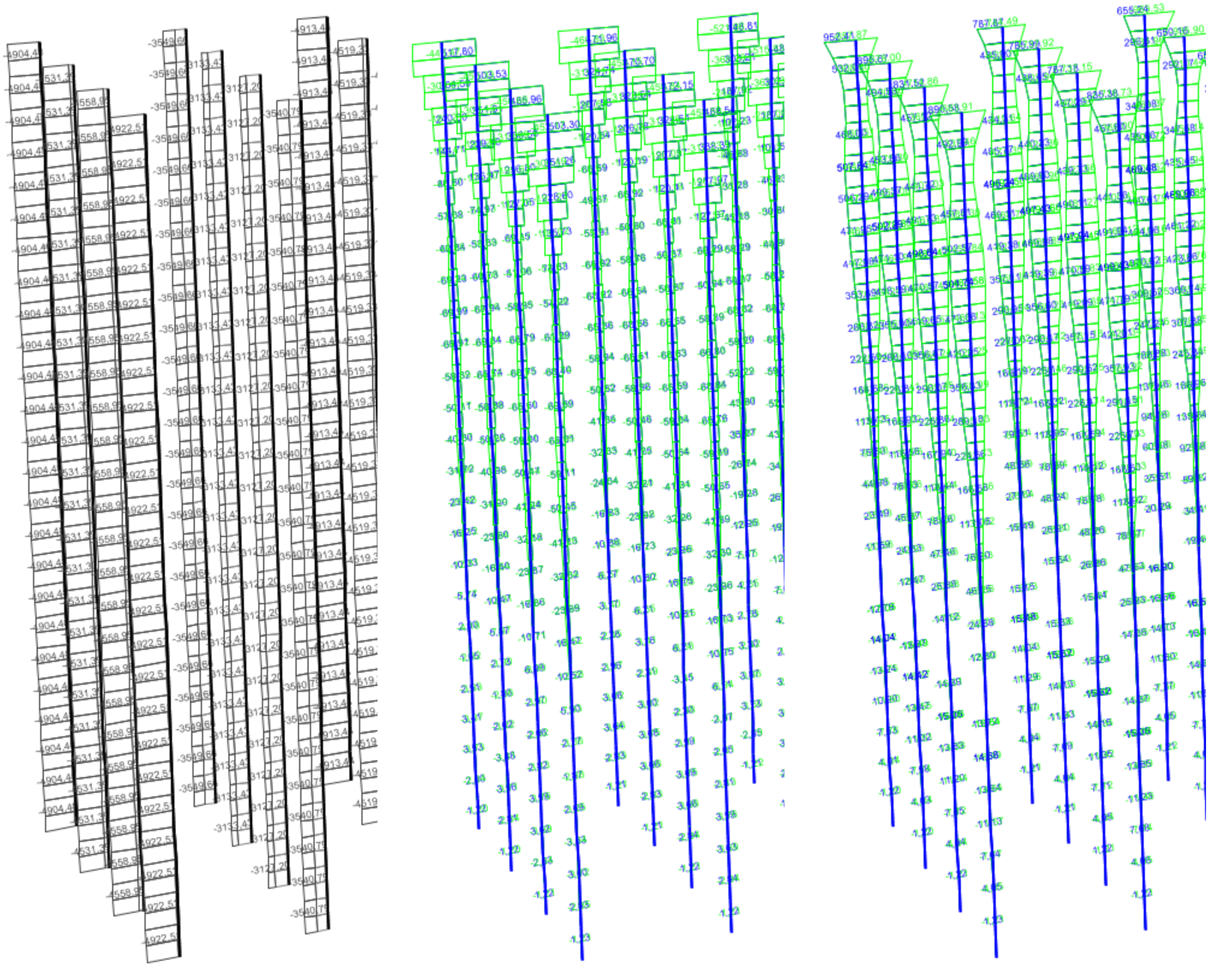

(a) (b) (c)

Figure 6.6: Piles internal forces for the most unfavorable seismic load combination (G_t+0.2Q+0.5DT'+Ex+0.3Ey-0.3Ez): (a) normal forces N; (b) Shear forces V_x ; (c) Moments M_y

Σχήμα 6.6: Εντατικά μεγέθη πασσάλων για το δυσμενέστερο σεισμικό συνδυασμό (G_t+0.2Q+0.5DT'+Ex+0.3Ey-0.3Ez): (a) αξονικές δυνάμεις N, (b) Διατμητικές δυνάμεις V_x , (c) Ροπές M_y

6.5.3. Pier's internal forces due to "Persistent design situation"

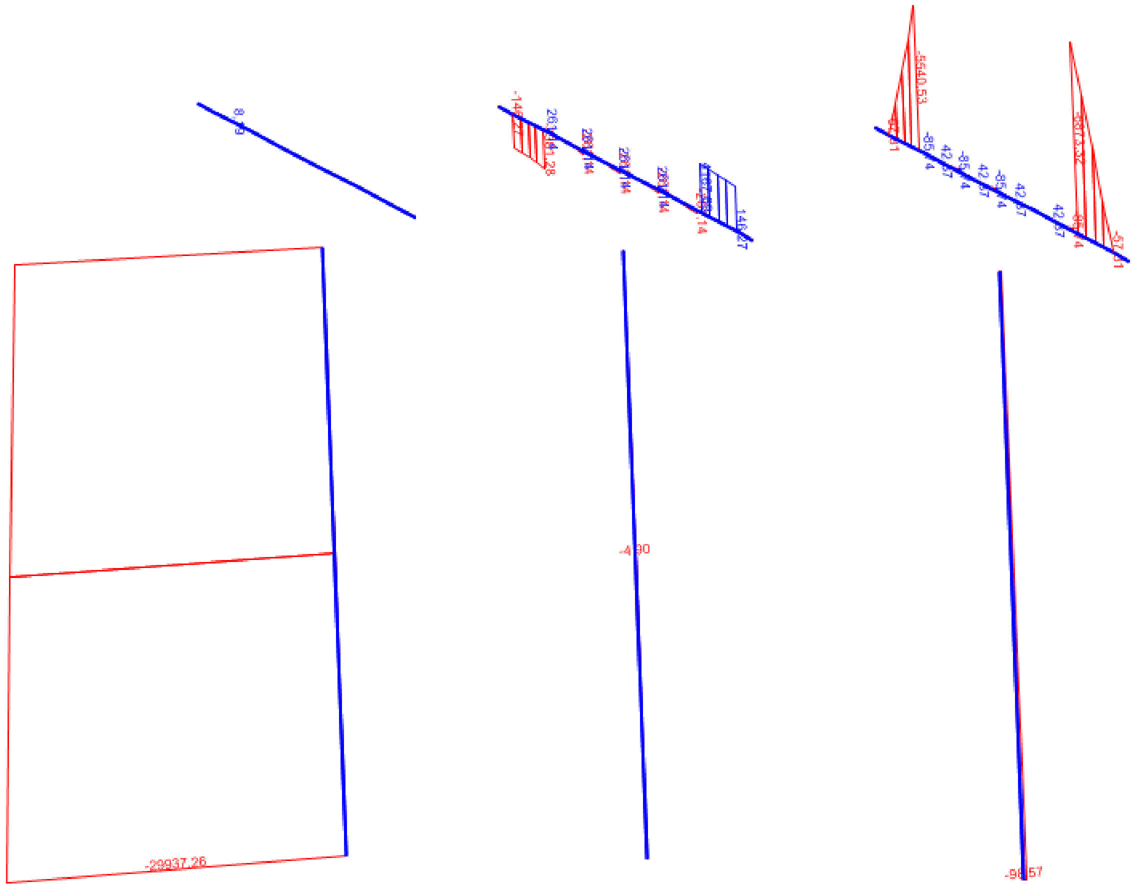

(a) (b) (c)

Figure 6.7: Pier internal forces due to persistent design situation: (a) normal forces N; (b) Shear forces V_x ; (c) Moments M_y

Σχήμα 6.7: Εντατικά μεγέθη στύλου μεσοβάθρου λόγω καταστάσεων σχεδιασμού με διάρκεια: (a) αξονικές δυνάμεις N, (b) Διατμητικές δυνάμεις V_x, (c) Ροπές M_y

6.5.4. Pier's internal forces due to "Seismic design situation"

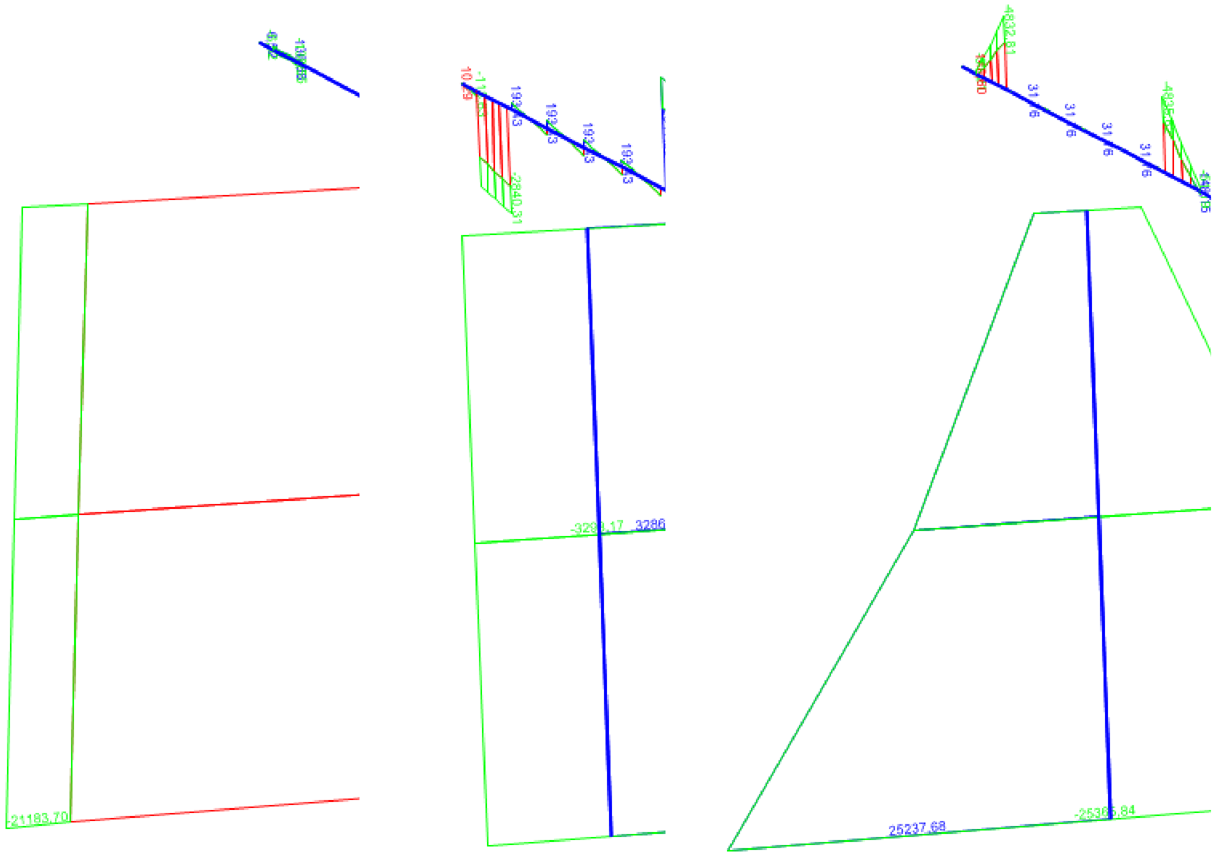

(a) (b) (c)

Figure 6.8: Pier internal forces for the most unfavorable seismic load combination (G_t+0.2Q+0.5DT'+Ex+0.3Ey-0.3Ez): (a) normal forces N; (b) Shear forces V_x ; (c) Moments M_y

Σχήμα 6.8: Εντατικά μεγέθη στύλου μεσοβάθρου για το δυσμενέστερο σεισμικό συνδυασμό (G_t+0.2Q+0.5DT'+Ex+0.3Ey-0.3Ez): (a) αξονικές δυνάμεις N, (b) Διατμητικές δυνάμεις V_x , (c) Ροπές M_y

6.6. Design of piles

6.6.1. Bearing capacity

According to the calculations presented in section 4.2, the bearing capacity of a single pile of diameter 1.0 m and length 25.00 m is 8.50 MN/2.00 = 4.25 MN for static loads and 8.50 MN/1.30 =6.54 MN for seismic loads. In these calculations, the considered safety factors were 2.00 for the static combinations and 1.30 for the seismic ones.

These values are compared with the maximum axial load at the top of the pier's piles (Figures 6.5 and 6.6):

Static combinations: minN = 4012 kN < 4250kN √

Seismic combinations: minN = 4923 kN < 6540kN √

6.6.2. Required reinforcements

Longitudinal reinforcement

Based on the results of the analyses, the max required longitudinal reinforcement of the piles for the most unfavorable seismic load combination (G_t+0.2Q+Ex+0.3Ey-0.3Ez), where P=-180.5kN, M_x=296.01kNm and M_y=952.41kNm, is equal to 48.8cm^2 (upper cross section). Taking under consideration that a minimum ratio of 1% is required by the Code, the piles' reinforcement was set to 16∅25 (78.56cm^2). This reinforcement was reduced to one half at the lower one half of the length of the piles (8∅25 = 39.3 cm^2).

Confining reinforcement

According to the results of the analyses, the max required shear reinforcement of the piles for the most unfavorable seismic load combination (G_t+0.2Q+Ex+0.3Ey-0.3Ez), where V_x=517.8kN and V_y=160.03kN, is equal to 7.5cm^2 (upper cross section). Nevertheless, the final ratio reinforcement is dictated by confining reasons.

For the most unfavorable load combination (G_t+0.2Q+Ex+Ey-0.3Ez), the maximum compressive load of the piles under seismic action is N_c=3295 kN.

Since

$$n_k = \frac{N_c}{f_{ck} A_c} = 4923 / (20000 \times 3.14 \times 1.0^2/4) = 0.31 > 0.08$$

i.e. the normalized axial force n_k exceeds the limit of 0.08, confining reinforcement should be provided. For spiral reinforcement:

$$\omega_{min} = 1.40 \cdot \frac{A_c}{A_{cc}} \cdot \lambda \cdot n_k \geq 0.18 = 1.40 \times 1.0^2 / 0.84^2 \times 0.37 \times 0.31 = 0.17 < 0.18 \rightarrow \omega = 0.18$$

The required confining reinforcement is defined by the mechanical reinforcement ratio which is:

$$\min \rho_w = \omega_{min} \frac{f_{cd}}{f_{yd}} \Rightarrow \min \rho_w = 0.18 \times \frac{\frac{20 \times 10^3}{1.5}}{\frac{500 \times 10^3}{1.15}} \Rightarrow \min\rho_w = 0.0055$$

A spiral ∅12/9 (25.1cm^2) is used accounting for a volumetric ratio equal to:

$$\rho_w = \frac{4A_{sp}}{D_{sp}s_L} = 4 \times 1.13\ cm^2 / (84\ cm \times 9\ cm) \Rightarrow \rho_w = 0.006 > min\rho_w$$

The spacing of the spiral should satisfy the limits:

$s_L = 9$ cm $< 6d_{bL} = 6 \times 2.5$ cm $= 15$ cm (where d_{bL} is the longitudinal bar diameter) and

$s_L = 9$ cm $< D_{cc}/5 = 84$ cm $/ 5 = 16.8$ cm (where D_{cc} is the diameter of the confined concrete core).

The required longitudinal and shear reinforcement of the pier is presented in Figure 6.9.

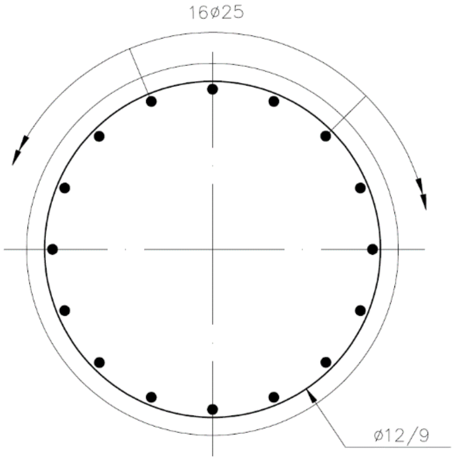

Figure 6.9: Pile reinforcement (upper section)
Σχήμα 6.9: Οπλισμός πασσάλων (διατομή άνω)

6.7. Design of the pier

According to the results of the calculations, for the base section of the pier and for the most unfavorable seismic load combination (G_t+0.2Q+Ex+0.3Ey-0.3Ez), it is: P=-17891.3kN, M_x=12963.8kNm, M_y=25237.7kNm, V_x=3286.8kN and V_y=1093.7kN. The max required longitudinal reinforcement of the base section for this case is 486.1 cm^2, which was finally set to 104Φ25 (510.6 cm^2). The required longitudinal and shear reinforcement of the pier is presented in Figure 6.10.

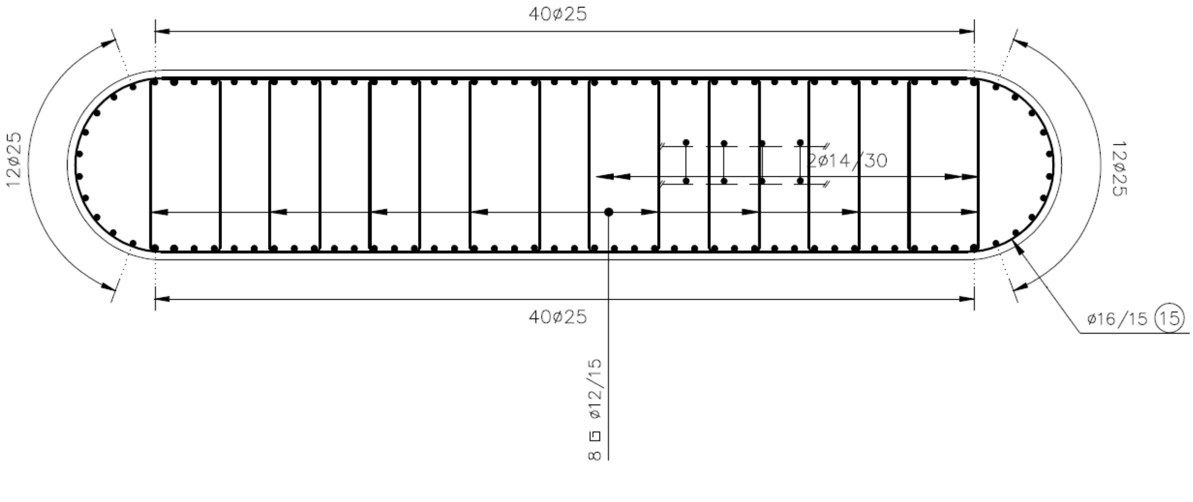

Figure 6.10: Pier reinforcement (base section)
Σχήμα 6.10: Οπλισμός μεσοβάθρου (διατομή βάσης)

6.8. Design of the pilecap

The required reinforcements of the pilecap against static and seismic actions are presented in Figure 6.11, where the main direction is parallel to the longitudinal direction of the pilecap and the cross one is parallel to the lateral one. A reinforcement grid of Φ20/10 is used for the upper reinforcement of the pilecap while a double reinforcement grid of Φ20/10 is used for the lower one.

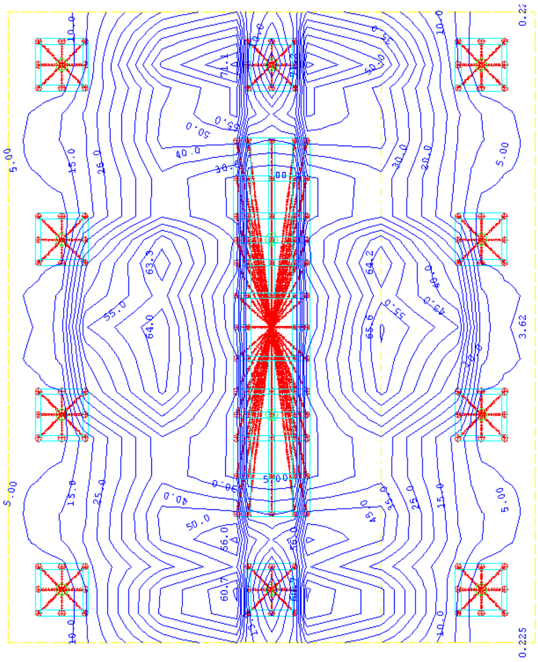

(a) Bottom cross reinforcements

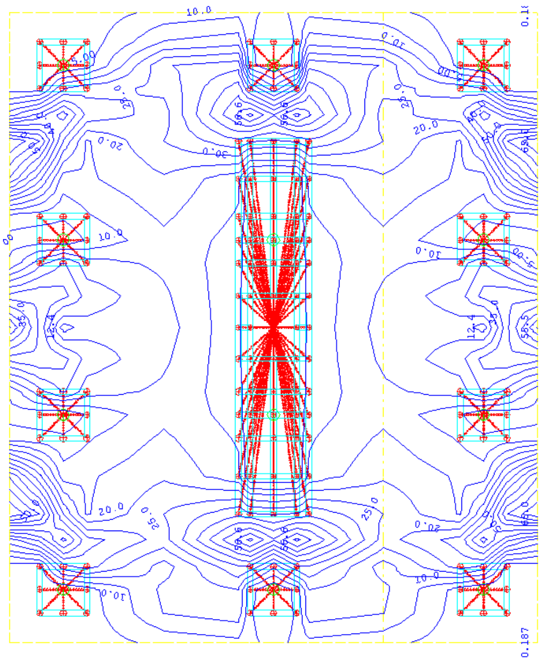

(b) Bottom main reinforcements

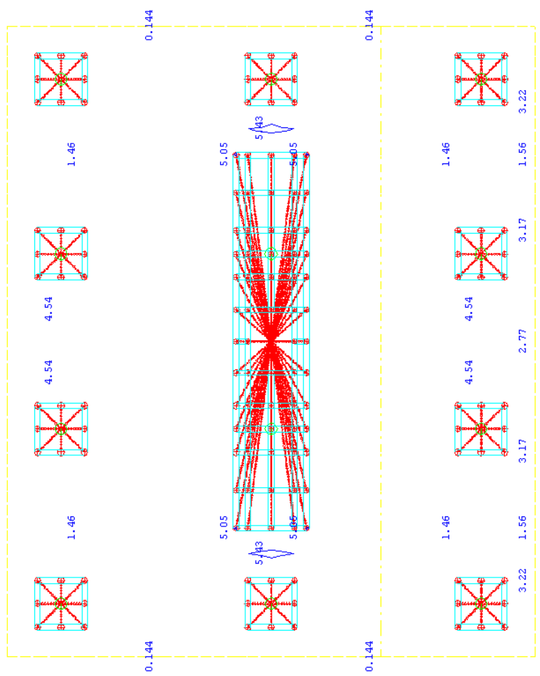

(a) Top cross reinforcements

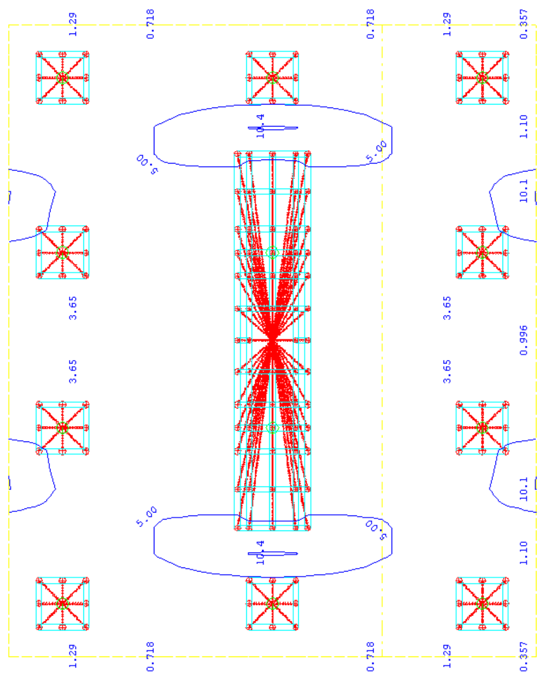

(b) Top main reinforcements

Figure 6.11: Pilecap reinforcement
Σχήμα 6.11: Οπλισμός κεφαλοδέσμου πασσάλων

7. DESIGN OF BEARINGS AND EXPANSION JOINTS

7.1. Abutment's bearings

1. CHECK OF BEARINGS FOR SEISMIC CONDITIONS

(ACCORDING TO EC8)

ABUTMENT

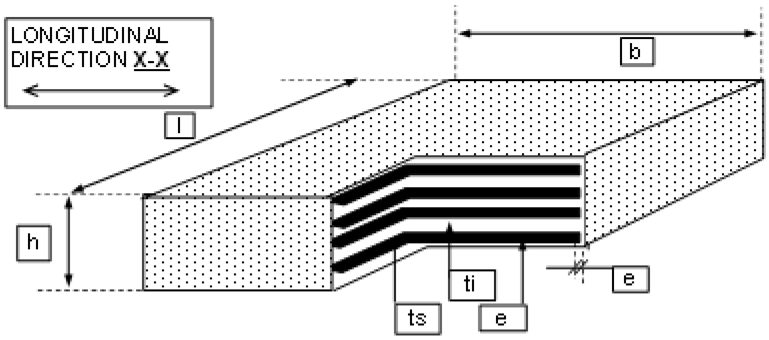

1. Geometrical characteristics

Width	b =	400	mm
Length	l =	500	mm
Overall thickness of bearing	h =	201	mm
Thickness of external rubber layer	t_o =	0	mm
Thickness of internal rubber layer	t_i =	11	mm
No of internal rubber layers		11	
No of external rubber layers		0	
Thickness of steel plate	t_s =	4	mm
No of steel plates		10	
Effective rubber thickness	Σt_i =	121	mm
Effective plan area of bearing	A_r=	195525	mm^2
Shape coefficient	S =	10,10	
Failure elongation	V_{bu} =	5	
Shear modulus G	G =	1,125	MPa
Horizontal stiffness of the bearing	K_h =	1817,9	KN / m
Vertical stiffness of the bearing	K_v=	720616	KN / m
Rotational stiffness of the bearing	$K\varphi_{yy}$=	7868	KNm/rad
Rotational stiffness of the bearing	$K\varphi_{xx}$=	19210	KNm/rad

2 . Loads - displacements - rotations

2.1 Vertical loads (Compression positive)

Dead loads	R_g =	796,17	KN
Super dead loads	R_{go} =	210,39	KN
Prestress and prestress losses	R_p =	0,00	KN
Live loads (MAX)	R_q =	463,96	KN
Uniform road traffic loads	R_{qo}=	163,92	KN
Longitudinal earthquake	RE_{Qxx}=	108,10	KN
Lateral earthquake	RE_{Qyy}=	304,96	KN
Vertical earthquake	RE_{Qzz}=	327,00	KN
Live loads (MIN)	R_q =	0,00	KN

2.2 Displacements

Displacement x-x			
Displacement due to dead load	d_{B1x}=	-3,50	mm
Displacement due to uniform road traffic loads	d_{B2x}=	-0,57	mm
Displacement due to creep and shrinkage	d_{B3x} =	12,71	mm
Displacement due to temperature	d_{Tx} =	14,36	mm
Displacement y-y			
Displacement due to dead load	d_{B1y}=	0,00	mm
Displacement due to uniform road traffic loads	d_{B2y}=	0,00	mm
Displacement due to creep and shrinkage	d_{B3y} =	0,00	mm
Displacement due to temperature	d_{Ty} =	0,00	mm

2.3 Rotations

Rotation αx			
Rotation due to dead load	α_{B1x}=	0,00	$x10^{-3}$rad
Rotation due to uniform road traffic loads	α_{B2x}=	0,00	$x10^{-3}$rad
Rotation due to creep and shrinkage	α_{B3x} =	0,00	$x10^{-3}$rad
Rotation due to temperature	α_{Tx} =	0,00	$x10^{-3}$rad
Rotation αy			
Rotation due to dead load	α_{B1y}=	4,55	$x10^{-3}$rad
Rotation due to uniform road traffic loads	α_{B2y}=	0,87	$x10^{-3}$rad
Rotation due to creep and shrinkage	α_{B3y} =	0,00	$x10^{-3}$rad
Rotation due to temperature	α_{Ty} =	0,00	$x10^{-3}$rad

3. Check in direction X-X (LONGITUDINAL DIRECTION)

3.1 Max displacements and rotations of bearing

From dynamic analysis	ds_{dx} =	209,10	mm
	ds_{dy} =	57,09	mm
Design displacement x-x	d_{Edx}=	224,92	mm
Design displacement y-y	d_{Edy}=	57,09	mm
	d_{Ed} =	232,05	mm
From dynamic analysis	α_{sx}=	0,00	$x10^{-3}$rad
	α_{sy}=	0,82	$x10^{-3}$rad
Design rotation αx	α_{Edx}=	0,00	$x10^{-3}$rad
Design rotation αy	α_{Edy}=	6,24	$x10^{-3}$rad

3.2 Design shear strain due to horizontal displacement

CHECK $\varepsilon_{q,d}= dE_d / \Sigma t_r < 2.0$ $\varepsilon_{q,d}$= **1,92 < 2,0 O.K**

3.3 Design shear strain due to compressive load

Seismic design displacement	d_{Ed} =	232,05	mm
Effective area of bearing in x-x	A_r=	94328	mm2
Max compressive load for the design earthquake	N_{sd} =	1337,0	KN
Max effective normal stress	σ_e =	14174	KN/m²
Shear modulus	G =	1,125	MPa
Deformation due to vertical loads	$\varepsilon_{c,d}$=1.5σ_e/SG=	**1,871**	

3.4 Design shear strain due to angular distortion

$\varepsilon_{\alpha,d} = (l^2 \alpha_x + b^2 \alpha_y)\, t_i / 2\Sigma t_i^3$ — $\varepsilon_{\alpha,d} =$ 0,375

CHECK Max design strain: $\varepsilon_{q,d}+\varepsilon_{c,d}+\varepsilon_{\alpha,d}<\varepsilon_{u,d}$ — **4,164 < 7,0 O.K**

3.5 Check against slip (anchorage)

Max shear force	V_{Ed} =	421,85 KN
Min vertical design force	N_{Ed} =	741,7 KN
CHECK $\sigma_e = N_{Ed} / A_r$ > = 3,0 MPa	=	7,86 > 3,0 O.K
V_{Ed} / N_{Ed}	=	0,57
$\alpha+\beta/\sigma_e$=0,10 + 1,5x0,6 / σ_e =	=	0,21
CHECK V_{Ed}/N_{Ed}<=0,10+0,9/σ_e	ANCHORAGE	FOR BEARINGS WITH EXTERNAL RUBBER LAYER
$\alpha+\beta/\sigma_e$=0,50 + 1,5x0,6 / σ_e =	=	0,61
CHECK V_{Ed}/N_{Ed}<=0,50+0,9/σ_e	O.K.	FOR BEARINGS WITH EXTERNAL STRIPED PLATES

3.6 Check against buckling

Max vertical design force	N_{Ed} =	1337,0 kN
$\sigma_e = N_{Ed} / A_r$	=	14,17 kN
2 min(b,l) G S / 3 Σti	=	25,04 kN
CHECK $\sigma_{e,d}$<2 min(b,l) G S / 3 Σt_i		O.K.

4. Check in direction Y-Y (LATERAL DIRECTION)

4.1 Max displacement of bearing

From dynamic analysis	ds_{dx} =	62,74 mm
	ds_{dy} =	190,31 mm
Design displacement x-x	d_{Edx}=	78,56
Design displacement y-y	d_{Edy}=	190,31 mm
	d_{Ed} =	205,89 mm
From dynamic analysis	α_{sx}=	0,28 $x10^{-3}$rad
	α_{sy}=	0,95 $x10^{-3}$rad
Design rotation αx	α_{Edx}=	0,28 $x10^{-3}$rad
Design rotation αy	α_{Edy}=	6,37 $x10^{-3}$rad

4.2 Design shear strain due to horizontal displacement

CHECK $\varepsilon_{q,d} = dE_d / \Sigma t_i < 2.0$ = **1,70 < 2.0 O.K**

4.3 Design shear strain due to compressive load

Seismic design displacement	d_{Ed} =	205,89 mm
Effective area of bearing in x-x	A_r=	88372 mm²
Max compressive load for the design earthquake	N_{sd} =	1474,8 KN
Max effective normal stress	σ_e =	16689 KN/m²

Shear modulus	$G =$	1,125 MPa
Deformation due to vertical loads	$\varepsilon_{c,d}=1.5\sigma_e/SG=$	**2,203**

4.4 Design shear strain due to angular distortion

$\varepsilon_{a,d} = (l^2\,\alpha_x + b^2\,\alpha_y)\,t_i\,/\,2\Sigma t_i^3$	$\varepsilon_{a,d}=$	**0,409**
CHECK Max design strain: $\varepsilon_{q,d}+\varepsilon_{c,d}+\varepsilon_{a,d}<\varepsilon_{u,d}$		**4,314 < 7,0 O.K**

4.5 Check against slip (anchorage)

Max shear force	$V_{Ed} =$	374,28 KN	
Min vertical design force	$N_{Ed} =$	603,9 KN	
CHECK $\sigma_e = N_{Ed}\,/\,A_r\ >= 3{,}0$ **MPa**	=	**6,83 > 3,0 O.K**	
$V_{Ed}\,/\,N_{Ed}$	=	0,62	
$\alpha+\beta/\sigma_e$=0,10 + 1,5x0,6 / σ_e =	=	0,23	
CHECK V_{Ed}/N_{Ed}<=0,10+0,9/σ_e		ANCHORAGE	FOR BEARINGS WITH EXTERNAL RUBBER LAYER
$\alpha+\beta/\sigma_e$=0,50 + 1,5x0,6 / σ_e =	=	0,63	
CHECK V_{Ed}/N_{Ed}<=0,50+0,9/σ_e		O .K	FOR BEARINGS WITH EXTERNAL STRIPED PLATES

4.6 Check against buckling

Max vertical design force	$N_{Ed} =$	1474,8 kN
$\sigma_e = N_{Ed}\,/\,A_r$	=	16,69 kN
2 min(b,l) G S / 3 Σti	=	25,04 kN
CHECK $\sigma_{e,d}$<2 min(b,l) G S / 3 Σt_i		**O.K.**

2. CHECK OF BEARINGS FOR STATIC CONDITIONS
(ACCORDING TO DIN 4141)

Dimensions of bearing	b=	400	mm
	l=	500	mm
Overall rubber thickness	Σt_i=	**121**	mm
Bearing area	A_e=	195525	mm^2
Total displacement : dG+1,5*0,6*dDT+1,5dbr=	**u=**	**41,78**	mm
Max vertical load	**Pmax=**	1470,5	KN
Min vertical load	**Pmin=**	1006,56	
Για Σt_i<=b/5 --> $\tan\gamma_{\varepsilon\pi\iota\tau}$=0.70	$\tan\gamma_{\varepsilon\pi\iota\tau}$=	–	
Για Σt_i>=b/5 --> $\tan\gamma_{\varepsilon\pi\iota\tau}$=0.70-[($\Sigma t_i$/b)-0.2]	$\tan\gamma_{\varepsilon\pi\iota\tau}$=	**0,5975**	
	$\tan\gamma=u/\Sigma t_i$	**0,345**	**O.K**
Max normal stress of bearing : σ_{max}=P/A=	σ_{max}=	**7,52**	**< 15,0 MPa**
Min normal stress of bearing : σ_{min}=P/A=	σ_{min}=	**5,15**	**> 5,0 Mpa**

7.2. Pier's bearings

1. CHECK OF BEARINGS FOR SEISMIC CONDITIONS
(ACCORDING TO EC8)

PIER

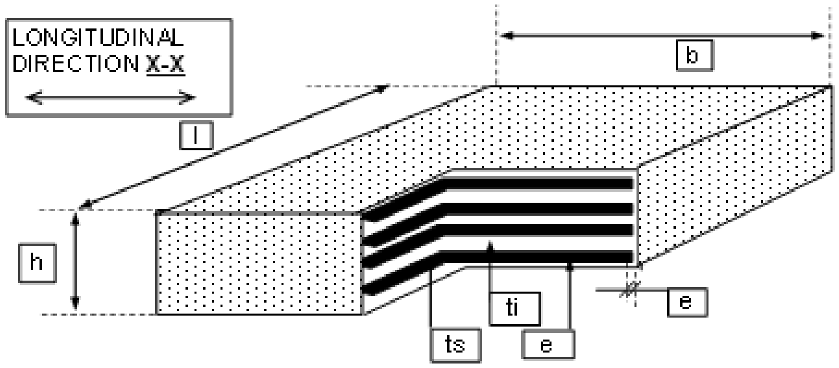

1 . Geometrical characteristics

Width	b =	350	mm
Length	l =	450	mm
Overall thickness of bearing	h =	171	mm
Thickness of external rubber layer	t_o =	0	mm
Thickness of internal rubber layer	t_i =	11	mm
No of internal rubber layers		9	
No of external rubber layers		0	
Thickness of steel plate	t_s =	4	mm
No of steel plates		8	
Effective rubber thickness	Σt_i =	99	mm
Effective plan area of bearing	A_e=	153525	mm^2
Shape coefficient	S =	8,95	
Failure elongation	V_{bu} =	5	
Shear modulus G	G =	1,125	MPa
Horizontal stiffness of the bearing	K_h =	1744,6	KN / m
Vertical stiffness of the bearing	K_v=	570144	KN / m
Rotational stiffness of the bearing	$K\varphi_{yy}$=	4439	KNm/rad
Rotational stiffness of the bearing	$K\varphi_{xx}$=	12131	KNm/rad

2 . Loads - displacements - rotations

2.1 Vertical loads (Compression positive)

Dead loads	R_g =	785,23	KN
Super dead loads	R_{go} =	213,92	KN
Prestress and prestress losses	R_p =	0,00	KN
Live loads (MAX)	R_q =	374,64	KN
Uniform road traffic loads	R_{qo}=	167,50	KN
Longitudinal earthquake	RE_{Qxx}=	313,26	KN
Lateral earthquake	RE_{Qyy}=	258,63	KN
Vertical earthquake	RE_{Qzz}=	325,18	KN
Live loads (MIN)	R_q =	0,00	KN

2.2 Displacements

Displacement x-x

Displacement due to dead load	$d_{\beta 1x}=$	7,89	mm
Displacement due to uniform road traffic loads	$d_{\beta 2x}=$	1,75	mm
Displacement due to creep and shrinkage	$d_{\beta 3x}=$	0,34	mm
Displacement due to temperature	$d_{Tx}=$	0,40	mm

Displacement y-y

Displacement due to dead load	$d_{\beta 1y}=$	0,00	mm
Displacement due to uniform road traffic loads	$d_{\beta 2y}=$	0,00	mm
Displacement due to creep and shrinkage	$d_{\beta 3y}=$	0,00	mm
Displacement due to temperature	$d_{Ty}=$	1,84	mm

2.3 Rotations

Rotation αx

Rotation due to dead load	$\alpha_{\beta 1x}=$	0,09	$x10^{-3}$rad
Rotation due to uniform road traffic loads	$\alpha_{\beta 2x}=$	0,04	$x10^{-3}$rad
Rotation due to creep and shrinkage	$\alpha_{\beta 3x}=$	0,00	$x10^{-3}$rad
Rotation due to temperature	$\alpha_{Tx}=$	0,00	$x10^{-3}$rad

Rotation αy

Rotation due to dead load	$\alpha_{\beta 1y}=$	-3,65	$x10^{-3}$rad
Rotation due to uniform road traffic loads	$\alpha_{\beta 2y}=$	-0,79	$x10^{-3}$rad
Rotation due to creep and shrinkage	$\alpha_{\beta 3y}=$	0,00	$x10^{-3}$rad
Rotation due to temperature	$\alpha_{Ty}=$	0,00	$x10^{-3}$rad

3. Check in direction X-X (LONGITUDINAL DIRECTION)

3.1 Max displacements and rotations of bearing

From dynamic analysis	$ds_{dx}=$	163,46	mm
	$ds_{dy}=$	53,69	mm
Design displacement x-x	$d_{Edx}=$	173,64	mm
Design displacement y-y	$d_{Edy}=$	54,61	mm
	$d_{Ed}=$	182,03	mm
From dynamic analysis	$\alpha_{sx}=$	0,00	$x10^{-3}$rad
	$\alpha_{sy}=$	5,84	$x10^{-3}$rad
Design rotation αx	$\alpha_{Edx}=$	0,13	$x10^{-3}$rad
Design rotation αy	$\alpha_{Edy}=$	10,28	$x10^{-3}$rad

3.2 Design shear strain due to horizontal displacement

CHECK $\varepsilon_{q,d}= dE_d / \Sigma t_r < 2.0$ $\varepsilon_{q,d}=$ **1,84 < 2,0 O.K**

3.3 Design shear strain due to compressive load

Seismic design displacement	$d_{Ed}=$	182,03	mm
Effective area of bearing in x-x	$A_r=$	81634	mm2
Max compressive load for the design earthquake	$N_{sd}=$	1521,1	KN
Max effective normal stress	$\sigma_e=$	18633	KN/m²
Shear modulus	$G=$	1,125	MPa
Deformation due to vertical loads	$\varepsilon_{c,d}=1.5\sigma_e/SG=$	**2,776**	

3.4 Design shear strain due to angular distortion

$\varepsilon_{\alpha,d} = (l^2 \alpha_x + b^2 \alpha_y)\, t_i / 2\Sigma t_i^3$	$\varepsilon_{\alpha,d}$=	0,590
CHECK Max design strain: $\varepsilon_{q,d}+\varepsilon_{c,d}+\varepsilon_{\alpha,d}<\varepsilon_{u,d}$		5,205 < 7,0 O.K

3.5 Check against slip (anchorage)

Max shear force	V_{Ed} =	317,56	KN
Min vertical design force	N_{Ed} =	544,2	KN
CHECK $\sigma_e = N_{Ed} / A_r$ >= 3,0 MPa	=	6,67 > 3,0 O.K	
V_{Ed} / N_{Ed}	=	0,58	
$\alpha+\beta/\sigma_e$=0,10 + 1,5x0,6 / σ_e =	=	0,23	
CHECK V_{Ed}/N_{Ed}<=0,10+0,9/σ_e		ANCHORAGE	FOR BEARINGS WITH EXTERNAL RUBBER LAYER
$\alpha+\beta/\sigma_e$=0,50 + 1,5x0,6 / σ_e =	=	0,63	
CHECK V_{Ed}/N_{Ed}<=0,50+0,9/σ_e		O.K.	FOR BEARINGS WITH EXTERNAL STRIPED PLATES

3.6 Check against buckling

Max vertical design force	N_{Ed} =	1521,1	kN
$\sigma_e = N_{Ed} / A_r$	=	18,63	kN
2 min(b,l) G S / 3 Σti	=	23,73	kN
CHECK $\sigma_{e,d}$<2 min(b,l) G S / 3 Σt_i		O.K.	

4. Check in direction Y-Y (LATERAL DIRECTION)

4.1 Max displacement of bearing

From dynamic analysis	ds_{dx} =	49,04	mm
	ds_{dy} =	178,98	mm
Design displacement x-x	d_{Edx}=	59,22	
Design displacement y-y	d_{Edy}=	179,90	mm
	d_{Ed} =	189,40	mm
From dynamic analysis	α_{sx}=	0,18	$x10^{-3}$rad
	α_{sy}=	0,99	$x10^{-3}$rad
Design rotation αx	α_{Edx}=	0,31	$x10^{-3}$rad
Design rotation αy	α_{Edy}=	5,43	$x10^{-3}$rad

4.2 Design shear strain due to horizontal displacement

CHECK $\varepsilon_{q,d}$= $dE_d / \Sigma t_i$<2.0	=	1,91 < 2.0 O.K

4.3 Design shear strain due to compressive load

Seismic design displacement	d_{Ed} =	189,40	mm
Effective area of bearing in x-x	A_r=	66472	mm²
Max compressive load for the design earthquake	N_{sd} =	1482,8	KN
Max effective normal stress	σ_e =	22307	KN/m²

Shear modulus — $G =$ 1,125 MPa

Deformation due to vertical loads — $\varepsilon_{c,d}=1.5\sigma_e/SG=$ **3,324**

4.4 Design shear strain due to angular distortion

$\varepsilon_{a,d} = (l^2\,\alpha_x + b^2\,\alpha_y)\,t_i \,/\, 2\Sigma t_i^3$ — $\varepsilon_{a,d}=$ **0,334**

CHECK Max design strain: $\varepsilon_{q,d}+\varepsilon_{c,d}+\varepsilon_{a,d}<\varepsilon_{u,d}$ — **5,571 < 7,0 O.K**

4.5 Check against slip (anchorage)

Max shear force — $V_{Ed} =$ 330,42 KN

Min vertical design force — $N_{Ed} =$ 582,5 KN

CHECK $\sigma_e = N_{Ed} / A_r >= 3{,}0$ MPa — = **8,76 > 3,0 O.K**

V_{Ed} / N_{Ed} — = 0,57

$\alpha+\beta/\sigma_e$=0,10 + 1,5x0,6 / σ_e = — = 0,20

CHECK V_{Ed}/N_{Ed}<=0,10+0,9/σ_e — ANCHORAGE — FOR BEARINGS WITH EXTERNAL RUBBER LAYER

$\alpha+\beta/\sigma_e$=0,50 + 1,5x0,6 / σ_e = — = 0,60

CHECK V_{Ed}/N_{Ed}<=0,50+0,9/σ_e — **O . K** — FOR BEARINGS WITH EXTERNAL STRIPED PLATES

4.6 Check against buckling

Max vertical design force — $N_{Ed} =$ 1482,8 kN

$\sigma_e = N_{Ed} / A_r$ — = 22,31 kN

2 min(b,l) G S / 3 Σti — = 23,73 kN

CHECK $\sigma_{e,d}$<2 min(b,l) G S / 3 Σt_i — **O.K.**

. CHECK OF BEARINGS FOR STATIC CONDITIONS
(ACCORDING TO DIN 4141)

Dimensions of bearing	b=	350	mm
	l=	450	mm
Overall rubber thickness	Σt_i=	**99**	mm
Bearing area	A_e=	153525	mm^2
Total displacement : dG+1,5*0,6*dDT+1,5dbr=	u=	**22,24**	mm
Max vertical load	Pmax=	1373,8	KN
Min vertical load	Pmin=	999,15	
Για Σt_i<=b/5 --> $\tan\gamma_{\epsilon\pi\iota\tau}$=0.70	$\tan\gamma_{\epsilon\pi\iota\tau}$=	–	
Για Σt_i>=b/5 --> $\tan\gamma_{\epsilon\pi\iota\tau}$=0.70-[($\Sigma t$/b)-0.2]	$\tan\gamma_{\epsilon\pi\iota\tau}$=	**0,617143**	
	$\tan\gamma=u/\Sigma t_i$	**0,225**	**O.K**
Max normal stress of bearing : σ_{max}=P/A=	σ_{max}=	**8,95**	**< 15,0 MPa**
Min normal stress of bearing : σ_{min}=P/A=	σ_{min}=	**6,51**	**> 5,0 Mpa**

7.3. Expansion joints

CHECK OF EXPANSION JOINTS

A) SEISMIC CONDITIONS

Design displacement for the loading direction i-i

$$d_{Edi}=\pm 0.4d_E+d_G\pm 0.5d_T$$

where:

d_E= Design seismic displacement

and $d_E=(d^2_{E1}+d^2_{E2})^{1/2}$ max relative displacement between two statically independent sections 1 and 2

d_G= Displacement of permanent or quasi-permanent actions (creep, shrinkage)

d_T= Displacement due to temperature actions (DT=-37/+57°C)

$$d_{Ed}=(d^2_{Edi}+d^2_{Edj})^{1/2}$$

where: d_{Edi} design displacement in main loading direction (i - i) and

d_{Edj} 30% of the design displacement in the lateral direction (j -j)

		OPENING	CLOSURE	GAP
● CHECK				
In direction x-x				
	d_{E1}=	222,44 mm	-222,44	
	d_{E2}=	0,00 mm	0,00	
	d_E=	222,44 mm	-222,44	
	dG=	20,47 mm	0,00	
	dT=	15,63 mm	-24,10	
$d_{Edx}=0.4d_E+d_G+0.5d_T$=		117,26 mm	-101,03 mm	250,73
In direction y - y				
	d_{E1}=	217,91 mm	-217,91	
	d_{E2}=	0,00 mm	0,00	
	d_E=	217,91 mm	-217,91	
	dG=	0,00 mm	0,00	
	dT=	0,00 mm	0,00	
$d_{Edy}=0.4d_E+d_G+0.5d_T$=		87,16 mm	-87,16 mm	217,91
Finally	$d_{Ed}=((0,3*d_{Edx})^2+d^2_{Edy})^{1/2}$=	94,00 mm	-92,28 mm	230,53
	$d_{Ed}=(d^2_{Edx}+(0,3*d_{Edy})^2)^{1/2}$=	120,14 mm	-104,36 mm	259,11

B) STATIC CONDITIONS

Design displacement for the loading direction i-i: **d=dG+-1,5*0,6*dT+1,5*dbr**

d_G= **Displacement of permanent or quasi-permanent actions**

d_T= **Displacement due to temperature actions (DT=-37/+57°C)**

d_{br}= **Displacement due to braking**

		OPENING	CLOSURE
● CHECK			
In direction x-x			
	d_{br}=	13,94 mm	-9,10
	dG=	20,47 mm	0,00
	dT=	15,63 mm	-24,10
d=dG+-1,5*0,6*dT+1,5*Dbr=		55,45 mm	-35,34 mm

An expansion joint type Algaflex or similar is chosen: **T 250** (+ - 125 mm)

PART B:

INNOVATIVE DESIGN OF THE BRIDGE

8. INTRODUCTION

8.1. Generally

In this part, the static and seismic design of the bridge will be repeated with a new methodology - that of "natural" seismic isolation (i.e. shallow foundation and partial improvement, of the top part only of the liquefiable soil), in connection with the allowable foundation movements which were established in work task 1 (see Deliverable D6a).

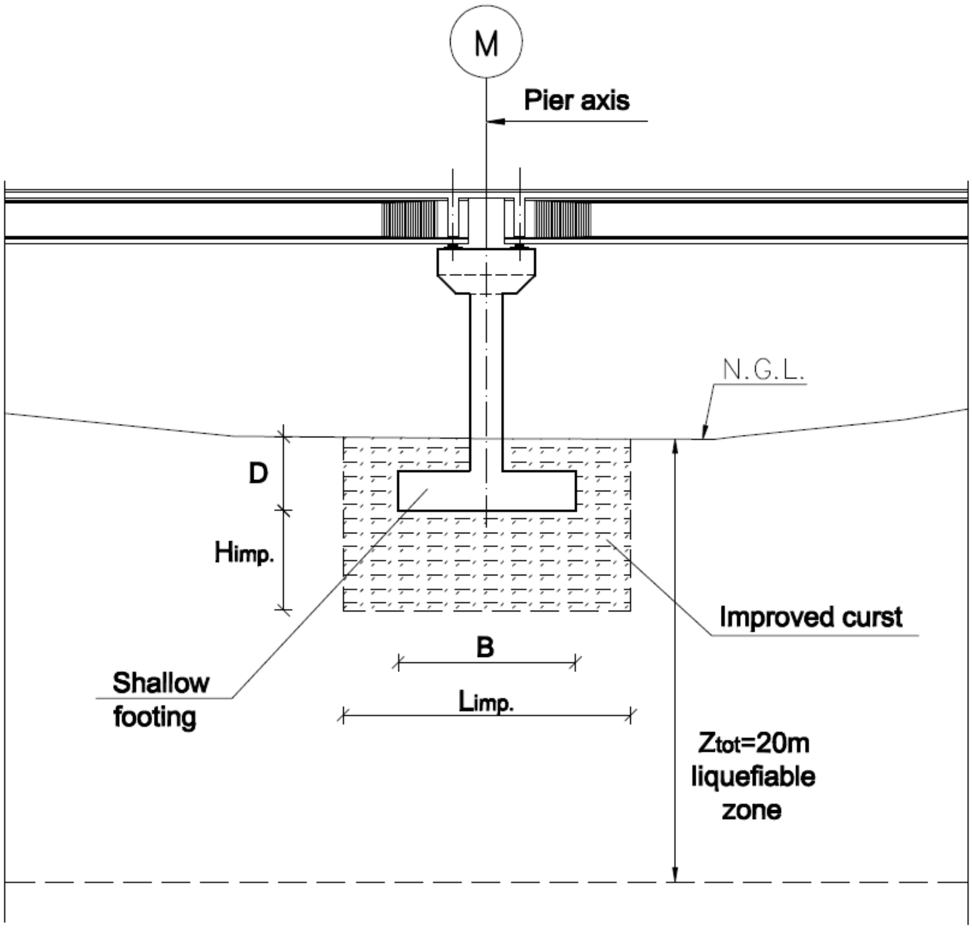

Figure 8.1: Description of the "natural" seismic isolation at pier site.
Σχήμα 8.1: Περιγραφή της "φυσικής" μόνωσης στη περιοχή του μεσοβάθρου

The steps to be followed are described hereafter:

1. A preliminary design of the innovative bridge with shallow foundation is carried out. In order to initially estimate the min dimensions of the footing, a check of its eccentricity against seismic loading is carried out. At this stage, the support conditions of the pier, i.e. the inertial characteristics of the springs at the base of the pier, are arbitrary assessed. For the rest of the members of the bridge, the dimensions defined in the conventional design are taken into account.

Two seismic loading cases are considered: a weak seismic motion with return period T_{ret} equal to 225years not causing liquefaction at the liquefiable sand and a strong motion with return period T_{ret} equal to 1000 years causing liquefaction at the liquefiable sand.

2. According to the results of the first step, the max allowable foundation movements ρ_{all} are calculated, taking also into account appropriate serviceability criteria. To this end, the diagram M-ρ of the moments at the base of the pier (where the first plastic hinge is formed) against imposed settlements is produced. This procedure has already been realized and presented in Deliverable D6a.

3. In this step, the final dimensions of the footing along with the dimensions of the improved curst are defined. Two conditions should be satisfied:

   - The static safety factor FS_{deg}, immediately after the seismic event should be greater than 1,0.
   - The remaining settlements ρ should be lower than the max allowable foundation movements ρ_{all} which were established in work task 1 (see Deliverable D6a).

   To this end, an iterative procedure is carried out, by means of an appropriate software in EXCEL form, prepared by the Geotechnical team.

4. Taking into account the dimensions of the footing and the curst defined in step 2, the static and dynamic characteristics of the support springs are defined by the Geotechnical Team.

5. Considering the dimensions of the footing and the characteristics of the support springs defined in the previous steps, the bridge is now redesigned against seismic actions, for the two following conditions:

   - No liquefaction state (weak motion): The bridge should perform practically elastically ($q \leq 1.5$). This check corresponds to "Immediate Occupancy" performance level.
   - Liquefaction state (strong motion): This check corresponds to "Life Safety" performance level. The bridge should tolerate loads and displacements imposed during and immediately after the seismic motion. The asynchrony motion of abutment and pier due to different foundation conditions should be considered.

   According to the results of the calculations the final dimensions and reinforcement of the various members of the bridge are defined.

6. In case where, from step 5, a different reinforcement ratio of the pier results, leading to a different resistance moment of the pier and, in consequence, to different max allowable foundation movements ρ_{all}, the whole process is repeated until convergence is succeeded.

9. BRIDGE DESCRIPTION

9.1. Geometry and cross sections

The longitudinal section of the bridge according to the innovative design, is shown in Figure 9.1. The dimensions of the foundation system will be estimated to the next section. For the rest of the members of the bridge, the dimensions defined in the conventional design are taken into account.

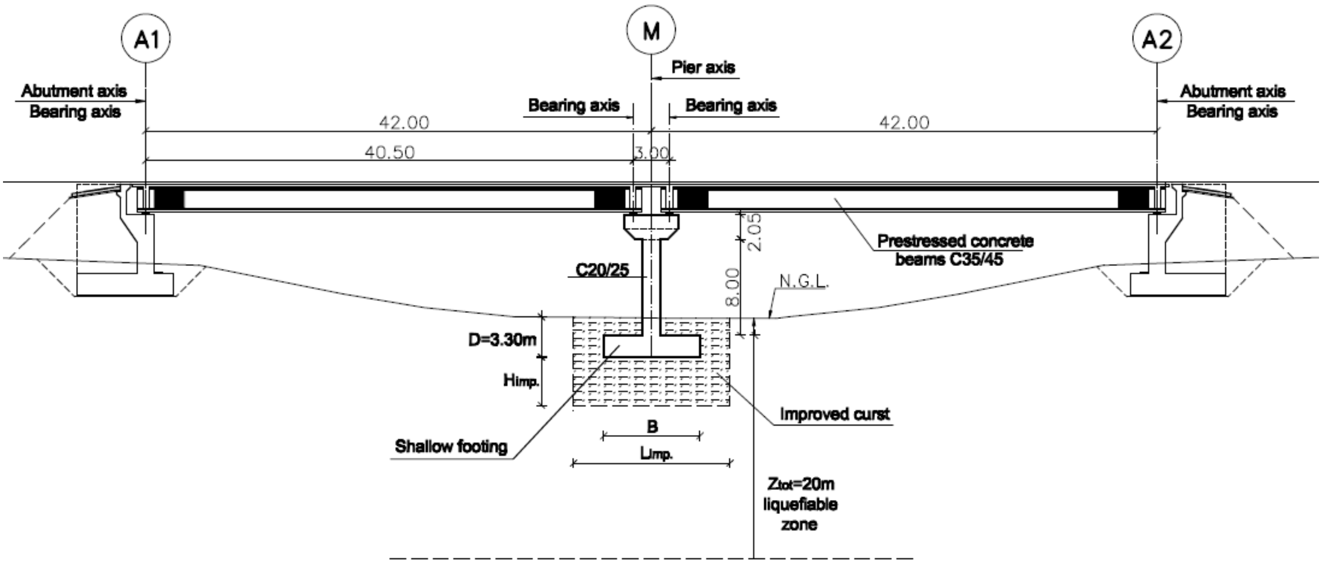

Figure 9.1: Londitudinal section of the bridge

Σχήμα 9.1: Κατά μήκος τομή γέφυρας

Namely, the deck is 11.25 m wide, plus 1.25 m wide pavements at each side and it is composed of 2×7 precast, prestressed concrete beams of length 40.50 m. A cast in-situ slab of 0.25 m min thickness is constructed. The concrete beams are resting upon the abutments and the mid-pier via elastomeric anchored bearings of Algabloc NB5 type with dimensions 400×500mm^2 (t_{el}=121mm) for the abutments and 350×450mm^2 (t_{el}=99 mm) for the pier. The pier is a wall-type column of cross section 1.50m × 8.35m.

9.2. Materials

The prestressed precast beams are made of concrete of grade C35/45, the cast in-situ reinforced concrete slabs of concrete C30/37, while the rest of concrete members are made of concrete C20/25. The reinforcing steel grade is B500C while the prestressing tendons are of steel 1600/1860.

10. DESIGN OF THE FOUNDATION

10.1. Check of eccentricity against seismic actions (Step 1)

A preliminary design of the innovative bridge with shallow foundation is carried out. In order to initially estimate the min dimensions of the footing, a check of its eccentricity against seismic loading is carried out. Eccentricity should satisfy the requirement to be less than the 1/3 of the length of the footing at the certain direction. A footing of dimensions BxL=8,0x13,0m^2 is initially selected.

10.1.1. Model

For the analysis, the model presented in Figure 10.1 was considered. The superstructure, the pier column-cap and the pier column were modeled with beam elements representing in detail the geometry and the stiffness characteristics of the members. The resistance of the foundation system was simulated using appropriate springs at the base of the pier, the inertial characteristics of which are, at this stage, arbitrary assessed. More specifically, the following values have been used:

K_{hx} = 5.3E+05 kN/m for the longitudinal direction,

K_{hy} = 5.5E+05 kN/m for the lateral direction,

K_z = 1.7E+06 kN/m for the vertical direction,

K_{Rx} = 3.3E+07 kNm/rad about the longitudinal direction, and

K_{Ry} = 2.6E+07 kNm/rad about the lateral direction.

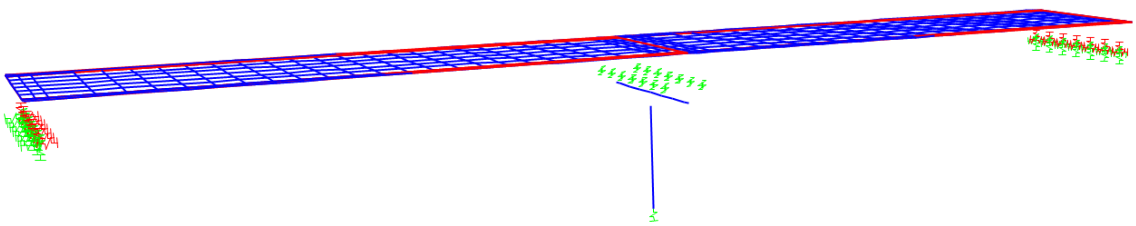

Figure 10.1: Finite element model of the bridge

Σχήμα 10.1: Προσομοίωμα πεπερασμένων στοιχείων της γέφυρας

10.1.2. Loads

(for details see Conventional Design, section 6)

The following load cases were considered:

10.1.2.1. Self weight

It is automatically calculated by the program for g_{con}=25 kN/m3

10.1.2.2. Additional dead loads

Pavement layer and lining concrete: 3.50 KN/m^2

Sidewalk with parapets: 8.50 kN/m

10.1.2.3. Shrinkage and creep

DT′ is taken equal to 32.7°C for the beams and to 30°C for the continuity slab.

10.1.2.4. Uniform road traffic loads

q = 5.45 kN/m^2

10.1.2.5. Uniform difference of temperature on deck

$\Delta T_{N,con} = -17°$ C

$\Delta T_{N,exp} = +37°$ C

10.1.2.6. Earthquake loads

Modal response spectrum analysis was performed. Two seismic loading cases were considered: a weak seismic motion with return period T_{ret} equal to 225 years not causing liquefaction at the liquefiable sand and a strong motion with return period T_{ret} equal to 1000 years causing liquefaction at the liquefiable sand.

According to the Geotechnical Report (see Deliverable D4), for the natural soil and the weak motion, the design spectrum of Eurocode 8 is used, for soil type D with soil factor S=0.96 and peak ground acceleration a_g=0.22g, while for the strong motion the design spectrum for soil type C with soil factor S=0.50 and peak ground acceleration a_g=0.32g is taken into account (see Figures 3.6 and 3.7 of this report respectively). For the design of the foundation, the behavior factor q was taken equal to 1.0.

The following load cases were examined:

Earthquake x-x (horizontal longitudinal direction of the bridge)

Earthquake y-y (horizontal lateral direction of the bridge)

Earthquake z-z (vertical direction of the bridge)

10.1.3. Load Combinations

For the seismic design situation the following load combination at ULS were considered:

(1) $G_t+0.2\times Q+0.5\times DT'\pm Ex\pm 0.3Ey\pm 0.3Ez$
(2) $G_t+0.2\times Q+0.5\times DT'\pm 0.3Ex\pm Ey\pm 0.3Ez$
(3) $G_t+0.2\times Q+0.5\times DT'\pm 0.3Ex\pm 0.3Ey\pm Ez$

10.1.4. Results

The most unfavorable load combination concerns the weak seismic motion with return period T_{ret}=225 years, not causing liquefaction at the liquefiable sand (maxa=0.528g).

Table 10.1: Forces and moments at the base of the pier

Πίνακας 10.1: Δυνάμεις και ροπές στη βάση του στύλου

Load Combinations	N	Vx	Vy	Mx	My
	KN	KN	KN	KNm	KNm
(1) min	20757,95	3971,04	1288,92	15745,53	31540,54
(1) max	18324,92	-3971,04	-1288,919	-15745,53	-31540,53
(2) min	20757,95	1191,31	4296,40	52485,10	9462,16
(2) max	18324,92	-1191,31	-4296,40	-52485,11	-9462,16
(3) min	23596,48	1191,31	1288,92	15745,54	9462,17
(3) max	15486,40	-1191,31	-1288,92	-15745,54	-9462,16

In Table 10.1 the forces and moments at the base of the pier are presented where, Mx the moment about the longitudinal direction of the bridge, My the moment about the lateral direction, Vx the shear force in the longitudinal direction, Vy the shear force in the lateral direction and N the vertical force.

Forces and moments at the center O of the footing are calculated as:

$M_x^O = M_x + V_y * H_f + G_f * \alpha_g * H_f/2$

$M_y^O = M_y + V_x * H_f + G_f * \alpha_g * H_f/2$

$N^O = N + G_f$

where, M_x^O the moment about the longitudinal direction of the bridge, M_y^O the moment about its lateral direction, N^O the vertical force, H_f the thickness of the footing equal to 1.80m, G_f the weight of the footing and α_g the seismic factor equal to 0.22x0.96=0.211. Forces and moments at the center O of the footing are shown in Table 10.2.

Table 10.2: Forces and moments at the center O of the footing

Πινακας 10.2: Δυνάμεις και ροπές στο κέντρο Ο του πεδίλου

Load Combinations	Mx^O KNm	My^O KNm	N^O KN	ex	ey
(1) min	18954.32	39577.14	25437.95	0.75	1.56
(1) max	-18954.32	-39577.14	23004.92	-0.82	-1.72
(2) min	61087.35	12475.25	25437.95	2.40	0.49
(2) max	-61087.35	-12475.25	23004.92	-2.66	-0.54
(3) min	18934.33	12495.25	28276.48	0.67	0.44
(3) max	-18934.33	-12495.25	20166.40	-0.93	-0.62

The max eccentricities satisfy the aforementioned requirement, namely:

ex = 2.66m < L/3 = 13.0/3 = 4.33m and

ey = 1.72m < B/3 = 8.0/3 = 2.66m

10.2. Estimation of max allowable foundation settlement ρ_{all} (step 2)

The max allowable foundation settlement ρ_{all} was established in work task 1 to be equal to approximately 23cm (see Deliverable D6a).

10.3. Estimation of footing and curst dimensions (step 3)

The final dimensions of the footing along with the dimensions of the improved curst were defined. To this end, an iterative procedure was carried out, by means of an appropriate software in EXCEL form, prepared by the Geotechnical team. Two conditions should be satisfied:

- The static safety factor FS_{deg}, immediately after the seismic event should be greater than 1.0.
- The remaining settlements ρ should be lower than the max allowable foundation settlement ρ_{all} which was established in work task 1 to be equal to approximately 23cm (see Deliverable D6a). It should be noted that the remaining settlements ρ is the sum of the settlements ρ_0 produced by the permanent loads and of the settlements ρ_{dyn} produced by the seismic event. From the

analysis, ρ_0 was found to be equal to 1.2cm. Thus, it should be: $\rho_{dyn} \leq \rho_{all} - \rho_0 = 23 - 1.2 = 21.8$cm.

Table 10.3: Iterative procedure (in EXCEL form) for the estimation of footing and curst dimensions
Πίνακας 10.3: Επαναληπτική διαδικασία (σε μορφή EXCEL) για τον υπολογισμό των διαστάσεων του πεδίλου και της κρούστας

Input		
Soil Properties		*Range*
Relative Density of the natural soil, $D_{r,o}$ (%)	60	*$D_{r,o}$ (%)=35-70*
Excess Pore Pressure ratio in the improved zone, $r_{u,design}$	0,3	*$r_{u,design}$=0.3-0.5*
Buoyant unit weight, γ' (kN/m^3)	9,81	
Soil Geometry		
Total Thickness of the liquefiable layer, Ztot (m)	20	
Thickness of the improved zone, H_{imp}(m)	4	*H_{imp}(m) = 1-10*
Thickness of the liquefiable layer, Z_{liq} (m)	12,7	
Width of the improved zone, L_{imp}(m)	13	
Excitation		
Maximum input acceleration, α_{max} (g)	0,17	
Predominant period, T (sec)	0,25	
Number of cycles, N	12	
Footing Properties		
Footing width, B(m)	8	
Footing Length, L(m)>B(m) [use 0 for strip footing]	15	
Embedmennt depth, D(m)	3,3	
Total static load from footing, q_o (kPa)	248	

Output	
Improved Soil	
Length of the imroved zone (m)	20
Volume of the imroved zone (m3)	1040
Replacement ratio, α_s	0,132
Relative Density of the improved zone, $D_{r,imp}$ (%)	81
Friction Angle of the improved zone, φ_{imp} (deg)	40
Permeability of the improved zone, k_{eq} (m/s)	1,50E-03
Pore Pressure Ratio below footing, U3	0,824
Infinite Improvement	
Degraded factor of safety, $F.S._{deg}^{inf}$	1,39
Seismic settlements, $\rho_{dyn,inf}$(m)	0,056
Differential settlements, δ(m)	0,038
Rotation, θ(degrees)	0,182
Finite Improvement	
Degraded factor of safety, $F.S._{deg}$	1,10
Seismic settlements, ρ_{dyn}(m)	0,068
Differential settlements, δ(m)	0,046
Rotation, θ(degrees)	0,222

According to the results of the calculations, it was found that a footing of $8x15m^2$ resting on an improved curst 4m thick, results to a degraded factor of safety FS_{deg} equal to 1.10 and a remaining settlement ρ_{dyn} equal to 6.8cm much lower than the max permissible 21.8cm (see Table 10.3).

The degraded factor of safety FS_{deg} (the lower limit of which was selected to be 1.10) proved to be the critical factor for the design of the foundation. The final dimensions of the footing and the improved curst are presented in Figure 10.2.

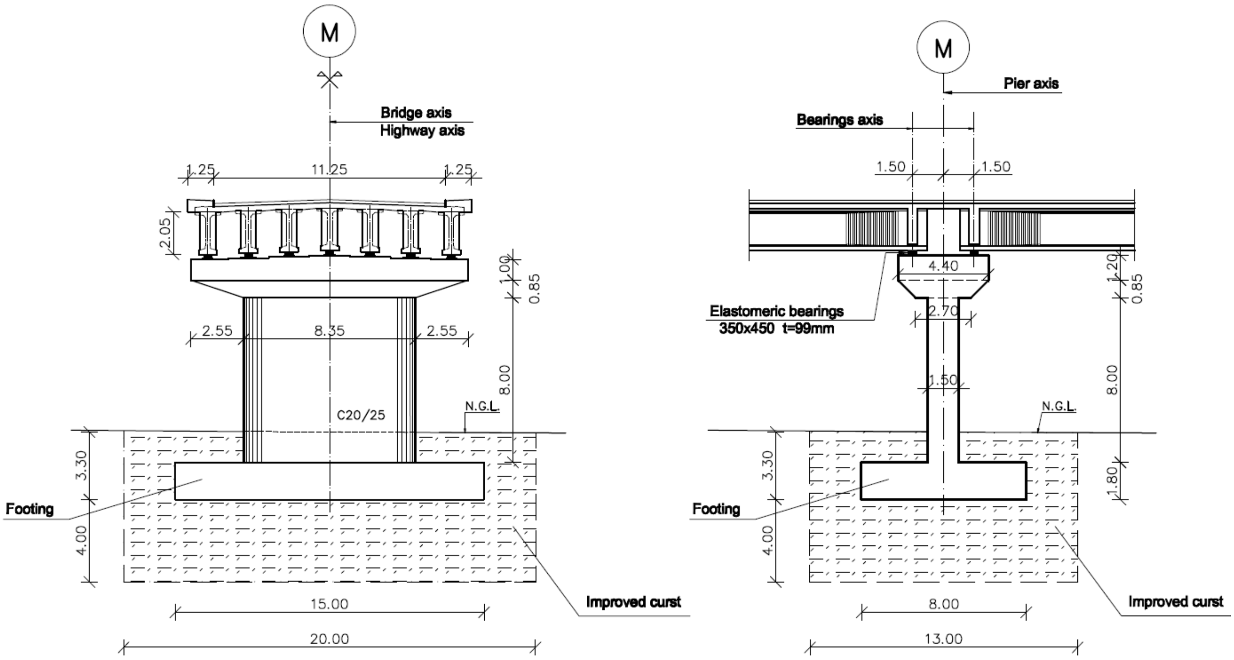

(a) (b)

Figure 10.2: Final dimensions of the footing and the improved curst: (a) in longitudinal direction , (b) in lateral direction of the bridge

Σχήμα 10.2: Τελικές διαστάσεις πεδίλου και βελτιωμένης κρούστας: (a) στη διαμήκη διεύθυνση, (b) στην εγκάρσια διεύθυνση της γέφυρας

10.4. Estimation of the stiffness characteristics of the support springs for the analysis (step 4)

Taking into account the dimensions of the footing and the curst, previously defined, the dynamic resistance of the pier support was defined by the Geotechnical Team, as a function of its static stiffness and the eigenperiod of the bridge. More specifically, the support was supposed to consist of a spring and a dashpot, whose the dynamic stiffness characteristics, were calculated according to the following formulae:

Dynamic Impedance: $K^* = K + i\,(2\pi/T)\,C = k_{static}\,(k_1(T) + i^*k_2(T))$

Spring Coefficient: $K = k_{static}{}^*k_1(T)$

Dashpot Coefficient: $C = k_{static}\,{}^*k_2(T)^*T/2\pi$

$k_1(T)$ and $k_2(T)$ are the dynamic correction factors of the static spring coefficients k_{static} , common for the longitudinal x and the lateral y direction of the bridge. They are presented in Table 10.3 as a function of the eigenperiod of the bridge.

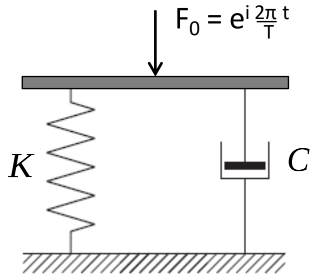

Figure 10.3: Model of pier support

Σχήμα 10.3: Προσομοίωση στήριξης μεσοβάθρου

Table 10.3: Dynamic correction factors of static spring coefficients (common for horizontal x and y direction) in case of liquefaction and non liquefaction

Πίνακας 10.3: Δυναμικοί διορθωτικοί συντελεστές των στατικών ελατηριακών σταθερών (κοινοί για τις οριζόντιες διευθύνσεις x και y) στην περίπτωση ρευστοποίησης και μη ρευστοποίησης

	NO LIQUEFACTION						
	$k_1(T)$						
	T (sec)						
MODE	0,2	0,4	0,6	0,8	1,0	1,25	1,5
VERTICAL	0,48	0,74	0,76	0,88	0,91	0,93	0,94
HORIZONTAL	1,00	0,85	0,86	0,87	0,88	0,91	0,95
ROCKING	0,80	0,93	0,97	0,98	0,99	0,99	1,00

	NO LIQUEFACTION						
	$k_2(T)$						
	T (sec)						
MODE	0,2	0,4	0,6	0,8	1,0	1,25	1,5
VERTICAL	0,84	0,31	0,12	0,11	0,06	0,06	0,06
HORIZONTAL	0,66	0,48	0,24	0,17	0,12	0,06	0,05
ROCKING	0,23	0,07	0,06	0,06	0,06	0,06	0,06

	WITH LIQUEFACTION						
	$k_1(T)$						
	T (sec)						
MODE	0,2	0,4	0,6	0,8	1,0	1,25	1,5
VERTICAL	0,20	0,67	0,78	0,51	0,54	0,62	0,68
HORIZONTAL	1,18	1,02	0,96	0,90	0,94	0,90	0,76
ROCKING	0,79	0,89	0,93	0,92	0,94	0,96	0,98

	WITH LIQUEFACTION						
	$k_2(T)$						
	T (sec)						
MODE	0,2	0,4	0,6	0,8	1,0	1,25	1,5
VERTICAL	2,40	1,20	1,10	0,81	0,53	0,36	0,28
HORIZONTAL	1,80	1,00	0,80	0,60	0,54	0,58	0,53
ROCKING	0,50	0,22	0,19	0,14	0,10	0,08	0,08

In Tables 10.4 and 10.5 are presented the dynamic stiffness coefficients of spring and dashpot simulating the resistance of pier support, in case the ground liquefies and in case the ground does not liquefy, respectively.

Table 10.4: Dynamic stiffness coefficients of spring and dashpot in case of non liquefaction

Πίνακας 10.4: Δυναμικά χαρακτηριστικά ακαμψίας ελατηρίου και αποσβεστήρα στην περίπτωση μη ρευστοποίησης

NO LIQUEFACTION	Static Stiffness k_{static}	Dynamic Impedance (T_{brid}=1,54sec)		Spring Coefficient K	Dashpot Coefficient C
		$K_1(T)$	$K_2(T)$		
Vertical, z (kN/m)	2.95E+06	0.94	0.06	2.77E+06	1.77E+05
Horizontal, x (kN/m)	2.28E+06	0.95	0.05	2.17E+06	1.14E+05
Horizontal, y (kN/m)	2.16E+06	0.95	0.05	2.05E+06	1.08E+05
Rocking, rx (around x axis) (kNm/rad)	1.17E+08	1.00	0.06	1.17+08	7.02E+06
Rocking, ry (around y axis) (kNm/rad)	4.66E+07	1.00	0.06	4.66E+07	2.79E+06

Table 10.5: Dynamic stiffness coefficients of spring and dashpot in case of liquefaction

Πίνακας 10.5: Δυναμικά χαρακτηριστικά ακαμψίας ελατηρίου και αποσβεστήρα στην περίπτωση ρευστοποίησης

WITH LIQUEFACTION	Static Stiffness k_{static}	Dynamic Impedance (T_{brid}=1,54sec)		Spring Coefficient K	Dashpot Coefficient C
		$K_1(T)$	$K_2(T)$		
Vertical, z (kN/m)	7.95E+05	0.68	0.28	5.40E+05	2.22E+05
Horizontal, x (kN/m)	1.19E+06	0.76	0.53	9.04E+05	6.31E+05
Horizontal, y (kN/m)	1.13E+06	0.76	0.53	8.58E+05	5.99E+05
Rocking, rx (around x axis) (kNm/rad)	7.18E+07	0.98	0.08	7.04E+07	5.74E+06
Rocking, ry (around y axis) (kNm/rad)	2.86E+07	0.98	0.08	2.80E+07	2.29E+06

11. FINAL DESIGN OF THE INNOVATIVE BRIDGE (step 5)

11.1. Introduction

In this section, the bridge is redesigned against seismic actions, taking into account both cases: the case of liquefaction and the case of no liquefaction. The geometry of pier footing, estimated in section 10 and illustrated in Figure 10.2 is used. For the rest of the members of the bridge, the dimensions defined in the conventional design are taken into account.

11.2. Model

For the analysis, the model presented in Figure 10.1 was considered. The resistance of the foundation system of the pier was now simulated using the spring and dashpot illustrated in Figure 10.3. Their dynamic stiffness coefficients are presented in Table 10.4 for the case of no liquefaction and in Table 10.5 for the case of liquefaction.

11.3. Loads

(for details see Conventional Design, section 6)

The following load cases were considered:

11.3.2. Self weight

It is automatically calculated by the program for g_{con}=25 kN/m3

11.3.3. Additional dead loads

Pavement layer and lining concrete: 3.50 KN/m^2
Sidewalk with parapets: 8.50 kN/m

11.3.4. Shrinkage and creep

DT' is taken equal to 32.7°C for the beams and to 30°C for the continuity slab.

11.3.5. Uniform road traffic loads

q = 5.45 kN/m^2

11.3.6. Uniform difference of temperature on deck

$\Delta T_{N,con} = -17°$ C
$\Delta T_{N,exp} = +37°$ C

11.3.7. Earthquake loads

Modal response spectrum analysis was performed. Two seismic loading cases were considered:

- No liquefaction case (weak motion): The bridge should perform practically elastically (q≤1.5). This check corresponds to "Immediate Occupancy" performance level.
- Liquefaction case (strong motion): This check corresponds to "Life Safety" performance level. The bridge should tolerate loads and displacements imposed during and immediately after the seismic motion. Since a uniform excitation was used for the whole bridge, the asynchrony motion between abutment and pier due to their different foundation conditions should also be considered. To this end, an additional horizontal displacement was imposed to the base of the pier, accounting for the max relative horizontal movement between abutment and pier.

Moreover, liquefaction-produced displacements, in the form of settlements and rotations, gradually accumulate during vibration, receiving their maximum value at the end of the seismic event (Karamitros et al. 2012, Karamitros et al. 2013a and Karamitros et al. 2013b). These displacements should be considered as **residual** actions, which may produce additional stress and deformations to the structural components of the structure (pier, deck, bearings, etc.). To this sense, settlements and relevant rotations of the pier along with accidentally residual horizontal displacements were taken into account immediately after the end of the seismic event. It should be noted, however, that the max allowable foundation settlement ρ_{all} of the pier established in work task 1 was approximately equal to 20cm (see Deliverable D6a), much lower than the seismic settlement of 6.8cm estimated for the foundation of the innovative design in case of liquefaction (see Table 10.3).

A. No liquefaction

A weak seismic motion with return period T_{ret} equal to 225 years not causing liquefaction at the liquefiable sand was considered. According to the Geotechnical Report (see Deliverable D4), for the natural soil and the weak motion, the design spectrum of Eurocode 8 was used, for soil type D with soil factor S=0.96 and peak ground acceleration a_g=0.22g (see Figure 3.6).

The following load cases were examined:

Earthquake x-x (horizontal longitudinal direction of the bridge)
Earthquake y-y (horizontal lateral direction of the bridge)
Earthquake z-z (vertical direction of the bridge)

B. With liquefaction

During seismic excitation

Inertial seismic loads "E", along with relative horizontal displacements "δ" were taken into account.

A strong seismic motion was taken into account with return period T_{ret} equal to 1000 years causing liquefaction at the liquefiable sand. A design spectrum for soil type C with soil factor S=0.50 and peak ground acceleration a_g=0.32g was considered (see Figure 3.7).

Table 11.1: Peak and average transient displacements of liquefied ground
Πίνακας 11.1: Μέγιστες και μέσες εδαφικές μετακινήσεις ρευστοποιημένου εδάφους

no	Excitation	Peak horizontal displacement, δ(cm)				
		Outcropping bedrock	Ground Surface			
			with improved top layer		without improved top layer	
			Absolute	Relative	Absolute	Relative
1	ITALY_BAG	13.13	19.12	10.49	27.64	20.59
2	ITALY_VLT	1.28	2.81	3.20	4.03	4.39
3	KOBE_TDO	13.47	17.17	20.00	14.46	21.47
4	LOMAP_AND	10.20	21.16	22.17	11.23	9.31
5	LOMAP_GIL	11.68	12.59	4.99	13.07	4.87
average		**9.95**	**14.57**	**12.17**	**14.09**	**21.07**

In Table 11.1 prepared by the Geotechnical Team, the average transient displacements of liquefied ground, for various seismic events are presented (see Annex A). Taking into account that the abutment is founded on the outcropping bedrock and the pier on an improved top layer of the liquefiable ground, the max relative horizontal displacements developed between abutment and pier due to liquefaction are presented at the fifth column. For the analysis the average value of δ=12.17cm was used.

Considering that the max values of ground acceleration and of ground displacements are not developed simultaneously (see time histories diagrams in Appendix A), inertial loads and relative horizontal displacements were combined according to the rule presented in Equ. 11.1 and 11.2 and justified in Appendix B:

(a) Inertial seismic loads and 30% of the relative horizontal displacements at the base of the pier, statistically summed:

- $[(\pm Ex \pm 0.3Ey \pm 0.3Ez)^2 + (0.3(\pm\delta x \pm 0.3\delta y))^2]^{1/2}$ (11.1a)
- $[(\pm 0.3Ex \pm Ey \pm 0.3Ez)^2 + (0.3(\pm 0.3\delta x \pm \delta y))^2]^{1/2}$ (11.1b)

(b) 30% Inertial seismic loads and relative horizontal displacements at the base of the pier, statistically summed:

- $[(0.3\ (\pm Ex \pm 0.3Ey \pm 0.3Ez))^2 + (\pm\delta x \pm 0.3\delta y)^2]^{1/2}$ (11.2a)
- $[(0.3\ (\pm 0.3Ex \pm Ey \pm 0.3Ez))^2 + (\pm 0.3\delta x \pm \delta y)^2]^{1/2}$ (11.2b)

<u>Immediately after the seismic excitation</u>

Liquefaction-produced displacements, in the form of settlements and rotations are taken into account at the base of the pier as residual actions. In addition, an amount of residual relative horizontal displacement is considered, as an accidental result of the seismic vibration.

According to Table 10.3 a residual seismic settlement ρ_{dyn} equal to 0,068m was taken into account. Settlements were considered to be related to accidental rotations, according to the following empirical relationship - though derived for buildings (Yasuda, 2014):

$\varphi_x = \varphi_y = 0.05 \cdot \rho_{dyn}$

where: ρ_{dyn} is the induced settlement (in cm) and φ_x, φ_y the resultant rotations about the strong and the weak axis of the pier, respectively (in degrees).

Moreover, a residual relative horizontal displacement δ_{res}=0.01m is considered.

Finally, the following loading cases are examined:

- $\delta_{res} + \rho_{dyn} + \varphi_y + 0.3\varphi_x$
- $\delta_{res} + \rho_{dyn} + \varphi_x + 0.3\varphi_y$

11.4. Load combinations

For the seismic design situation examined, the seismic loads described in paragraph 11.3.7 were combined with G_t+0.2Q+0.5DT’.

11.5. Vibration modes and natural frequencies

A. No liquefaction

The natural frequencies and periods of the first six vibration modes are listed in Table 11.2, while in Figure 11.1 the corresponding modal shapes are depicted.

Table 11.2: First six eigenfrequencies and eigenperiods of the bridge in case of no liquefaction

Πίνακας 11.2: Έξι πρώτες ιδιοσυχνότητες και ιδιοπερίοδοι της γέφυρας στην περίπτωση μη ρευστοποίησης

Mode number	Eigenfrequency (rad/sec)	Eigenfrequency (Hz)	Period (sec)
1	4.15	0.66	1.51
2	4.23	0.67	1.48
3	4.88	0.78	1.29
4	12.37	1.97	0.51
5	14.35	2.28	0.44
6	14.45	2.30	0.43

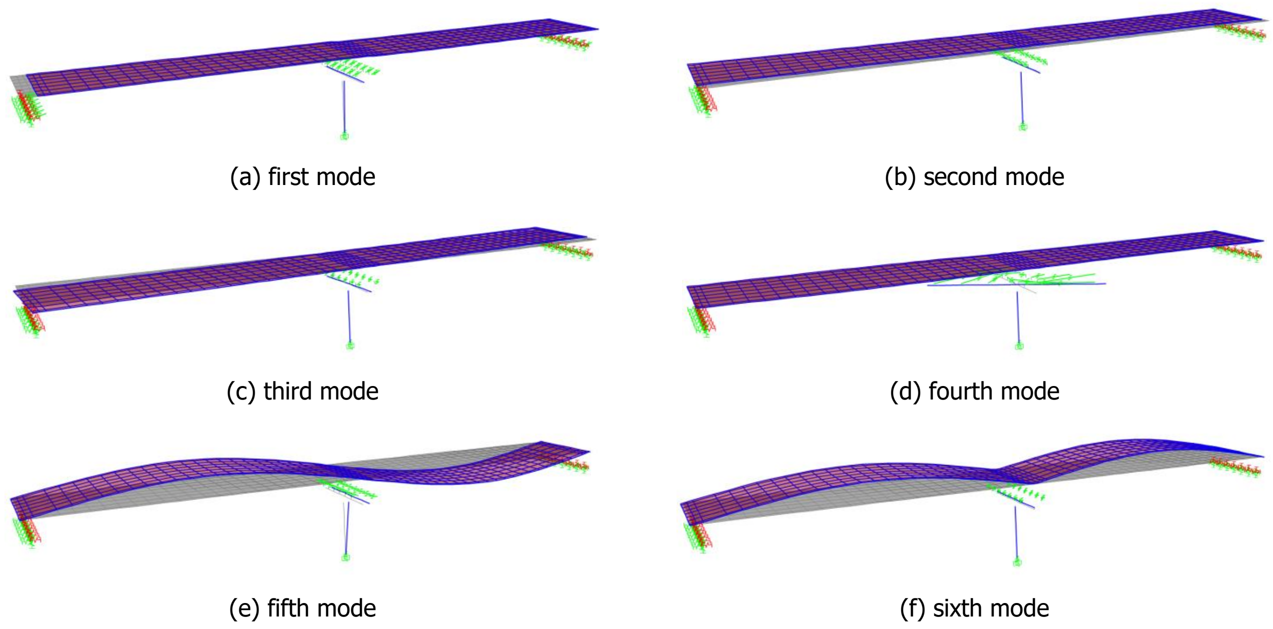

(a) first mode (b) second mode

(c) third mode (d) fourth mode

(e) fifth mode (f) sixth mode

Figure 11.1: Six first eigenmodes of the bridge in case of no liquefaction

Σχήμα 11.1: Έξι πρώτες ιδιομορφές γέφυρας στην περίπτωση μη ρευστοποίησης

C. ***Liquefaction***

The natural frequencies and periods of the first six vibration modes are listed in Table 11.3, while in Figure 11.2 the corresponding modal shapes are depicted.

Table 11.3: First six eigenfrequencies and eigenperiods of the bridge in case of liquefaction

Πίνακας 11.3: Έξι πρώτες ιδιοσυχνότητες και ιδιοπερίοδοι της γέφυρας στην περίπτωση ρευστοποίησης

Mode number	Eigenfrequency (rad/sec)	Eigenfrequency (Hz)	Period (sec)
1	4,12	0,66	1,53
2	4,19	0,67	1,50
3	4,88	0,78	1,29
4	12,37	1,97	0,51
5	12,88	2,05	0,49
6	14,32	2,28	0,44

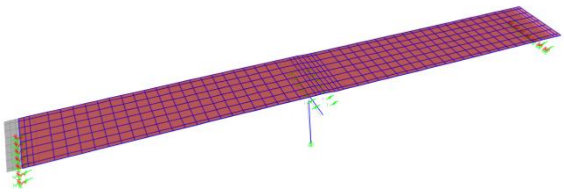

(a) first mode

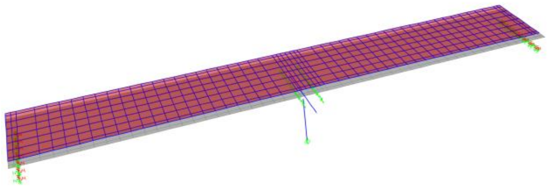

(b) second mode

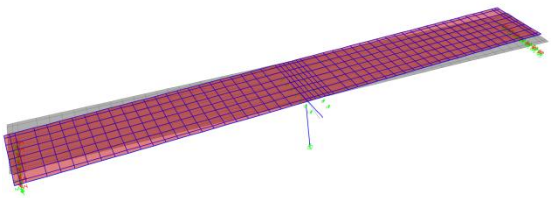

(c) third mode

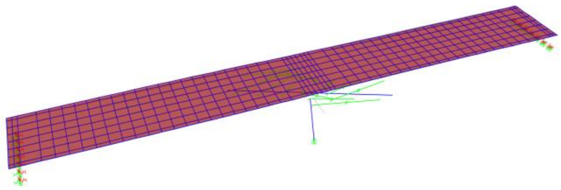

(d) fourth mode

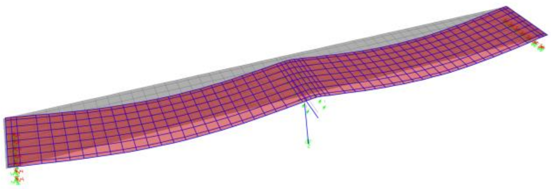

(e) fifth mode

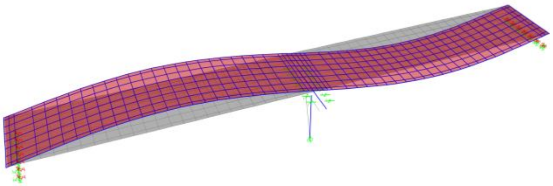

(f) sixth mode

Figure 11.2: Six first eigenmodes of the bridge in case of liquefaction

Σχήμα 11.2: Έξι πρώτες ιδιομορφές γέφυρας στην περίπτωση ρευστοποίησης

11.6. Results

11.6.1. No liquefaction - Pier's internal forces

In Figure 11.3 the internal forces for the seismic load combination in case of no liquefaction are depicted. According to the results of the calculations, for the base section of the pier and for the most unfavorable seismic load combination (G_t+0.2Q+0.5DT'+Ex+0.3Ey-0.3Ez), it is:

P=-18580.28kN, M_x=10930.21kNm, M_y=21636.23kNm, V_x=2599.30kN and V_y=866.59kN.

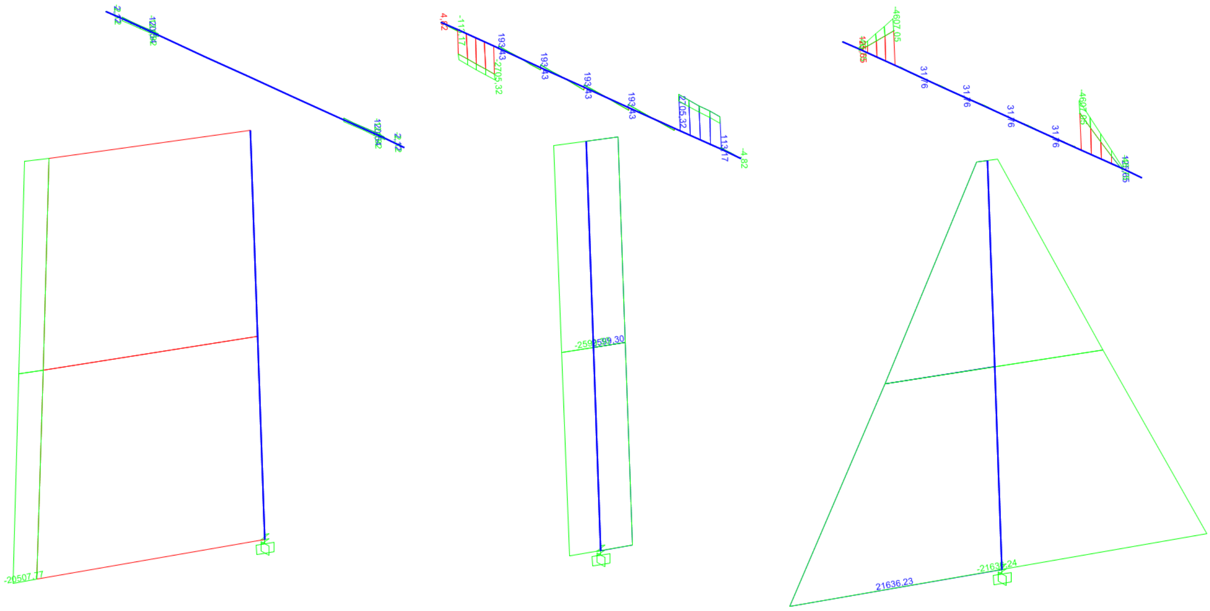

(a) (b) (c)

Figure 11.3: Pier forces for the most unfavorable seismic load combination (G_t+0.2Q+0.5DT'+Ex+0.3Ey-0.3Ez), in case of no liquefaction: (a) normal forces N; (b) Shear forces V_x ; (c) Moments M_y

Σχήμα 11.3: Εντατικά μεγέθη στύλου μεσοβάθρου για το δυσμενέστερο σεισμικό συνδυασμό (G_t+0.2Q+0.5DT'+Ex+0.3Ey-0.3Ez), σε περίπτωση μη ρευστοποίησης : (a) αξονικές δυνάμεις N, (b) Διατμητικές δυνάμεις V_x , (c) Ροπές M_y

11.6.2. Liquefaction - Pier's internal forces

<u>During seismic excitation</u>

From the results of the analysis it was found that the most unfavorable seismic combination includes the 30% of the inertial seismic loads and full horizontal relative displacements at the base of the pier, namely:

$$G_t+0.2\times Q+0.5\times DT'+ [(0.3\ (E_x+0.3E_y-0.3E_z))^2 + (\delta_x+0.3\delta_y)^2]^{1/2}$$

In Figure 11.4 and 11.5 the internal forces of the pier due to inertial seismic loads and to relative horizontal displacements "δx+0.3δy" respectively are depicted. For the most unfavorable seismic load combination, presented above, the internal forces at the base section of the pier were found to be:

P=-19310.38kN, M_x=5460.67kNm, M_y=13075.77kNm, V_x=1555.05kN and V_y=461.13kN.

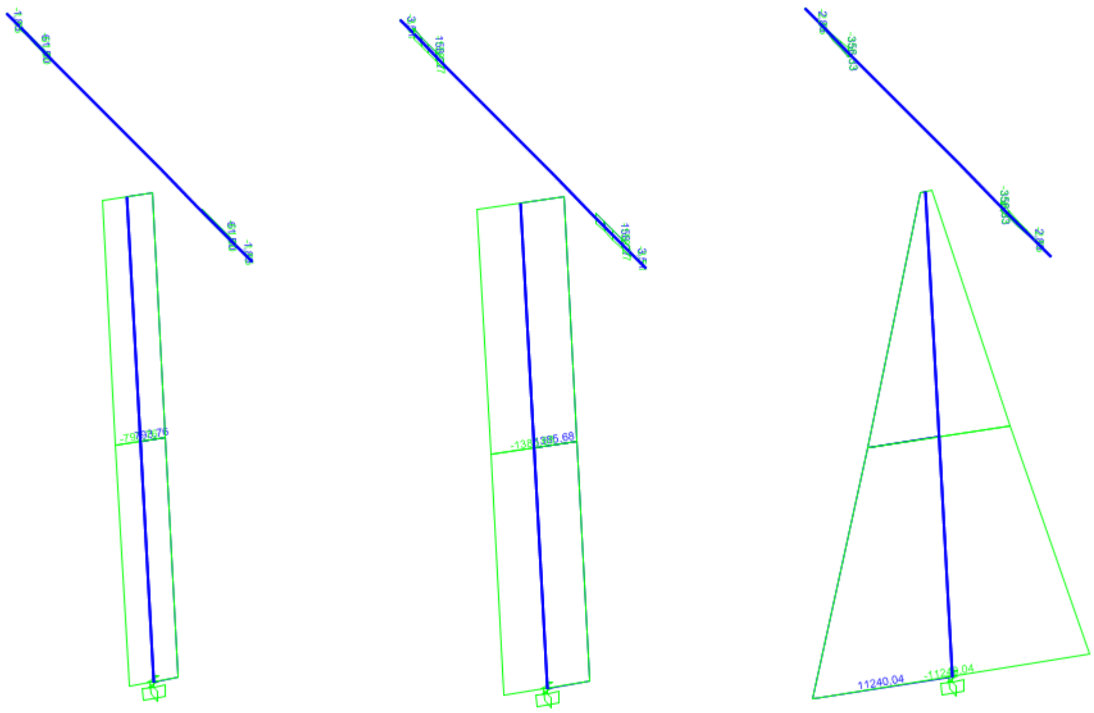

(a) (b) (c)

Figure 11.4: Pier's internal forces due to inertial seismic loads for the most unfavorable seismic loading (Ex+0.3Ey-0.3Ez), in case of liquefaction: (a) normal forces N; (b) Shear forces V_x ; (c) Moments M_y

Σχήμα 11.4: Εντατικά μεγέθη στύλου μεσοβάθρου λόγω αδρανειακών σεισμικών φορτίων για τη δυσμενέστερη σεισμική δράση (Ex+0.3Ey-0.3Ez), σε περίπτωση ρευστοποίησης: (a) αξονικές δυνάμεις N, (b) Διατμητικές δυνάμεις V_x , (c) Ροπές M_y

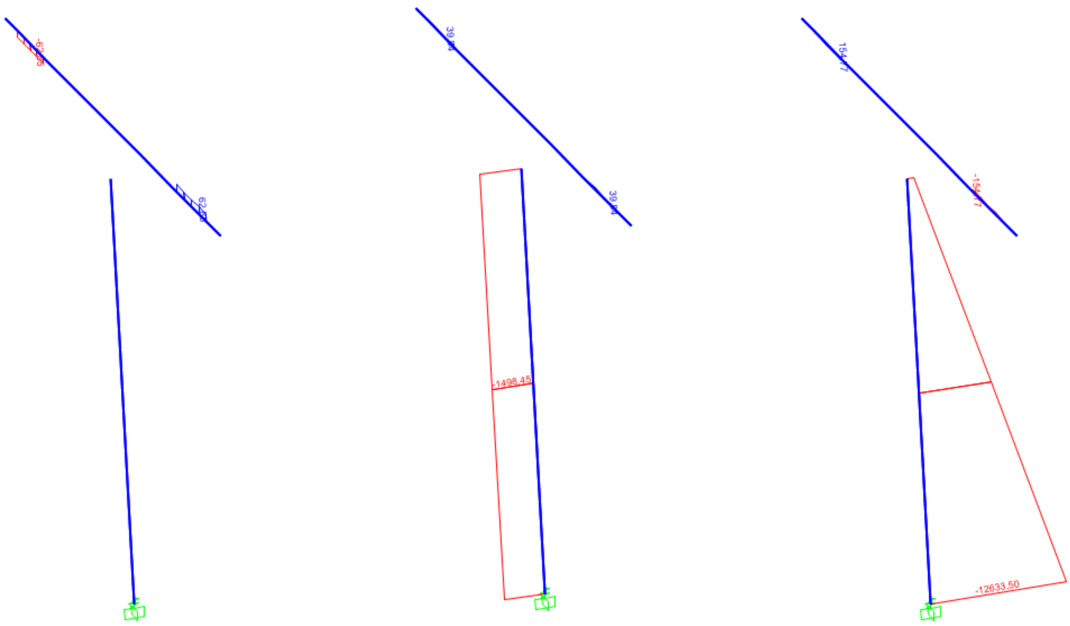

(a) (b) (c)

Figure 11.5: Pier's internal forces due to relative horizontal displacements "δx+0.3δy", in case of liquefaction: (a) normal forces N; (b) Shear forces V_x ; (c) Moments M_y

Σχήμα 11.5: Εντατικά μεγέθη στύλου μεσοβάθρου λόγω σχετικών οριζοντίων μετακινήσεων "δx+0.3δy", σε περίπτωση ρευστοποίησης: (a) αξονικές δυνάμεις N, (b) Διατμητικές δυνάμεις V_x , (c) Ροπές M_y

Immediately after the seismic excitation

In Figure 11.6, the moments developed at pier, immediately after the seismic excitation, due to residual relative horizontal displacement δ_{res}, settlement ρ_{dyn} and the most unfavorable rotations combination φ_y+0.3φ_x separately are presented, where it is shown that the pier is very sensitive to imposed rotations about its weak axis. Moreover, in Figure 11.7 are shown the internal forces developed at the pier for the most unfavorable seismic load combination (G_t+0.2Q+0.5DT'+δ_{res}+ρ_{dyn}+φ_y+0.3φ_x). For this combination, the internal forces at the base section of the pier were found to be:

P=19508.84kN, Mx=3730.76kNm, My=-13313.89kNm, Vx=-735.60kN and Vy=256.12kN.

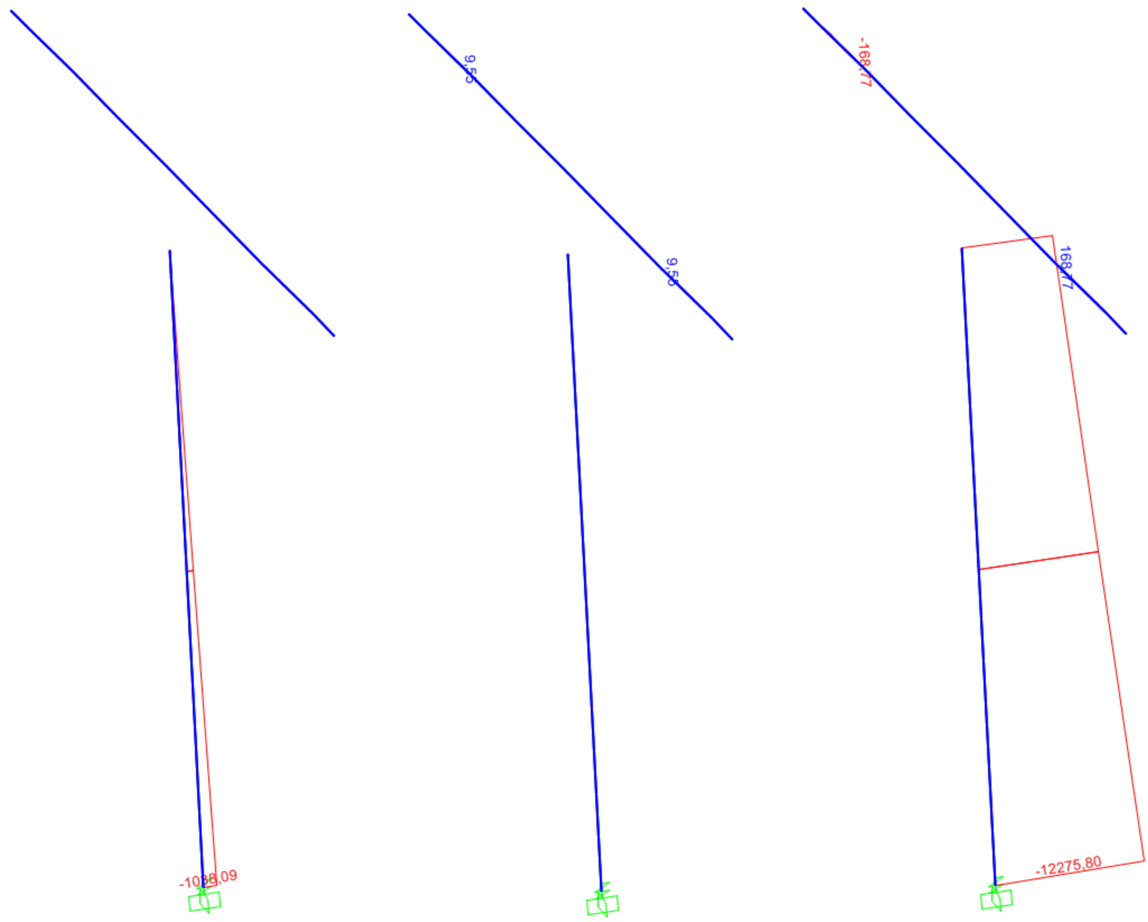

(a) (b) (c)

Figure 11.6: Pier's moments immediately after liquefaction due to: (a) residual relative horizontal displacement δ_{res}; (b) Settlement ρ_{dyn} ; (c) Rotations φ_y+0.3φ_x

Σχήμα 11.6: Καμπτικές ροπές στύλου μεσοβάθρου αμέσως μετά τη ρευστοποίηση λόγω,: (α) απομένουσας σχετικής οριζόντιας μετακίνησης δ_{res} , (b) καθίζησης ρ_{dyn} , (c) Στροφής φ_y+0.3φ_x

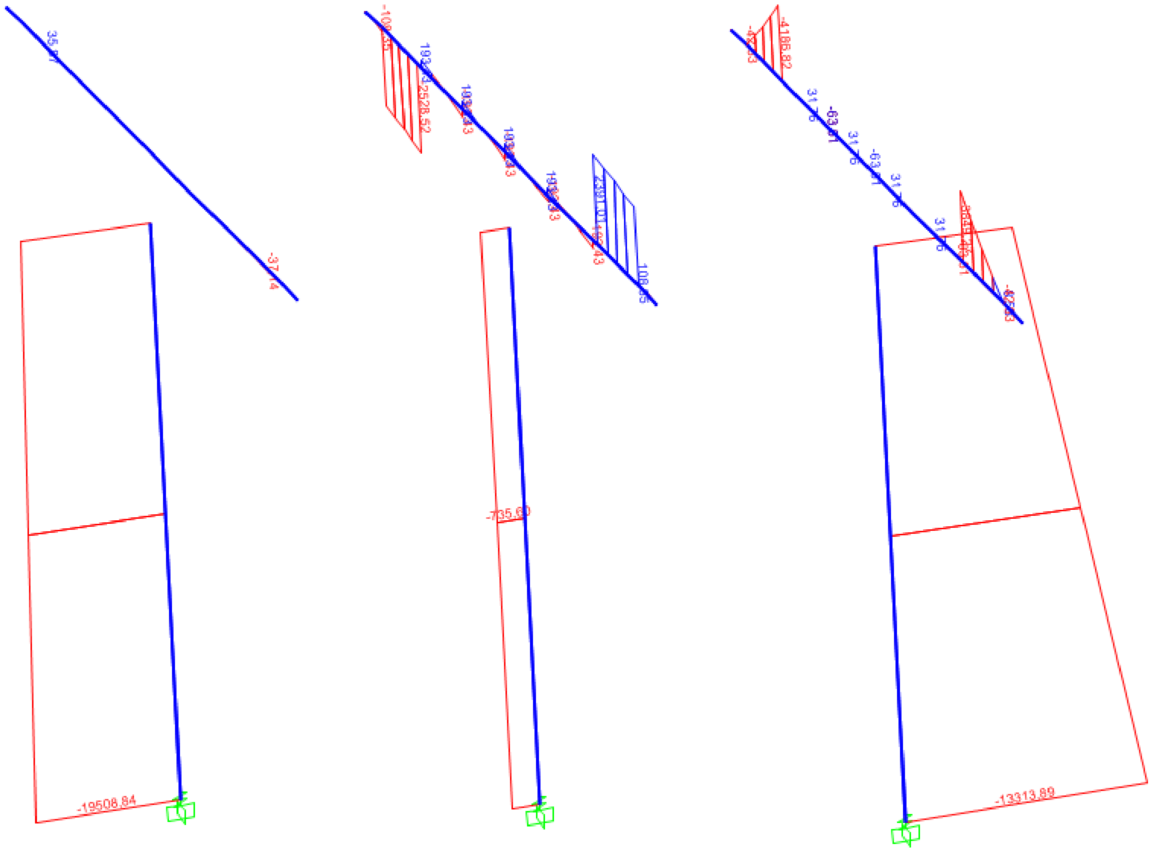

(a) (b) (c)

Figure 11.7: Pier's internal forces immediately after liquefaction, for the most unfavorable seismic load combination $G_t+0.2Q+0.5DT'+\delta_{res}+\rho_{dyn}+\varphi_y+0.3\varphi_x$: (a) normal forces N; (b) Shear forces V_x ; (c) Moments M_y

Σχήμα 11.7: Εντατικά μεγέθη στύλου μεσοβάθρου αμέσως μετά τη ρευστοποίηση για το δυσμενέστερο σεισμικό συνδυασμό $G_t+0.2Q+0.5DT'+\delta_{res}+\rho_{dyn}+\varphi_y+0.3\varphi_x$: (a) αξονικές δυνάμεις N, (b) Διατμητικές δυνάμεις V_x , (c) Ροπές M_y

11.6.3. Design of the pier

According to the results of the calculations presented in 11.6.2 and 11.6.3 the most unfavorable load combination for the seismic design situation refers to no liquefaction case. The max required longitudinal reinforcement of the base section for this case is 345.4 cm^2 and it was finally set to 114Φ20 (357.96 cm^2). In Figure 11.8, the longitudinal and shear reinforcements of the base section of the pier are presented.

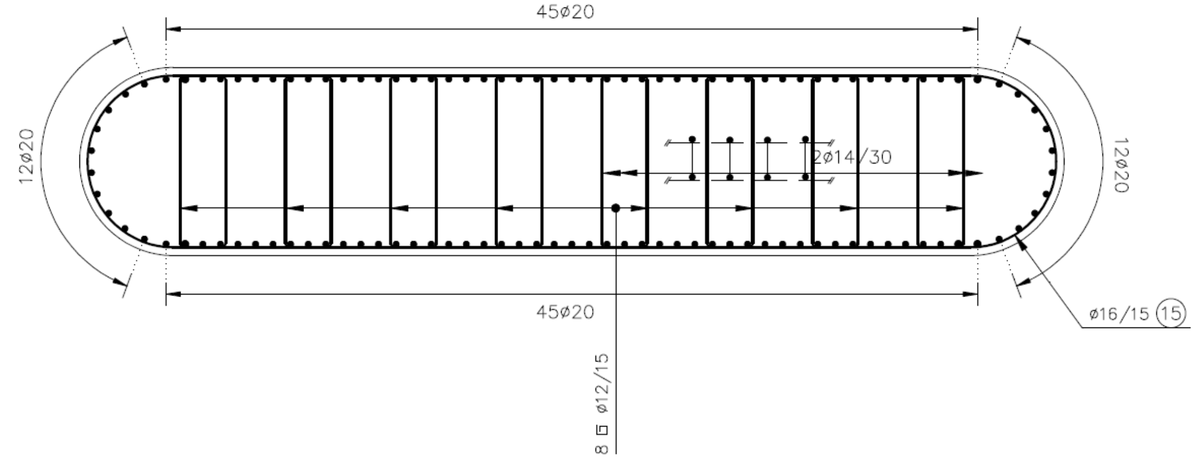

Figure 11.8: Pier reinforcement (base section)

Σχήμα 11.8: Οπλισμός μεσοβάθρου (διατομή βάσης)

11.6.4. Design of the footing

The model presented in Figure 11.9 was used in order to calculate the required reinforcements of the footing against static and seismic actions. The slab with dimensions 8.0x15.0m^2 and a thickness of 1.8m was simulated using shell elements. The soil-structure interaction was taken into account with equivalent springs. The spring constants were calculated based on the values of Table 3.1. The most unfavorable case of no liquefaction was considered, as nodal loads at the pier basis.

In **Error! Reference source not found.**Figure 11.10 the required reinforcements of the footing are presented, where the main direction is parallel to the longitudinal direction of the slab and the cross one is parallel to its lateral one. Finally, a reinforcement grid of Φ20/10 is used for the upper reinforcement of the footing while a double reinforcement grid of Φ20/10 is used for the lower one.

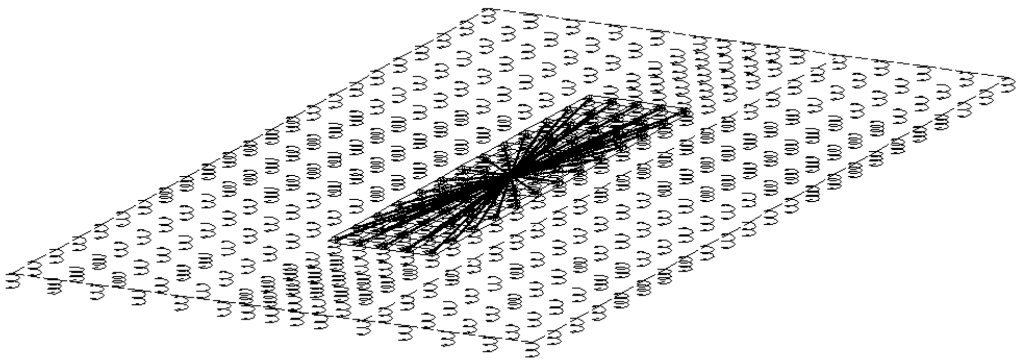

Figure 11.9: Model of the footing

Σχήμα 11.9: Προσομοίωμα πλάκας θεμελίωσης

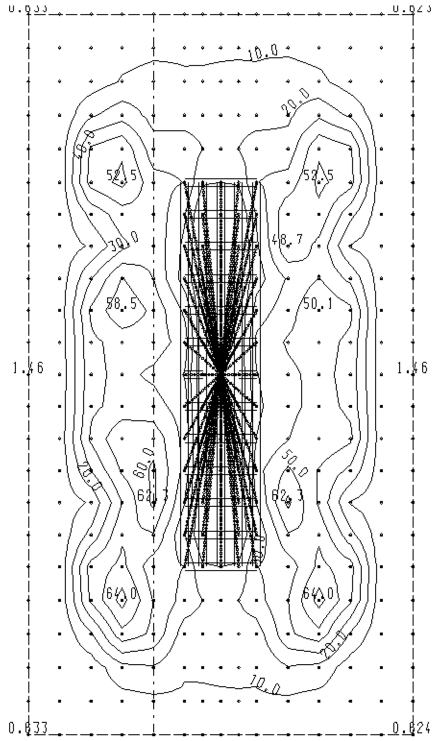

(a) Bottom cross reinforcements

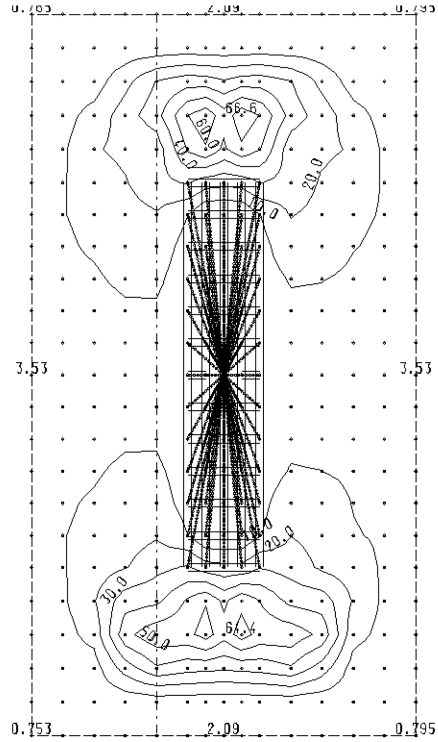

(b) Bottom main reinforcements

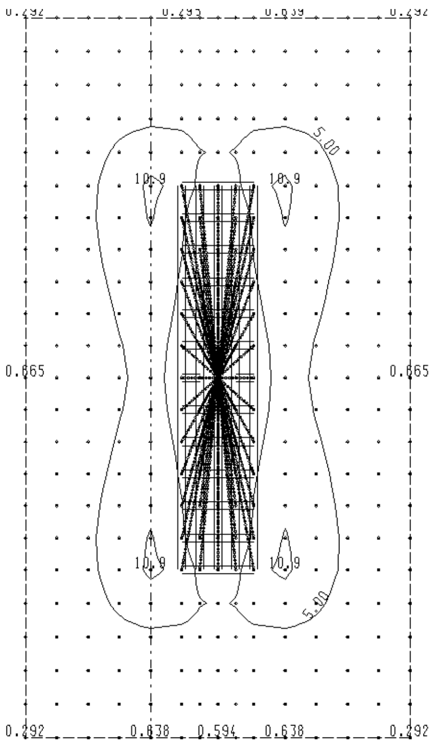

(a) Top cross reinforcements

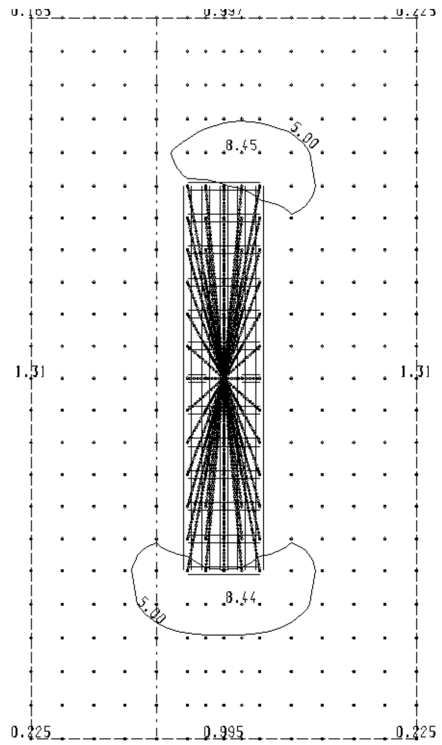

(b) Top main reinforcements

Figure 11.10: Footing reinforcement
Σχήμα 11.10: Οπλισμός πλάκας θεμελίωσης

11.7 DESIGN OF THE OTHER MEMBERS OF THE BRIDGE

11.7.1. Design of the superstructure

Considering that the prestressed superstructure of the bridge was designed against persistent design situations, the design process presented in the conventional design is also here taken into account.

Moreover, an additional check of the superstructure was carried out, for the case of soil liquefaction immediately after and after the seismic excitation. To this end, the displacements Δ at the base of the pier bearings, resulted under liquefaction-produced settlements at the base of the pier, i.e. residual seismic settlement ρ_{dyn} =6,8cm along with the relevant rotations (see section 11.3.7), were induced in the model of Figure 11.11.

The seismic combination (G+0.2Q+S) and the persistent combination (1.15G+1.35Q+S) were examined. The results showed that all checks at the Serviceability Limit State as well as at the Ultimate Limit State were satisfied.

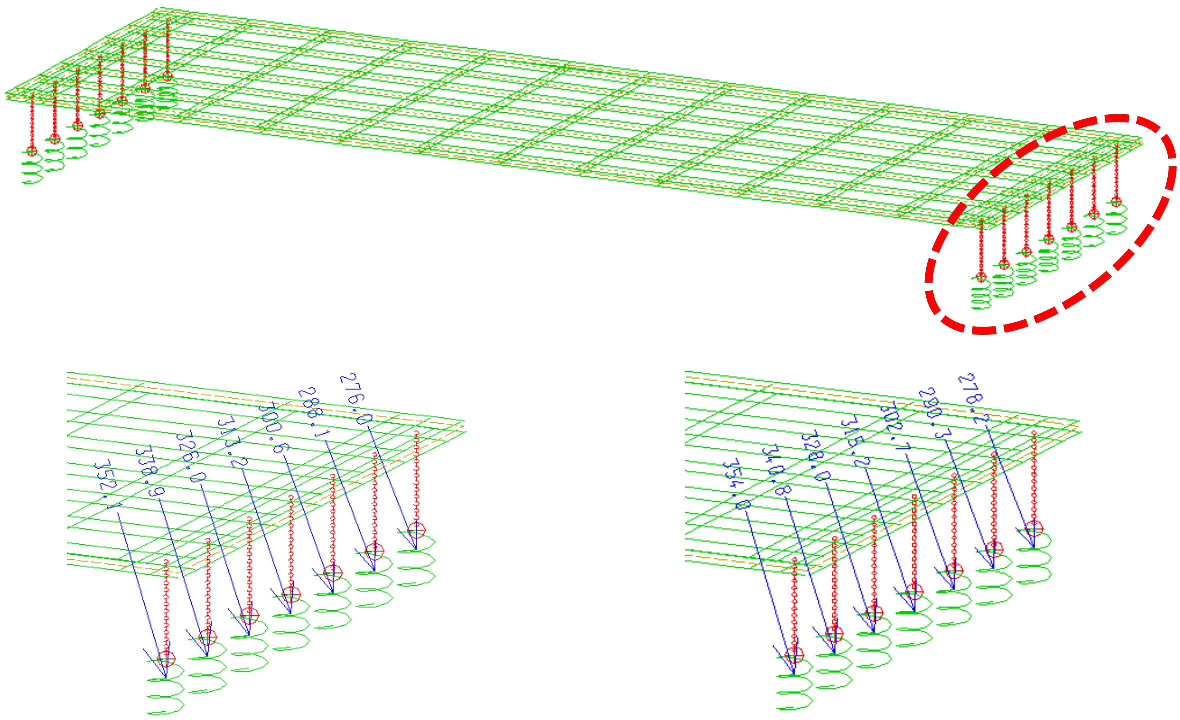

(a) (b)

Figure 11.11: Model of the superstructure and the imposed displacements at the base of pier bearings for a) the seismic and b) the persistent combination

Σχήμα 11.11: Προσομοίωμα ανωδομής και οι επιβαλλόμενες μετατοπίσεις στη βάση των εφεδράνων του μεσοβάθρου για a) το σεισμικό και b) το μόνιμο συνδυασμό.

11.7.2. Design of bearings and expansion joints

11.7.2.1. Abutments's bearings

1. CHECK OF BEARINGS FOR SEISMIC CONDITIONS
(ACCORDING TO EC8)

ABUTMENT

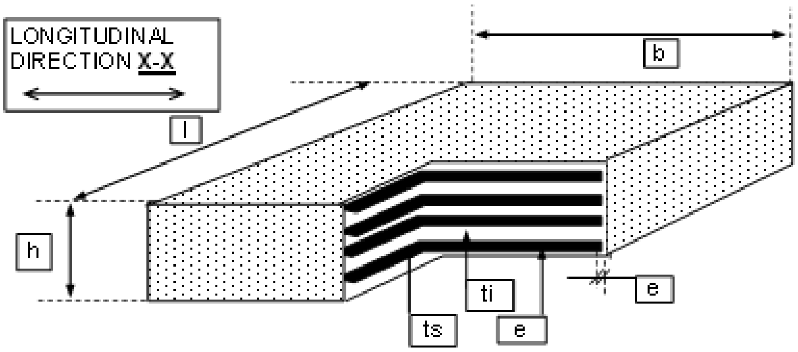

1 . Geometrical characteristics

Width	b =	400	mm
Length	l =	500	mm
Overall thickness of bearing	h =	171	mm
Thickness of external rubber layer	t_o =	0	mm
Thickness of internal rubber layer	t_i =	11	mm
No of internal rubber layers		9	
No of external rubber layers		0	
Thickness of steel plate	t_s =	4	mm
No of steel plates		8	
Effective rubber thickness	Σt_i =	99	mm
Effective plan area of bearing	A_e=	195525	mm^2
Shape coefficient	S =	10,10	
Failure elongation	V_{bu} =	5	
Shear modulus G	G =	1,125	MPa
Horizontal stiffness of the bearing	K_h =	2221,9	KN / m
Vertical stiffness of the bearing	K_v=	880753	KN / m
Rotational stiffness of the bearing	$K\varphi_{yy}$=	9617	KNm/rad
Rotational stiffness of the bearing	$K\varphi_{xx}$=	23479	KNm/rad

2 . Loads - displacements - rotations

2.1 Vertical loads (Compression positive)

Dead loads	R_g =	796,07	KN
Super dead loads	R_{go} =	210,31	KN
Prestress and prestress losses	R_p =	0,00	KN
Live loads (MAX)	R_q =	463,46	KN
Uniform road traffic loads	R_{qo}=	163,93	KN
Longitudinal earthquake	RE_{Qxx}=	36,26	KN
Lateral earthquake	RE_{Qyy}=	184,89	KN
Vertical earthquake	RE_{Qzz}=	165,38	KN
Live loads (MIN)	R_q =	0,00	KN

2.2 Displacements

Displacement x-x			
Displacement due to dead load	$d_{\beta 1x}$=	-3,04	mm
Displacement due to uniform road traffic loads	$d_{\beta 2x}$=	-0,60	mm
Displacement due to creep and shrinkage	$d_{\beta 3x}$ =	12,71	mm
Displacement due to temperature	d_{Tx} =	14,40	mm
Displacement y-y			
Displacement due to dead load	$d_{\beta 1y}$=	0,00	mm
Displacement due to uniform road traffic loads	$d_{\beta 2y}$=	0,00	mm
Displacement due to creep and shrinkage	$d_{\beta 3y}$ =	0,00	mm
Displacement due to temperature	d_{Ty} =	1,05	mm

2.3 Rotations

Rotation αx			
Rotation due to dead load	$\alpha_{\beta 1x}$=	0,00	$x10^{-3}$rad
Rotation due to uniform road traffic loads	$\alpha_{\beta 2x}$=	0,00	$x10^{-3}$rad
Rotation due to creep and shrinkage	$\alpha_{\beta 3x}$ =	0,00	$x10^{-3}$rad
Rotation due to temperature	α_{Tx} =	0,00	$x10^{-3}$rad
Rotation αy			
Rotation due to dead load	$\alpha_{\beta 1y}$=	4,27	$x10^{-3}$rad
Rotation due to uniform road traffic loads	$\alpha_{\beta 2y}$=	0,90	$x10^{-3}$rad
Rotation due to creep and shrinkage	$\alpha_{\beta 3y}$ =	0,00	$x10^{-3}$rad
Rotation due to temperature	α_{Ty} =	0,00	$x10^{-3}$rad

3. Check in direction X-X (LONGITUDINAL DIRECTION)

3.1 Max displacements and rotations of bearing

From dynamic analysis	ds_{dx} =	162,54	mm
	ds_{dy} =	43,47	mm
Design displacement x-x	d_{Edx}=	178,81	mm
Design displacement y-y	d_{Edy}=	44,00	mm
	d_{Ed} =	184,14	mm
From dynamic analysis	α_{sx}=	0,00	$x10^{-3}$rad
	α_{sy}=	0,20	$x10^{-3}$rad
Design rotation αx	α_{Edx}=	0,00	$x10^{-3}$rad
Design rotation αy	α_{Edy}=	5,37	$x10^{-3}$rad

3.2 Design shear strain due to horizontal displacement

CHECK $\varepsilon_{q,d} = dE_d / \Sigma t_r < 2.0$	$\varepsilon_{q,d}$=	**1,86 < 2,0 O.K**

3.3 Design shear strain due to compressive load

Seismic design displacement	d_{Ed} =	184,14	mm
Effective area of bearing in x-x	A_r=	114345	mm2
Max compressive load for the design earthquake	N_{sd} =	1180,5	KN
Max effective normal stress	σ_e =	10324	KN/m²
Shear modulus	G =	1,125	MPa
Deformation due to vertical loads	$\varepsilon_{c,d}=1.5\sigma_e/SG$=	**1,363**	

3.4 Design shear strain due to angular distortion

$\varepsilon_{\alpha,d} = (l^2\,\alpha_x + b^2\,\alpha_y)\,t_i \,/\, 2\Sigma t_i^3$	$\varepsilon_{\alpha,d}$ =	0,395
CHECK Max design strain: $\varepsilon_{q,d}+\varepsilon_{c,d}+\varepsilon_{\alpha,d}<\varepsilon_{u,d}$		3,618 < 7,0 O.K

3.5 Check against slip (anchorage)

Max shear force	V_{Ed} =	409,14	KN
Min vertical design force	N_{Ed} =	897,8	KN
CHECK $\sigma_e = N_{Ed} / A_r$ > = 3,0 MPa	=	7,85 > 3,0 O.K	
V_{Ed} / N_{Ed}	=	0,46	
$\alpha+\beta/\sigma_e$= 0,10 + 1,5x0,6 / σ_e =	=	0,21	
CHECK V_{Ed}/N_{Ed}<=0,10+0,9/σ_e		ANCHORAGE	FOR BEARINGS WITH EXTERNAL RUBBER LAYER
$\alpha+\beta/\sigma_e$= 0,50 + 1,5x0,6 / σ_e =	=	0,61	
CHECK V_{Ed}/N_{Ed}<=0,50+0,9/σ_e		O.K.	FOR BEARINGS WITH EXTERNAL STRIPED PLATES

3.6 Check against buckling

Max vertical design force	N_{Ed} =	1180,5	kN
$\sigma_e = N_{Ed} / A_r$	=	10,32	kN
2 min(b,l) G S / 3 Σti	=	30,61	kN
CHECK $\sigma_{e,d}$<2 min(b,l) G S / 3 Σt_i		O.K.	

4. Check in direction Y-Y (LATERAL DIRECTION)

4.1 Max displacement of bearing

From dynamic analysis	ds_{dx} =	48,76	mm
	ds_{dy} =	144,92	mm
Design displacement x-x	d_{Edx}=	65,03	
Design displacement y-y	d_{Edy}=	145,45	mm
	d_{Ed} =	159,32	mm
From dynamic analysis	α_{sx}=	0,18	x10^{-3}rad
	α_{sy}=	0,16	x10^{-3}rad
Design rotation αx	α_{Edx}=	0,18	x10^{-3}rad
Design rotation αy	α_{Edy}=	5,33	x10^{-3}rad

4.2 Design shear strain due to horizontal displacement

CHECK $\varepsilon_{q,d} = dE_d \,/\, \Sigma t_i < 2.0$ = **1,61 < 2.0 O.K**

4.3 Design shear strain due to compressive load

Seismic design displacement	d_{Ed} =	159,32	mm
Effective area of bearing in x-x	A_r=	110724	mm²
Max compressive load for the design earthquake	N_{sd} =	1284,5	KN
Max effective normal stress	σ_e =	11601	KN/m²

Shear modulus	$G =$	1,125 MPa
Deformation due to vertical loads	$\varepsilon_{c,d}=1.5\sigma_e/SG=$	**1,531**

4.4 Design shear strain due to angular distortion

$\varepsilon_{\alpha,d} = (l^2\,\alpha_x + b^2\,\alpha_y)\,t_i\,/\,2\Sigma t_i^3$	$\varepsilon_{\alpha,d}=$	**0,412**
CHECK Max design strain: $\varepsilon_{q,d}+\varepsilon_{c,d}+\varepsilon_{\alpha,d}<\varepsilon_{u,d}$		**3,553 < 7,0 O.K**

4.5 Check against slip (anchorage)

Max shear force	$V_{Ed} =$	353,99 KN	
Min vertical design force	$N_{Ed} =$	793,8 KN	
CHECK $\sigma_e = N_{Ed}/A_r >= 3{,}0$ **MPa**	=	**7,17 > 3,0 O.K**	
V_{Ed}/N_{Ed}	=	0,45	
$\alpha+\beta/\sigma_e=0{,}10 + 1{,}5x0{,}6/\sigma_e =$	=	0,23	
CHECK $V_{Ed}/N_{Ed}<=0{,}10+0{,}9/\sigma_e$		ANCHORAGE	FOR BEARINGS WITH EXTERNAL RUBBER LAYER
$\alpha+\beta/\sigma_e=0{,}50 + 1{,}5x0{,}6/\sigma_e =$	=	0,63	
CHECK $V_{Ed}/N_{Ed}<=0{,}50+0{,}9/\sigma_e$		**O . K**	FOR BEARINGS WITH EXTERNAL STRIPED PLATES

4.6 Check against buckling

Max vertical design force	$N_{Ed} =$	1284,5 kN
$\sigma_e = N_{Ed}/A_r$	=	11,60 kN
$2\min(b,l)\,G\,S\,/\,3\,\Sigma ti$	=	30,61 kN
CHECK $\sigma_{e,d}<2\min(b,l)\,G\,S\,/\,3\,\Sigma t_i$		**O.K.**

2. CHECK OF BEARINGS FOR STATIC CONDITIONS
(ACCORDING TO DIN 4141)

Dimensions of bearing	b=	400	mm
	l=	500	mm
Overall rubber thickness	Σt_i=	**99**	mm
Bearing area	A_e=	195525	mm^2
Total displacement : dG+1,5*0,6*dDT+1,5dbr=	**u=**	**42,28**	mm
Max vertical load	**Pmax=**	1469,8	KN
Min vertical load	**Pmin=**	1006,38	
Για $\Sigma t_i<=b/5$ --> $\tan\gamma_{\varepsilon\pi\iota\tau}=0.70$	$\tan\gamma_{\varepsilon\pi\iota\tau}$=	–	
Για $\Sigma t_i>=b/5$ --> $\tan\gamma_{\varepsilon\pi\iota\tau}=0.70-[(\Sigma t_i/b)-0.2]$	$\tan\gamma_{\varepsilon\pi\iota\tau}$=	**0,6525**	
	$\tan\gamma=u/\Sigma t_i$	**0,427**	**O.K**
Max normal stress of bearing : $\sigma_{max}=P/A=$	σ_{max}=	**7,52**	**< 15,0 MPa**
Min normal stress of bearing : $\sigma_{min}=P/A=$	σ_{min}=	**5,15**	**> 5,0 Mpa**

11.7.2.2. *Pier's bearings*

1. CHECK OF BEARINGS FOR SEISMIC CONDITIONS
(ACCORDING TO EC8)

PIER

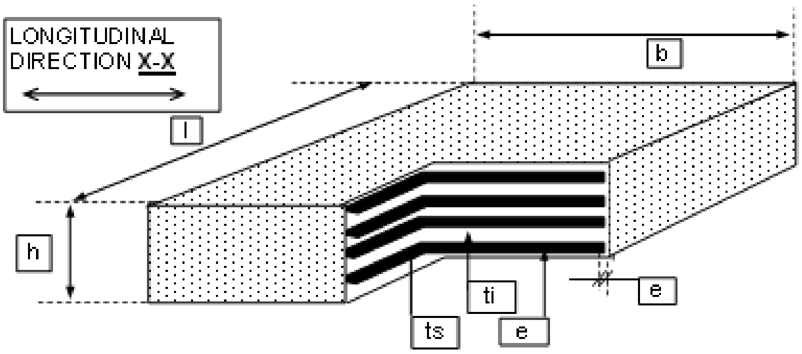

1 . Geometrical characteristics

Width	b =	350	mm
Length	l =	450	mm
Overall thickness of bearing	h =	160	mm
Thickness of external rubber layer	t_o =	0	mm
Thickness of internal rubber layer	t_i =	11	mm
No of internal rubber layers		8	
No of external rubber layers		0	
Thickness of steel plate	t_s =	4	mm
No of steel plates		8	
Effective rubber thickness	Σt_i =	88	mm
Effective plan area of bearing	A_e=	153525	mm^2
Shape coefficient	S =	8,95	
Failure elongation	V_{bu} =	5	
Shear modulus G	G =	1,125	MPa
Horizontal stiffness of the bearing	K_h =	1962,7	KN / m
Vertical stiffness of the bearing	K_v=	641411	KN / m
Rotational stiffness of the bearing	$K\varphi_{yy}$=	4994	KNm/rad
Rotational stiffness of the bearing	$K\varphi_{xx}$=	13647	KNm/rad

2 . Loads - displacements - rotations

2.1 Vertical loads (Compression positive)

Dead loads	R_g =	784,32	KN
Super dead loads	R_{go} =	213,82	KN
Prestress and prestress losses	R_p =	0,00	KN
Live loads (MAX)	R_q =	349,62	KN
Uniform road traffic loads	R_{qo}=	167,33	KN
Longitudinal earthquake	RE_{Qxx}=	198,59	KN
Lateral earthquake	RE_{Qyy}=	179,04	KN
Vertical earthquake	RE_{Qzz}=	181,78	KN
Live loads (MIN)	R_q =	0,00	KN

2.2 Displacements

Displacement x-x

Displacement due to dead load	$d_{\beta 1x}$=	8,58	mm
Displacement due to uniform road traffic loads	$d_{\beta 2x}$=	1,79	mm
Displacement due to creep and shrinkage	$d_{\beta 3x}$ =	0,00	mm
Displacement due to temperature	d_{Tx} =	0,40	mm

Displacement y-y

Displacement due to dead load	$d_{\beta 1y}$=	0,00	mm
Displacement due to uniform road traffic loads	$d_{\beta 2y}$=	0,00	mm
Displacement due to creep and shrinkage	$d_{\beta 3y}$ =	0,00	mm
Displacement due to temperature	d_{Ty} =	1,20	mm

2.3 Rotations

Rotation αx

Rotation due to dead load	$\alpha_{\beta 1x}$=	0,00	$x10^{-3}$rad
Rotation due to uniform road traffic loads	$\alpha_{\beta 2x}$=	0,00	$x10^{-3}$rad
Rotation due to creep and shrinkage	$\alpha_{\beta 3x}$ =	0,00	$x10^{-3}$rad
Rotation due to temperature	α_{Tx} =	0,00	$x10^{-3}$rad

Rotation αy

Rotation due to dead load	$\alpha_{\beta 1y}$=	-3,17	$x10^{-3}$rad
Rotation due to uniform road traffic loads	$\alpha_{\beta 2y}$=	-0,80	$x10^{-3}$rad
Rotation due to creep and shrinkage	$\alpha_{\beta 3y}$ =	0,00	$x10^{-3}$rad
Rotation due to temperature	α_{Ty} =	0,00	$x10^{-3}$rad

3. Check in direction X-X (LONGITUDINAL DIRECTION)

3.1 Max displacements and rotations of bearing

From dynamic analysis	ds_{dx} =	138,83	mm
	ds_{dy} =	47,27	mm
Design displacement x-x	d_{Edx}=	149,40	mm
Design displacement y-y	d_{Edy}=	47,87	mm
	d_{Ed} =	156,88	mm
From dynamic analysis	α_{sx}=	0,00	$x10^{-3}$rad
	α_{sy}=	3,87	$x10^{-3}$rad
Design rotation αx	α_{Edx}=	0,00	$x10^{-3}$rad
Design rotation αy	α_{Edy}=	7,84	$x10^{-3}$rad

3.2 Design shear strain due to horizontal displacement

CHECK $\varepsilon_{q,d} = dE_d / \Sigma t_r < 2.0$ $\varepsilon_{q,d}$= **1,78 < 2,0 O.K**

3.3 Design shear strain due to compressive load

Seismic design displacement	d_{Ed} =	156,88	mm
Effective area of bearing in x-x	A_r=	90820	mm2
Max compressive load for the design earthquake	N_{sd} =	1338,4	KN
Max effective normal stress	σ_e =	14737	KN/m²
Shear modulus	G =	1,125	MPa
Deformation due to vertical loads	$\varepsilon_{c,d}=1.5\sigma_e/SG$=	**2,196**	

3.4 Design shear strain due to angular distortion

$\varepsilon_{a,d} = (l^2 \alpha_x + b^2 \alpha_y)\, t_i / 2\Sigma t_i^3$ $\varepsilon_{a,d}$= 0,496

CHECK Max design strain: $\varepsilon_{q,d}+\varepsilon_{c,d}+\varepsilon_{a,d}<\varepsilon_{u,d}$ 4,475 < 7,0 O.K

3.5 Check against slip (anchorage)

Max shear force	V_{Ed} =	307,91 KN
Min vertical design force	N_{Ed} =	724,8 KN
CHECK $\sigma_e = N_{Ed} / A_r$ > = 3,0 MPa	=	7,98 > 3,0 O.K
V_{Ed} / N_{Ed}	=	0,42
$\alpha+\beta/\sigma_e$= 0,10 + 1,5x0,6 / σ_e =	=	0,21
CHECK V_{Ed}/N_{Ed}<=0,10+0,9/σ_e	ANCHORAGE	FOR BEARINGS WITH EXTERNAL RUBBER LAYER
$\alpha+\beta/\sigma_e$= 0,50 + 1,5x0,6 / σ_e =	=	0,61
CHECK V_{Ed}/N_{Ed}<=0,50+0,9/σ_e	O.K.	FOR BEARINGS WITH EXTERNAL STRIPED PLATES

3.6 Check against buckling

Max vertical design force	N_{Ed} =	1338,4 kN
$\sigma_e = N_{Ed} / A_r$	=	14,74 kN
2 min(b,l) G S / 3 Σti	=	26,69 kN
CHECK $\sigma_{e,d}$<2 min(b,l) G S / 3 Σt_i		O.K.

4. Check in direction Y-Y (LATERAL DIRECTION)

4.1 Max displacement of bearing

From dynamic analysis	ds_{dx} =	41,65 mm
	ds_{dy} =	157,56 mm
Design displacement x-x	d_{Edx}=	52,22
Design displacement y-y	d_{Edy}=	158,16 mm
	d_{Ed} =	166,56 mm
From dynamic analysis	α_{sx}=	0,15 $x10^{-3}$rad
	α_{sy}=	0,04 $x10^{-3}$rad
Design rotation αx	α_{Edx}=	0,15 $x10^{-3}$rad
Design rotation αy	α_{Edy}=	4,01 $x10^{-3}$rad

4.2 Design shear strain due to horizontal displacement

CHECK $\varepsilon_{q,d} = dE_d / \Sigma t_i$<2.0 = 1,89 < 2.0 O.K

4.3 Design shear strain due to compressive load

Seismic design displacement	d_{Ed} =	166,56 mm
Effective area of bearing in x-x	A_r=	76310 mm²
Max compressive load for the design earthquake	N_{sd} =	1324,8 KN
Max effective normal stress	σ_e =	17360 KN/m²

Shear modulus	$G =$	1,125 MPa
Deformation due to vertical loads	$\varepsilon_{c,d}=1.5\sigma_e/SG=$	**2,587**

4.4 Design shear strain due to angular distortion

$\varepsilon_{\alpha,d} = (l^2\alpha_x + b^2\alpha_y)\,t_i / 2\Sigma t_i^3$	$\varepsilon_{\alpha,d}=$	**0,269**
CHECK Max design strain: $\varepsilon_{q,d}+\varepsilon_{c,d}+\varepsilon_{\alpha,d}<\varepsilon_{u,d}$		**4,749 < 7,0 O.K**

4.5 Check against slip (anchorage)

Max shear force	$V_{Ed} =$	326,90 KN	
Min vertical design force	$N_{Ed} =$	738,5 KN	
CHECK $\sigma_e = N_{Ed}/A_r >= 3{,}0$ MPa	=	**9,68 > 3,0 O.K**	
V_{Ed}/N_{Ed}	=	0,44	
$\alpha+\beta/\sigma_e = 0{,}10 + 1{,}5x0{,}6 / \sigma_e =$	=	0,19	
CHECK $V_{Ed}/N_{Ed}<=0{,}10+0{,}9/\sigma_e$		ANCHORAGE	FOR BEARINGS WITH EXTERNAL RUBBER LAYER
$\alpha+\beta/\sigma_e = 0{,}50 + 1{,}5x0{,}6 / \sigma_e =$	=	0,59	
CHECK $V_{Ed}/N_{Ed}<=0{,}50+0{,}9/\sigma_e$		**O . K**	FOR BEARINGS WITH EXTERNAL STRIPED PLATES

4.6 Check against buckling

Max vertical design force	$N_{Ed} =$	1324,8 kN
$\sigma_e = N_{Ed}/A_r$	=	17,36 kN
2 min(b,l) G S / 3 Σti	=	26,69 kN
CHECK $\sigma_{e,d}<2\min(b,l)\,G\,S/3\,\Sigma t_i$		**O.K.**

. CHECK OF BEARINGS FOR STATIC CONDITIONS
(ACCORDING TO DIN 4141)

Dimensions of bearing	b=	350	mm
	l=	450	mm
Overall rubber thickness	Σt_i=	88	mm
Bearing area	A_e=	153525	mm^2
Total displacement : dG+1,5*0,6*dDT+1,5dbr=	**u=**	**22,59**	mm
Max vertical load	Pmax=	1347,8	KN
Min vertical load	Pmin=	998,14	
Για $\Sigma t_i<=b/5$ --> $\tan\gamma_{\varepsilon\pi\iota\tau}=0.70$	$\tan\gamma_{\varepsilon\pi\iota\tau}$=	–	
Για $\Sigma t_i>=b/5$ --> $\tan\gamma_{\varepsilon\pi\iota\tau}=0.70-[(\Sigma t_i/b)-0.2]$	$\tan\gamma_{\varepsilon\pi\iota\tau}$=	**0,648571**	
	$\tan\gamma=u/\Sigma t_i$	**0,257**	**O.K**
Max normal stress of bearing : $\sigma_{max}=P/A=$	σ_{max}=	**8,78**	**< 15,0 MPa**
Min normal stress of bearing : $\sigma_{min}=P/A=$	σ_{min}=	**6,50**	**> 5,0 Mpa**

11.7.2.3. *Expansion joints*

A) SEISMIC CONDITIONS

Design displacement for the loading direction i-i

$$d_{Edi}=\pm 0.4d_E+d_G\pm 0.5d_T$$

where:

d_E= Design seismic displacement

and $d_E=(d^2_{E1}+d^2_{E2})^{1/2}$ max relative displacement between two statically independent sections 1 and 2

d_G= Displacement of permanent or quasi-permanent actions (creep, shrinkage)

d_T= Displacement due to temperature actions (DT=-37/+57°C)

$$d_{Ed}=(d^2_{Edi}+d^2_{Edj})^{1/2}$$

where: d_{Edi} design displacement in main loading direction (i - i) and

d_{Edj} 30% of the design displacement in the lateral direction (j -j)

• CHECK	OPENING	CLOSURE	GAP
In direction x-x			
d_{E1}=	172,93 mm	-179,93	
d_{E2}=	0,00 mm	0,00	
d_E=	172,93 mm	-179,93	
dG=	20,33 mm	0,00	
dT=	15,64 mm	-24,09	
$d_{Edx}=0.4d_E+d_G+0.5d_T$=	97,32 mm	-84,02 mm	201,08
In direction y - y			
d_{E1}=	165,93 mm	-165,93	
d_{E2}=	0,00 mm	0,00	
d_E=	165,93 mm	-165,93	
dG=	0,00 mm	0,00	
dT=	0,00 mm	0,00	
$d_{Edy}=0.4d_E+d_G+0.5d_T$=	66,37 mm	-66,37 mm	165,93
Finally $d_{Ed}=((0,3*d_{Edx})^2+d^2_{Edy})^{1/2}$=	72,51 mm	-71,00 mm	176,56
$d_{Ed}=(d^2_{Edx}+(0,3*d_{Edy})^2)^{1/2}$=	99,34 mm	-86,34 mm	207,15

B) STATIC CONDITIONS

Design displacement for the loading direction i-i: **d=dG+-1,5*0,6*dT+1,5*dbr**

d_G= Displacement of permanent or quasi-permanent actions

d_T= Displacement due to temperature actions (DT=-37/+57°C)

d_{br}= Displacement due to braking

• CHECK	OPENING	CLOSURE
In direction x-x		
d_{br}=	13,38 mm	-9,10
dG=	20,33 mm	0,00
dT=	15,64 mm	-24,09
d=dG+-1,5*0,6*dT+1,5*Dbr=	54,48 mm	-35,33 mm

An expansion joint type Algaflex or similar is chosen: <u>**T 200** (+ - 100 mm)</u>

12. VERIFICATION (step 6)

According to the final design of the bridge presented in section 11, the reinforcement ratio of the pier was modified as presented in Figure 11.8. Thus, an iteration of the design procedure from step 2 had to be carried out.

Firstly, the yield bending moment $M_{Rd,y}$ of the bottom section of the pier was recalculated. The bending moment – curvature curve of this section was constructed by means of the software Opensees. The design values of the properties of the materials were used.

Two load combinations were examined, in order to account for the maximum and the minimum axial load of the pier, namely:

for N_{max} : $\xi \cdot \gamma_G \cdot (G+S)$ "+" $\gamma_P \cdot P$ "+" $\gamma_Q \cdot Q$ => $(0.85x1.35) \cdot G$ "+" P "+" 1.35Q =>

1.15G + 1.15S "+" P "+" 1.35Q (12.1)

for N_{min} : G + $\xi \cdot \gamma_G \cdot S$ "+" P => G + 1.15S "+" P (12.2)

The moment – curvature curve at the base of the pier is illustrated in Figure 12.1 and 12.2 for N_{max} and N_{min} respectively. The bilinear approximation of the original curves is also shown. The rule of almost equal areas above and below the actual curve is used, along with the fact that the initial branch of the bilinear curve passes from that point of the actual curve which corresponds to 60% of the resulting yield moment $M_{Rd,y}$.

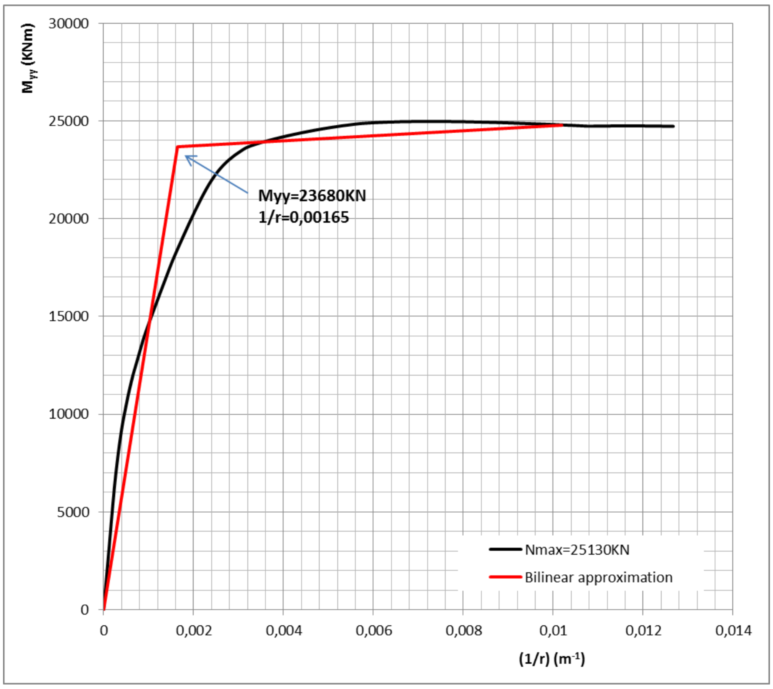

Figure 12.1: Moment- curvature curve at the base of the pier and its bilinear approximation (for N_{max})

Σχήμα 12.1: Διάγραμμα ροπών-καμπυλοτήτων στη βάση του μεσοβάθρου και η διγραμμική του προσέγγιση (για N_{max})

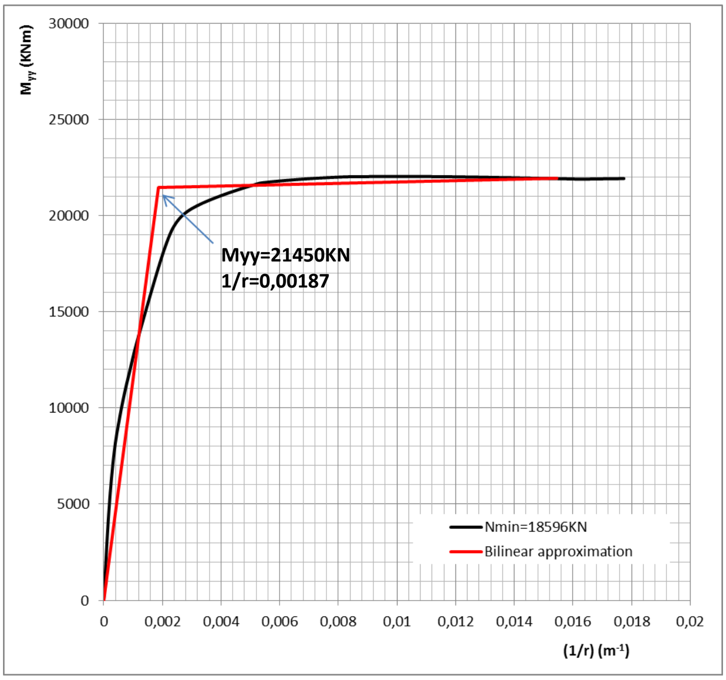

Figure 12.2: Moment- curvature curve at the base of the pier and its bilinear approximation (for N_{min})

Σχήμα 12.2: Διάγραμμα ροπών-καμπυλοτήτων στη βάση του μεσοβάθρου και η διγραμμική του προσέγγιση (για N_{min})

The results are summarized in Table 12.1, where the yield moment at the base of the pier $M_{Rd,y}$, the corresponding curvature $(1/r)_y$, the failure moment $M_{Rd,u}$ and the corresponding curvature $(1/r)_u$ are given. Also k_e is the initial elastic stiffness and K_p the stiffness of the plastic branch.

Table 12.1: Bilinear approximations of moment-curvature curves at the base of the pier

Πίνακας 12.1: Διγραμμικές προσεγγίσεις του διαγράμματος ροπών-καμπυλοτήτων στη βάση του μεσοβάθρου

	$M_{Rd,y}$ (kNm)	$(1/r)_y$ (m^{-1})	$M_{Rd,u}$ (kNm)	$(1/r)_u$ (m^{-1})	$a=K_p/k_e$
N_{max}	23680	1.65×10^{-3}	24793	10.20×10^{-3}	0.91%
N_{min}	21450	1.87×10^{-3}	21917	15.50×10^{-3}	0.30%

Then, a refined finite element model of the studied bridge, through the software Opensees, was prepared and the maximum allowable settlement ρ_{all} of the pier was calculated, as the settlement at which the yield moment at the base of the pier was reached, under the persistent combinations of loads, presented in equations (12.1) and (12.2). To this end, a nonlinear static (pushover) analysis was performed through a step-wise procedure of gradually simultaneously increasing settlements and rotations S at the base of the pier, according to equations (12.3) or (12.4).

$$S = \rho + \varphi_y + 0.3\varphi_x \quad (12.3)$$

$$S = \rho + \varphi_x + 0.3\varphi_y \quad (12.4)$$

Moreover, settlements and rotations are considered to be related according to the following empirical relationship, though derived for buildings (Yasuda, 2014):

$\varphi_x = \varphi_y = 0.05 \cdot \rho$ (12.5)

where: ρ is the induced settlement (in cm) and φ_x, φ_y the resultant rotations about the strong and the weak axis of the pier, respectively (in degrees).

A distributed plasticity model was adopted for the non-linear behaviour of the pier.

It was found that the most critical combination of imposed deformations S, is that of equation (12.3), namely $\Delta = \rho + \varphi_y + 0.3\varphi_x$, mainly due to the imposed rotation φ_y about the weak axis of the section. In Figures 12.6 and 12.7 the moment M_{yy} developed about the weak axis of the pier is computed against the imposed settlement at the base of the pier, for N_{max} and N_{min} respectively. Then, the allowable settlement is defined as the critical settlement producing the yield moment $M_{Rd,y}$ at the base of the pier.

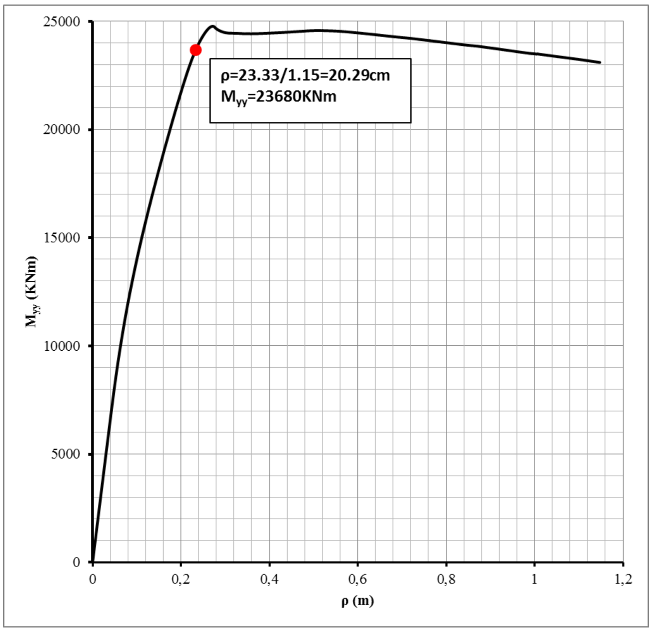

Figure 12.6: Moments at the base of the pier against imposed settlements derived from pushover analysis (for N_{max})

Σχήμα 12.6: Διάγραμμα ροπών στη βάση του μεσοβάθρου έναντι επιβαλλόμενων καθιζήσεων, όπως προέκυψε από τη μη γραμμική ανάλυση (για N_{max})

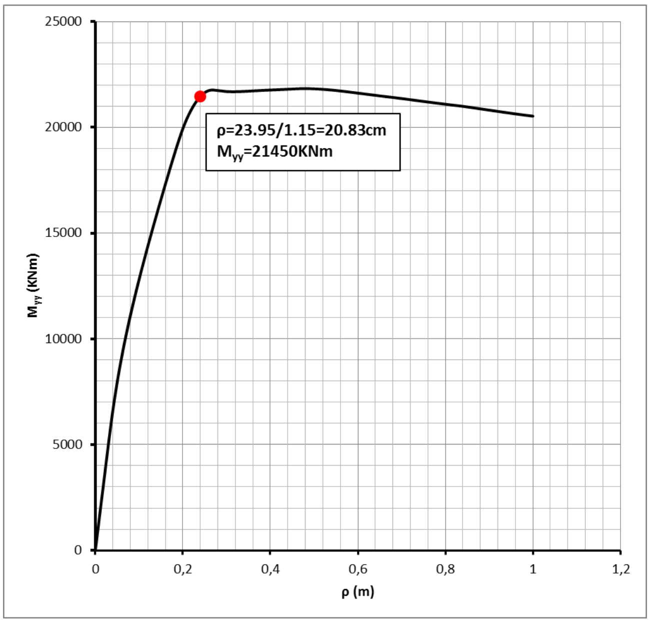

Figure 8: Moment at the base of the pier against imposed settlement derived from pushover analysis (for N_{min})

Σχήμα 8: Διάγραμμα ροπών στη βάση του μεσοβάθρου έναντι επιβαλλόμενων καθιζήσεων όπως προέκυψε από τη μη γραμμική ανάλυση (για N_{min})

The allowable values of the critical parameters for the design of the innovative bridge, according to the aforementioned results are summarized in Table 12.2, along with the corresponding inclination angles (drifts) θ of the pier, defined as θ=δ/h, where δ the relative displacement between the top and the bottom of the pier and h the height of the pier.

Table 12.2: Allowable values of critical parameters for the design of the innovative bridge derived from the non-linear analysis

Πίνακας 12.2: Μέγιστες επιτρεπτές τιμές κρίσιμων παραμέτρων για το σχεδιασμό της πρωτότυπης γέφυρας, που προέκυψαν από τη μη γραμμική ανάλυση

Combination	ρ_{all} **(cm)**	$\varphi_{y,y}$ **(rad)**	$\varphi_{x,x}$ **(rad)**	θ_y **(rad)**	$M_{Rd,y}$ **(kNm)**
1.15(G+S)+P+1.35Q (for N_{max})	20.3	0.018	0.006	0.0116	23680
G+1.15S+P (for N_{min})	20.8	0.018	0.006	0.0108	21450

As a conclusion, for the most unfavorable loading case of N_{max}, the allowable settlement of the foundation was estimated equal to 20.3cm. Taking into account that, for the certain dimensions of the footing and the curst, the value of the max settlement produced after liquefaction is limited to 6.8cm (as defined in section 10), there was no need to proceed to the next steps of the process.

13. COMPARISON OF THE RESULTS

13.1 Technical Comparison

As described in details previously, the concept of the innovative design is to allow to the ground beneath the foundation system (the shallow footing and the curst) to liquefy. Thus, essentially lower inertial seismic loads are induced into the structure, as it is clearly presented in Figure 13.1, where the elastic response spectra for the cases of the conventional and of the innovative design are illustrated. In fact, the accelerations developed in the structure in the latter case (innovative design and seismic event with T_{ret}=1000years which produces soil liquefaction) have been reduced to almost the half values as compared to those of the conventional design. More specifically, $S_{e,conv.}$=3.22m/sec^2 in the case of the conventional design where the predominant eigenperiod of the bridge is T_{br}=1.56sec, while $S_{e,innov.}$=1.54m/sec^2 in the case where the soil is allowed to liquefy (innovative design for T_{ret}=1000years and T_{br}=1.53sec).

On the other hand, the asynchrony motion between abutment and pier (due to their different foundation conditions) resulted to additional horizontal displacements at the base of the pier, which produced additional stress and deformations to the structural components of the structure. The magnitude of these relative displacements, however, was limited to about 12 cm, as indicated by appropriate data (time histories, see Appendix A) provided by the Geotechnical Team.

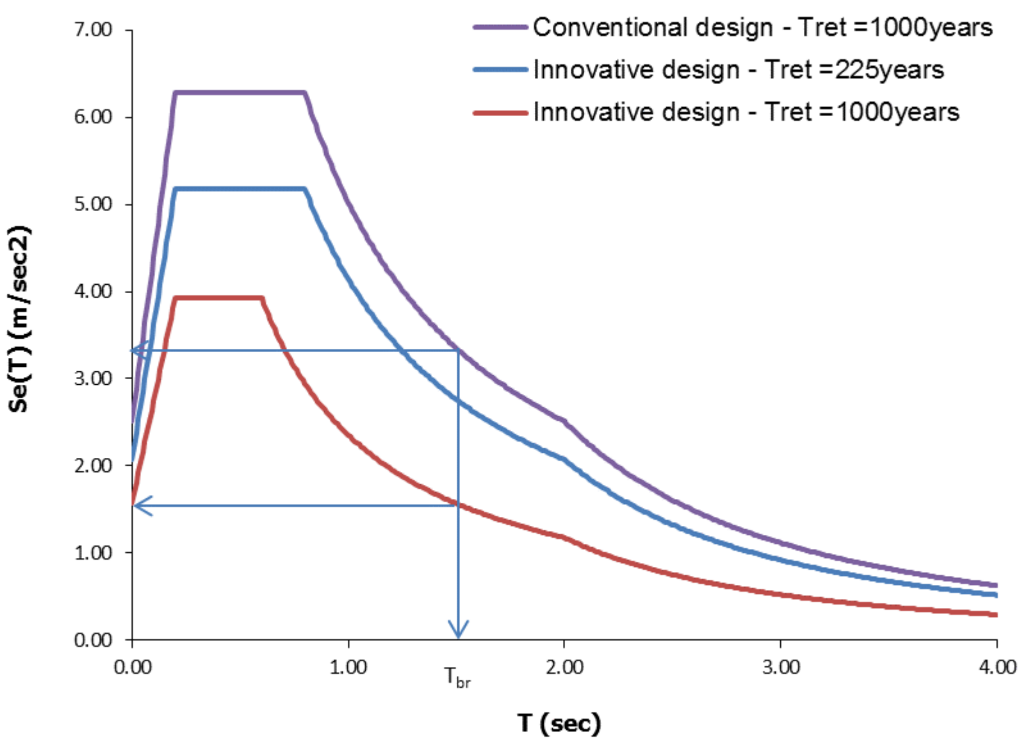

Figure 13.1: Elastic response spectra taken into account in the conventional and the innovative bridge design

Σχήμα 13.1: Ελαστικά φάσματα απόκρισης που λήφθηκαν υπόψη κατά το συμβατικό και τον πρωτότυπο σχεδιασμό της γέφυρας

As expected for statically determinate bridges, the most critical structural member of the bridge proved to be the pier, which essentially dictated the behavior of the entire system against seismic actions and liquefaction-induced deformations. In Table 13.1 are displayed the moments M_y at the base of the pier developed for the conventional and for the innovative bridge design (about the weak axis of the pier). Although the pier suffered essentially lower stress due to inertial seismic loads in case of liquefaction, it proved to be sensitive to the imposed horizontal displacements. However, for the magnitude of the displacements applied, the stress developed in total was significantly lower than that of the conventional design.

Finally, for the innovative design, it was proved that the decisive seismic load combination was that of the case of no liquefaction, obtained for the seismic event with T_{ret} of 225 years. The stress developed at the pier for this case, was by 15% lower than that of the conventional design, thus leading to a lower required reinforcement ratio of the pier.

Table 13.1: Moments M_y at the base of the pier developed for the conventional and for the innovative bridge design (about the weak axis of the pier)

Πίνακας 13.1: Καμπτικές ροπές M_y στη βάση του μεσοβάθρου για το συμβατικό και τον πρωτότυπο σχεδιασμό της γέφυρας (γύρω από τον ασθενή άξονα του βάθρου)

	M_y due to inertial seismic loads (kNm)	**M_y due to relative horizontal displacements (kNm)**	**M_y for the seismic load combination (kNm)**
Conventional design - T_{ret}=1000years	25238	-	25238
Innovative design - T_{ret}=225years (no liquefaction)	21636	-	21636
Innovative design - T_{ret}=1000years (liquefaction)	11240	12634	13076

As far as the rest of the members of the bridge concerns, the design of superstructure was not modified, while the required quantities of the bearings and the expansion joints were slightly reduced as compared with the relevant ones of the conventional design.

It should also be noted that the liquefaction-produced settlements and rotations at the base of the pier, after the end of the excitation, were not proved critical for the design.

13.1 Economical Comparison

In Table 13.2 the final quantities of required materials for the foundation and the pier of the bridge are shown, regarding the conventional and the innovative design.

It is observed that, for the innovative design as compared to the conventional one, a reduction of 80% was achieved for the ground improvement by means of gravel piles. In addition, about 60% of the quantities of foundation concrete and steel reinforcement were saved, mainly due to non-use of foundation piles. A reduction of 12% for steel reinforcement of the pier was also succeeded.

Moreover, it should be noted that a small decrease of the required quantities of bearings and joints was also obtained, as presented in the following table.

Table 13.2: Bill of quantities for foundation materials

Πίνακας 13.2: Προμέτρηση υλικών θεμελίωσης

	CONVENTIONAL DESIGN			**INNOVATIVE DESIGN**			**Difference (I/C)**
Gravel piles D=0.80m	1387m			273m			-80%
Reinforced concrete	Concrete m^3	Steel Kgr	Kgr/m^3	Concrete m^3	Steel Kgr	Kgr/m^3	(Concrete , Steel)
Piles	236	23000	98	-	-		
Foundation slab	276	28000	102	216	22000	102	
Sum	512	51000		216	22000		-58% , -57%
Pier	97	10500	108	97	9200	95	0% , -12%
Bearings	740lt			623lt			-16%
Expansion Joints	27.5m of width 250mm			27.5m of width 200mm			-20%

The overall cost of the bridge is estimated as 1000÷1500€/m^2. Taking into account the dimensions of the bridge, with width 13.75m and length 85.20m, the total cost arises at 1171500.00÷1757250.00€. The itemized budget regarding the differences between the two solutions is presented in Table 13.3 for the conventional solution and in Table 13.4 for the innovative one. These budgets are based on nominal prices for construction of public works issued by the Ministry of Infrastructure for 2013. The total cost of the foundation for the conventional design is 218104€, while for the innovative one is 73062€, that is a saving of 67%. The difference between the total costs for two solutions is 310694.00-149036.00=161658.00€ with the cost of the innovative solution being smaller. This difference arises at 9.2%÷13.7% of the total cost of the bridge, with a mean value of about 11.5%.

Table 13.3: Itemized budget for the conventional solution

Πίνακας 13.3: Αναλυτικός προϋπολογισμός για τη συμβατική λύση

Description	Quantity	Unit	Unit value (€)	Cost (€)
Gravel piles	1387	m	58.00	80446.00
Piles Φ100	300	m	135.00	40500.00
Pier's pilecap	276	m^3	158.00	43608.00
Reinforcement (foundation)	51000	kg	1.05	53550.00
Reinforcement (pier)	10500	kg	1.05	11025.00
Expansion joints	27.5	m	473.80*4.17	54333.00
Bearings	740	lt	36.80	27232.00
Sum				**310694.00**

Table 13.4: Itemized budget for the innovative solution

Πίνακας 13.4: Αναλυτικός προϋπολογισμός για την καινοτόμο λύση

Description	Quantity	Unit	Unit value (€)	Cost (€)
Gravel piles	273	m	58.00	15834.00
Pier's footing	216	m^3	158.00	34128.00
Reinforcement (foundation)	22000	kg	1.05	23100.00
Reinforcement (pier)	9200	kg	1.05	9660.00
Expansion joints	27.5	m	473.80*3.33	43388.00
Bearings	623	lt	36.80	22926.00
Sum				**149036.00**

APPENDIX A

Available Data of Time Histories

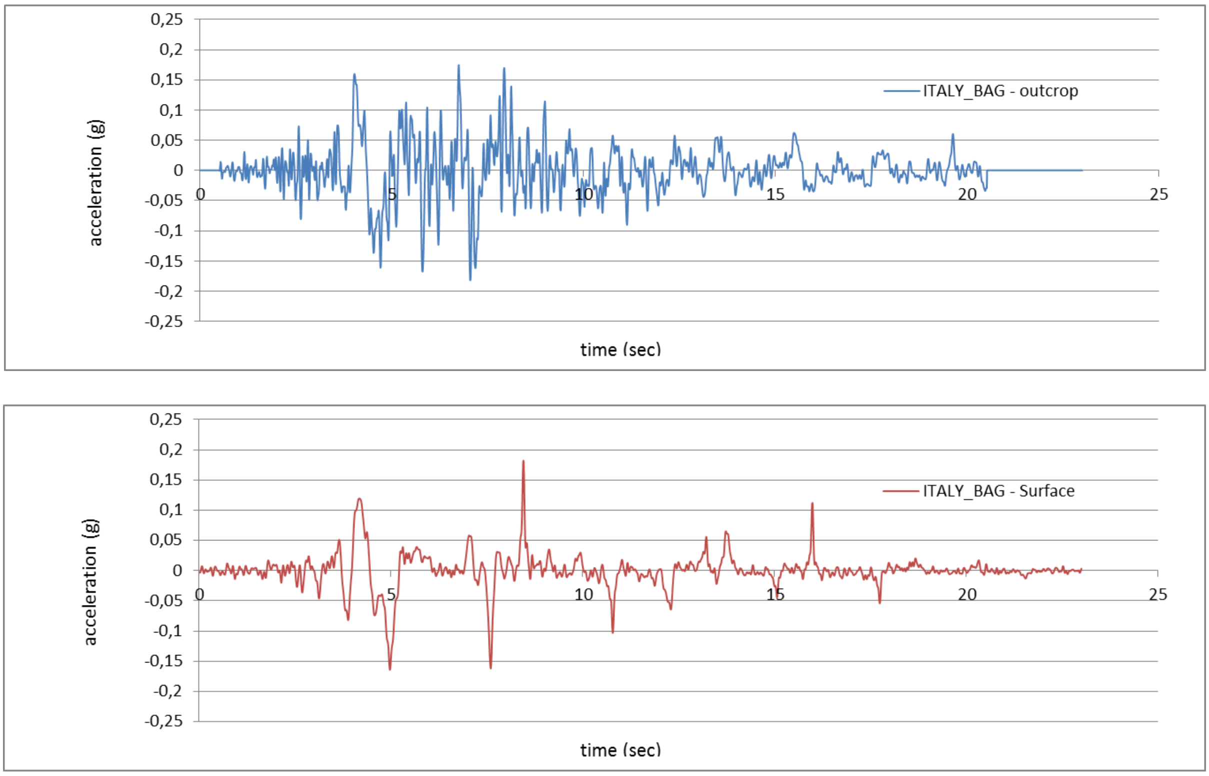

Figure A.1: Excitation ITALY_BAG - Accelerations time histories at the outcrop and the surface

Σχήμα Α.1: Καταγραφή ITALY_BAG - Χρονοϊστορίες επιταχύνσεων στο βραχώδες υπόβαθρο και στην επιφάνεια

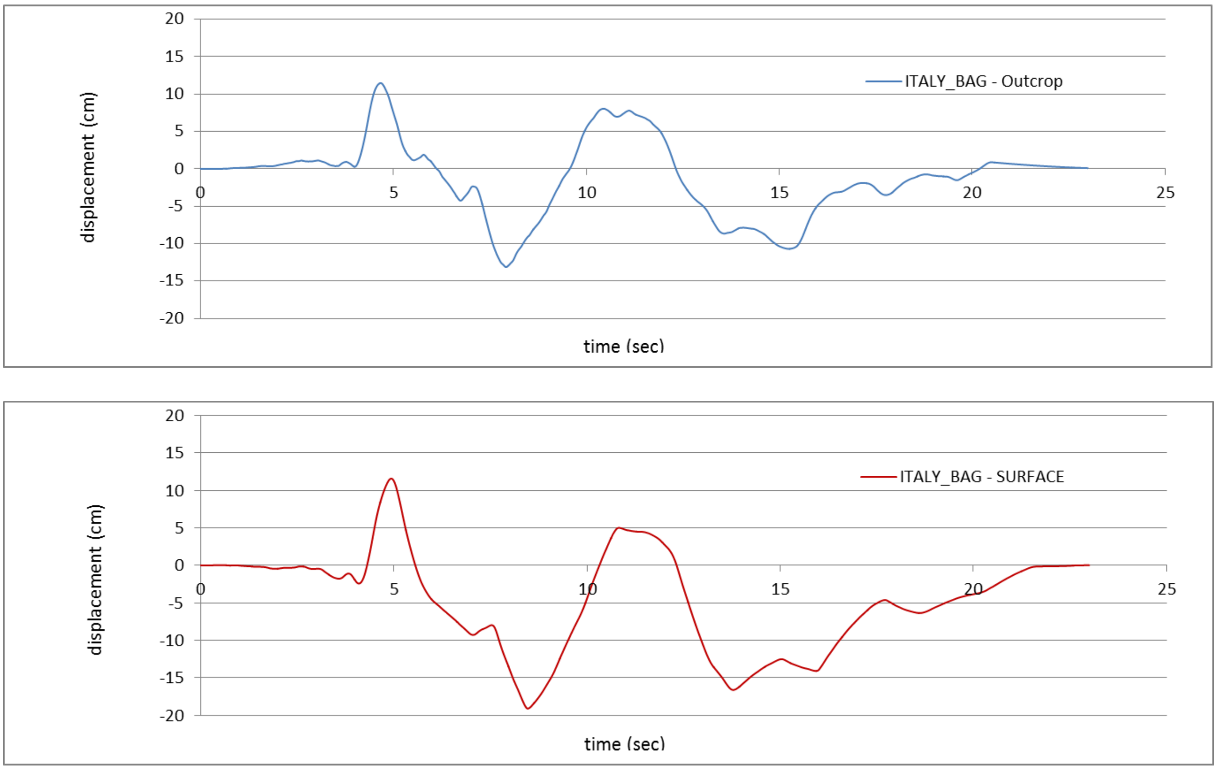

Figure A.2: Excitation ITALY_BAG – Displacements time histories at the outcrop and the surface

Σχήμα Α.2: Καταγραφή ITALY_BAG - Χρονοϊστορίες μετατοπίσεων στο βραχώδες υπόβαθρο και στην επιφάνεια

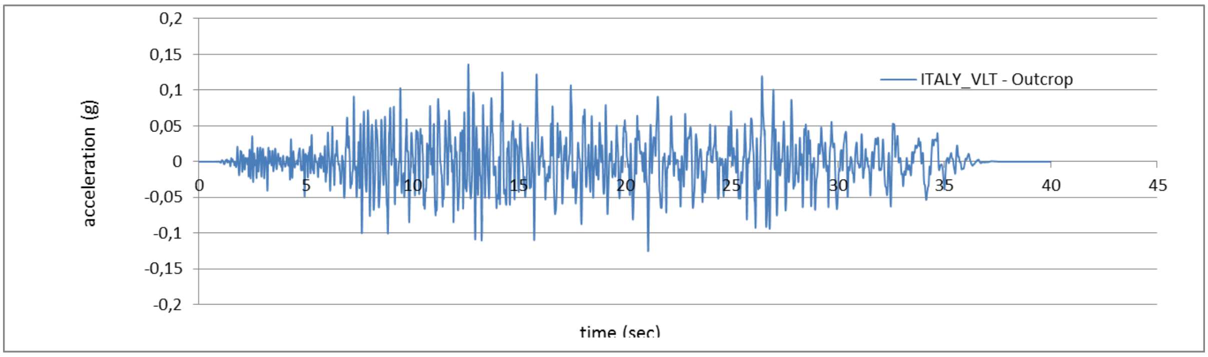

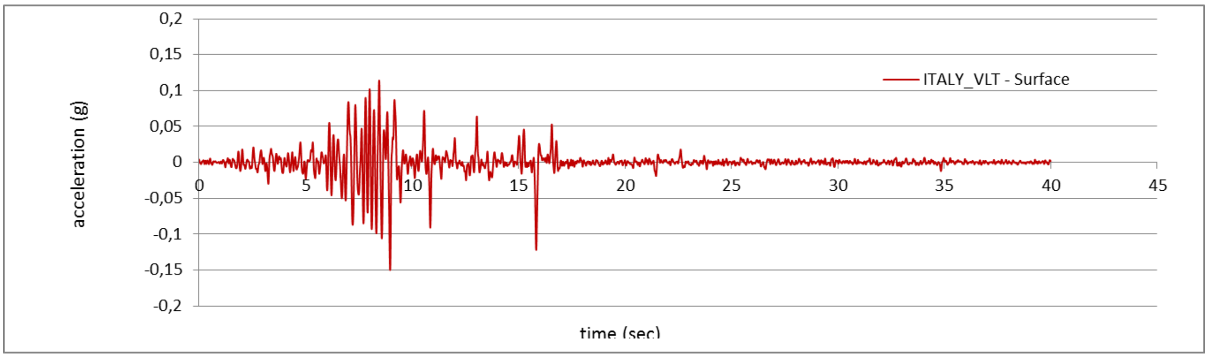

Figure A.3: Excitation ITALY_VLT - Accelerations time histories at the outcrop and the surface

Σχήμα A.3: Καταγραφή ITALY_VLT - Χρονοϊστορίες επιταχύνσεων στο βραχώδες υπόβαθρο και στην επιφάνεια

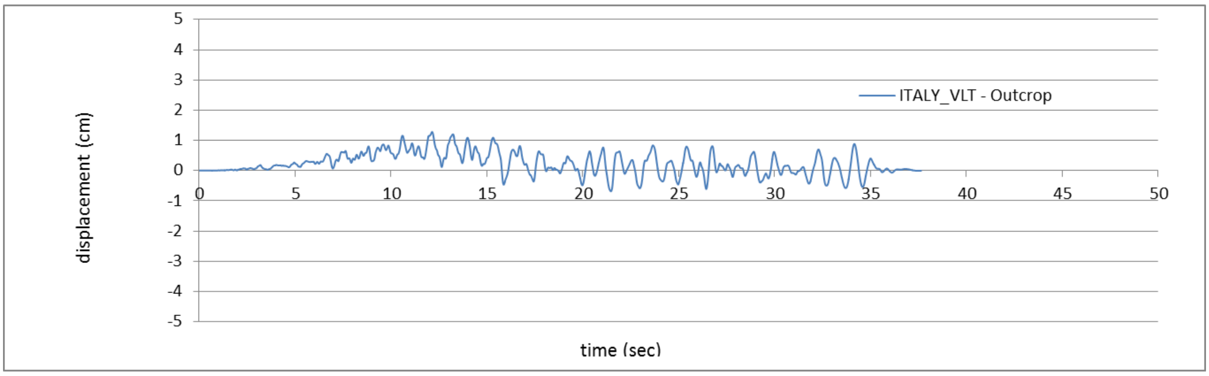

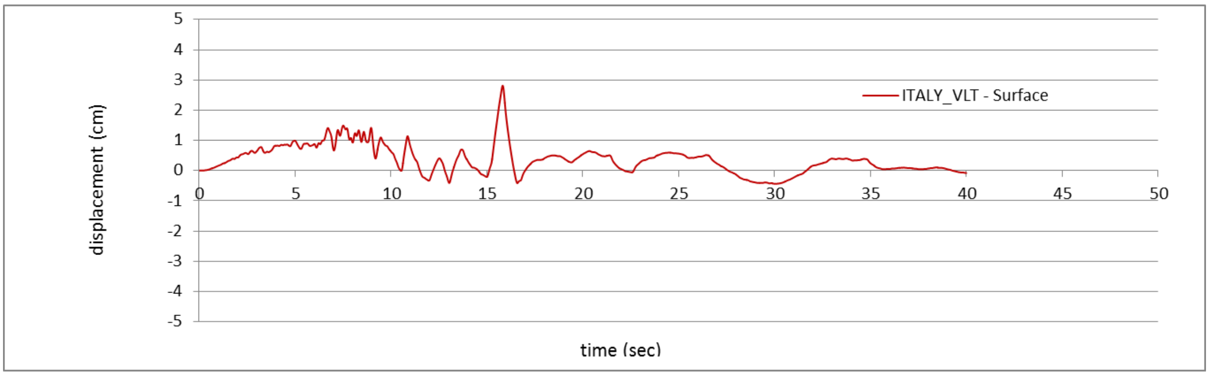

Figure A.4: Excitation ITALY_VLT – Displacements time histories at the outcrop and the surface

Σχήμα A.4: Καταγραφή ITALY_VLT - Χρονοϊστορίες μετατοπίσεων στο βραχώδες υπόβαθρο και στην επιφάνεια

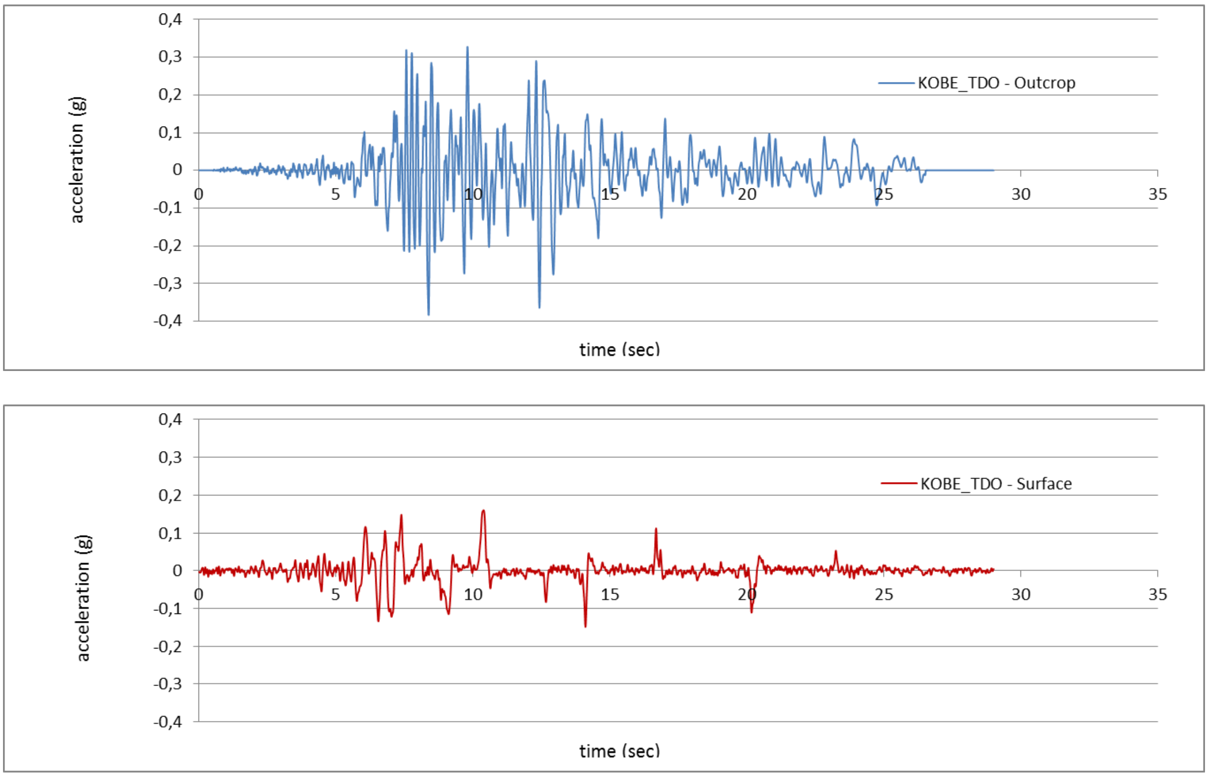

Figure A.5: Excitation KOBE_TDO - Accelerations time histories at the outcrop and the surface

Σχήμα Α.5: Καταγραφή KOBE_TDO - Χρονοϊστορίες επιταχύνσεων στο βραχώδες υπόβαθρο και στην επιφάνεια

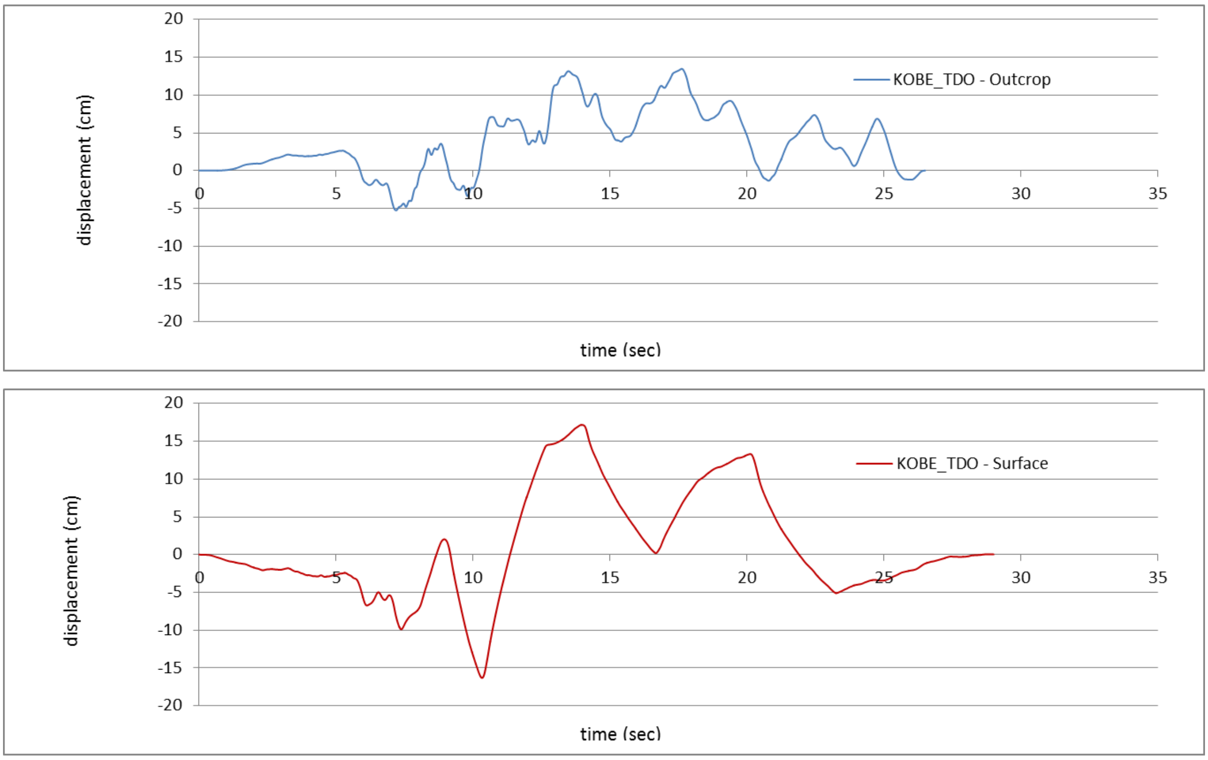

Figure A.6: Excitation KOBE_TDO – Displacements time histories at the outcrop and the surface

Σχήμα Α.6: Καταγραφή KOBE_TDO - Χρονοϊστορίες μετατοπίσεων στο βραχώδες υπόβαθρο και στην επιφάνεια

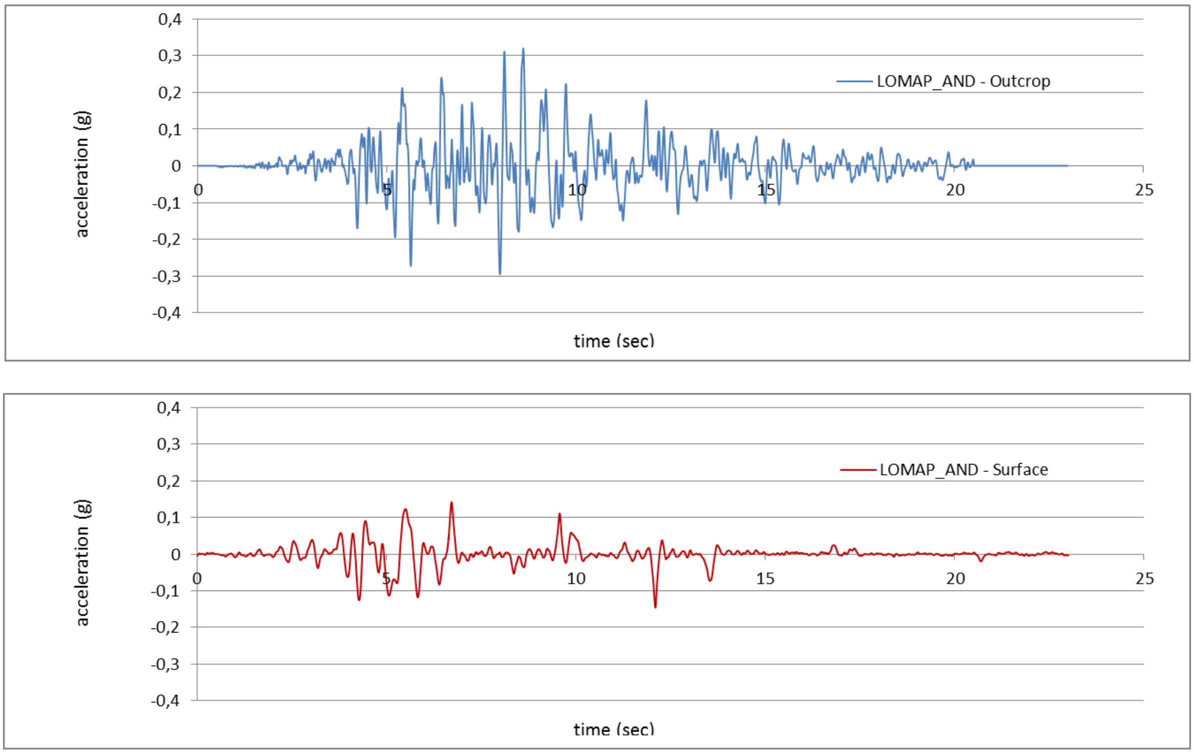

Figure A.7: Excitation LOMAP_AND - Accelerations time histories at the outcrop and the surface

Σχήμα A.7: Καταγραφή LOMAP_AND - Χρονοϊστορίες επιταχύνσεων στο βραχώδες υπόβαθρο και στην επιφάνεια

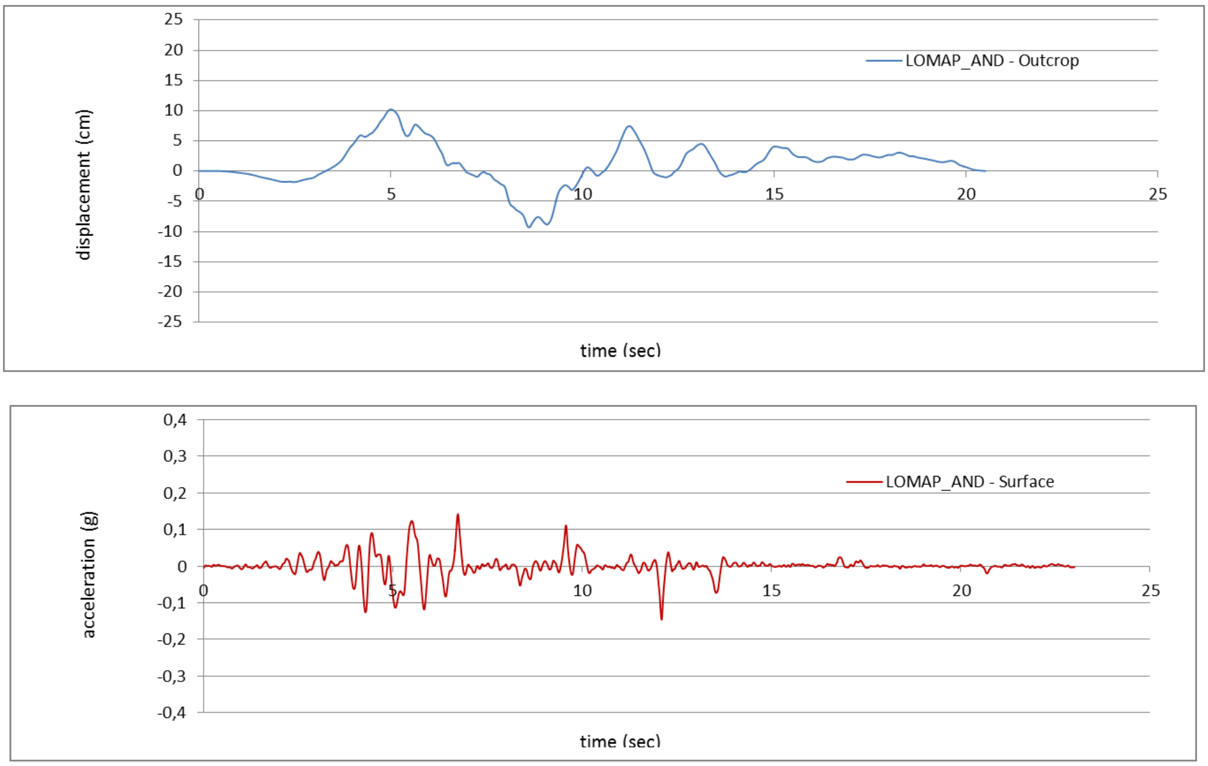

Figure A.8: Excitation LOMAP_AND – Displacements time histories at the outcrop and the surface

Σχήμα A.8: Καταγραφή LOMAP_AND - Χρονοϊστορίες μετατοπίσεων στο βραχώδες υπόβαθρο και στην επιφάνεια

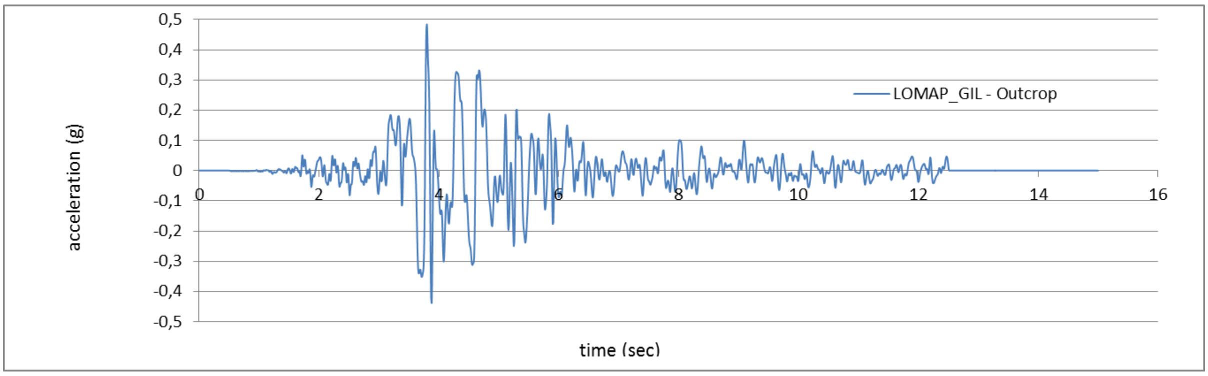

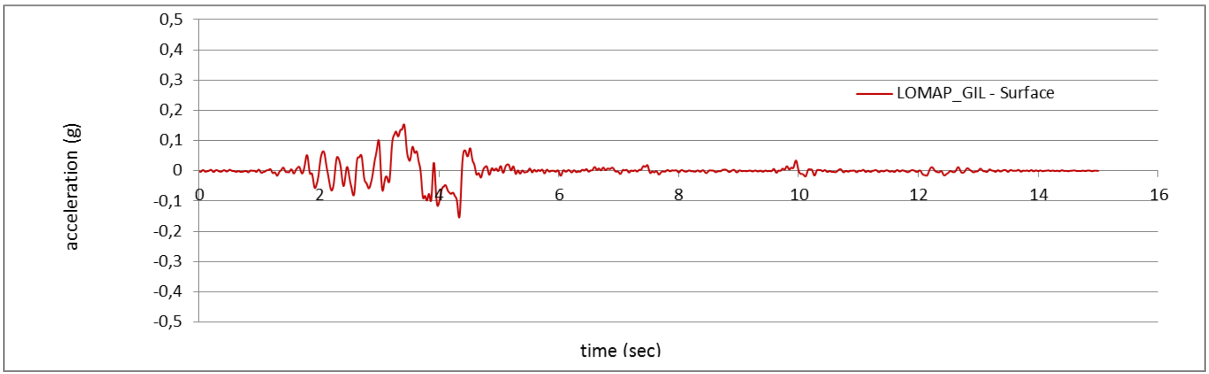

Figure A.9: Excitation LOMAP_GIL - Accelerations time histories at the outcrop and the surface

Σχήμα A.9: Καταγραφή LOMAP_GIL - Χρονοϊστορίες επιταχύνσεων στο βραχώδες υπόβαθρο και στην επιφάνεια

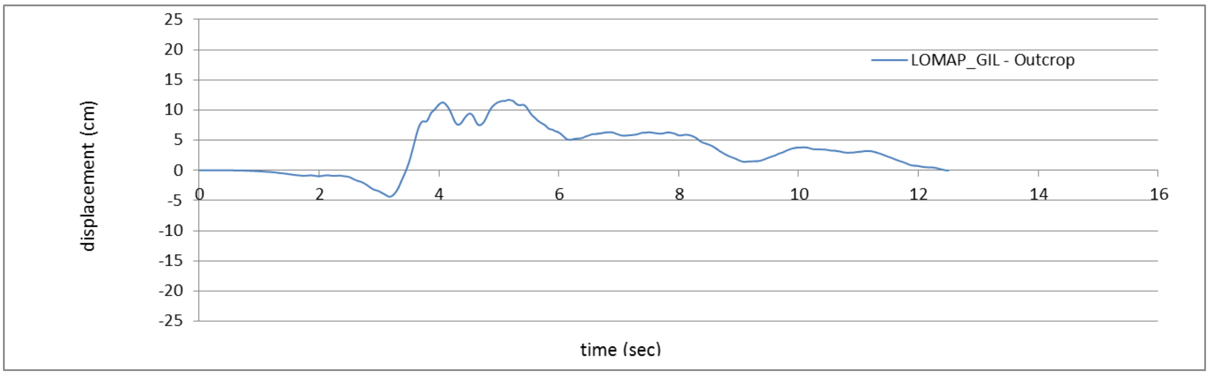

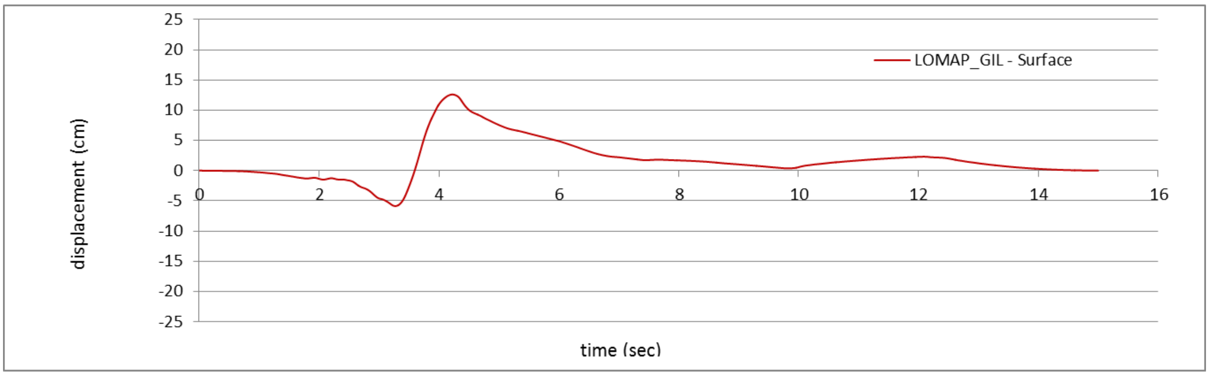

Figure A.10: Excitation LOMAP_AND – Displacements time histories at the outcrop and the surface

Σχήμα A.10: Καταγραφή LOMAP_AND - Χρονοϊστορίες μετατοπίσεων στο βραχώδες υπόβαθρο και στην επιφάνεια

APPENDIX B

Justification of the relationship adopted to express the asynchronous application of the inertial seismic loads and of the relative horizontal displacements at the base of the pier

In the following, a comparative study is carried out for the justification of the relationship adopted to express the asynchronous application of the inertial seismic loads and of the relative horizontal displacements at the base of the pier. To this end, the results of the accurate non-linear analyses were compared to those of the rougher linear elastic ones.

For the non-linear analyses the refined model of the bridge presented in Figure B.1 was used. Five excitations provided by the Geotechnical Team were taken into account (see Appendix A), via the software Opensees. More specifically, the displacement time histories referring to the rocky outcrop were imposed to the abutments, while the relevant ones for the soil surface were applied to the base of the pier (Dynamic Multiple-Support Excitation), for each seismic excitation separately.

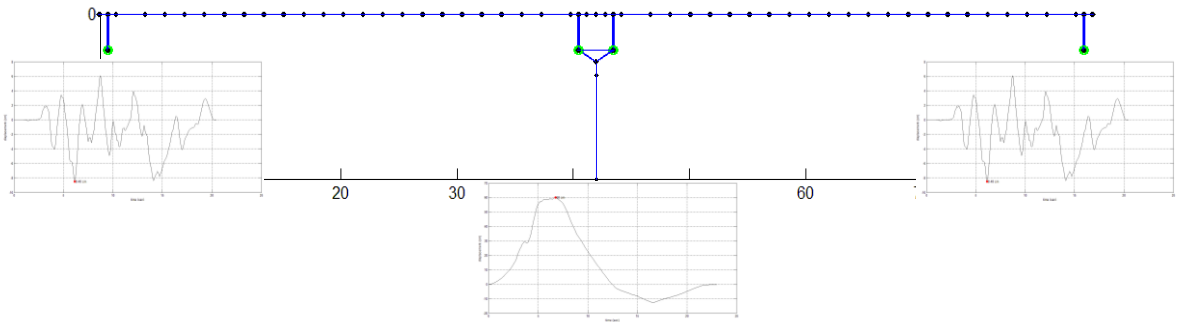

Figure B.1: Model of the bridge and displacement time histories applied to the foundation of the abutments and of the pier

Σχήμα B.1: Προσομοίωμα της γέφυρας και χρονοϊστορίες μετατοπίσεων που εφαρμόζονται στη βάση των ακροβάθρων και του μεσοβάθρου

In Figure B.2, the time histories of the moments M_{yy}, developed for each excitation at the base of the pier about its weak axis, are presented.

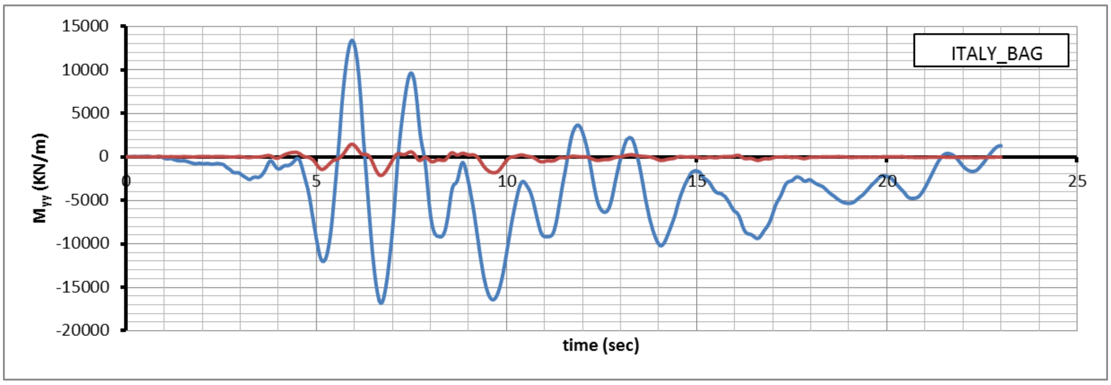

Figure B.2: Time histories of the moments M_{yy} developed for each excitation at the base of the pier about its weak axis

Σχήμα B.2: Χρονοϊστορίες αναπτυσσόμενων ροπών M_{yy} στη βάση του μεσοβάθρου (γύρω από τον ασθενή του άξονα) για τις διεγέρσεις που εξετάστηκαν.

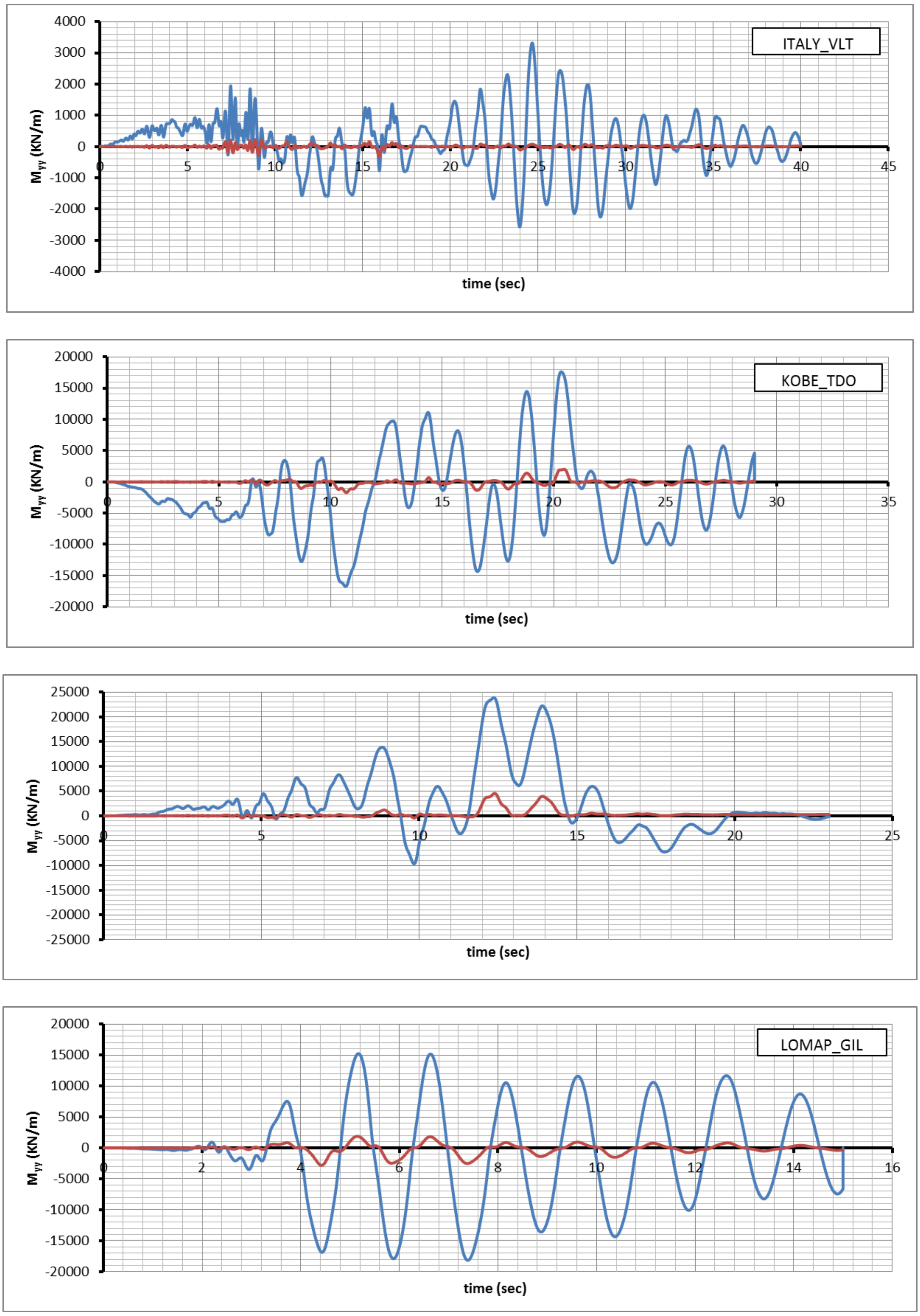

Figure B.2: Continued

Σχήμα B.2: Συνέχεια.

Subsequently, five linear elastic analyses were carried out for each excitation separately. The model of Figure 10.1 was used via the software SAP. Since, for such types of analyses, a uniform excitation is used for the whole bridge, the asynchrony motion between abutment and pier due to their different foundation conditions should also be considered. To this end, seismic loading consisted of two items:

- The spectrum of each excitation, as provided by the Geotechnical Team for the soil surface where the pier is founded (see Figure B.3 and Deliverable D4).
- Relative horizontal displacements developed between abutment and pier due to liquefaction and applied at the base of the pier. Their max values for each excitation are illustrated in Table B.1, as provided by the Geotechnical Team (see also Deliverable D4).

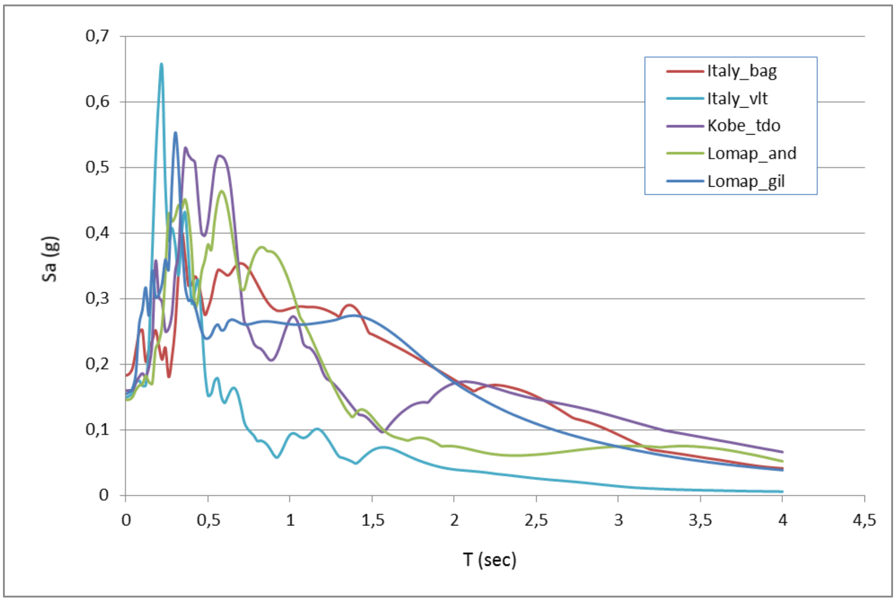

Figure B.3: Spectra of examined excitations for the soil surface where the pier is founded

Σχήμα B.3: Τα φάσματα των διεγέρσεων που εξετάστηκαν, στην επιφάνεια του εδάφους (θέση θεμελίωσης μεσοβάθρου)

Table B.1: Peak and average transient displacements between abutment and pier due to soil liquefaction

Πίνακας B.1: Μέγιστες οριζόντιες σχετικές εδαφικές μετακινήσεις μεταξύ ακροβάθρου και μεσοβάθρου λόγω ρευστοποίησης

no	**Excitation**	**Relative displacement δ (cm)**
1	ITALY_BAG	10.49
2	ITALY_VLT	3.20
3	KOBE_TDO	20.00
4	LOMAP_AND	22.17
5	LOMAP_GIL	4.99

In Table B.2 the max values of the moments Myy at the base of the pier, as derived from the inelastic and the elastic analyses are presented. For the elastic analyses the moments developed as a result of inertial E_{iner} and of the imposed displacements E_{disp} are depicted seperately. Then, two different relationships were adopted to express the asynchronous application of the inertial seismic loads and of the relative horizontal displacements at the base of the pier, namely:

a) $E_{iner}+0.3\ E_{disp}$ or $0.3\ E_{iner}+E_{disp}$ (B.1)

and

b) $(E_{iner}^2+(0.3E_{disp})^2)^{1/2}$ or $((0.3\ E_{iner})^2+E_{disp}^2)^{1/2}$ (B.2)

In both cases the results of the elastic solution proved more unfavorable than those of the accurate inelastic one (see Table B.2). Nevertheless, as shown in Figure B.4, the results of the elastic analysis better adapted to those of the exact solution when the rule of the statistical aggregation was used (Equation B.2).

Table B.2: Results derived from the elastic and the inelastic analyses for the five excitations examined

Πίνακας Β.2: Αποτελέσματα γραμμικών ελαστικών και μη γραμμικών αναλύσεων για τις πέντε διεγέρσεις που εξετάστηκαν

no	Excitation	M_{yy} at the base of the pier (KN)				
		Time history analysis	Elastic static analysis			
			Due to inertial loads E_{iner}	Due to imposed displacements E_{disp}	$E_{iner}+0.3\ E_{disp}$ or $0.3\ E_{iner}+E_{disp}$	$(E_{iner}^2+(0.3E_{disp})^2)^{1/2}$ or $((0.3\ E_{iner})^2+E_{disp}^2)^{1/2}$
1	ITALY_BAG	16818	16797	10890	20064	17111
2	ITALY_VLT	3317	5582	3322	6579	5670
3	KOBE_TDO	17611	7500	20762	23012	20884
4	LOMAP_AND	23872	8228	23014	25482	23146
5	LOMAP_GIL	18166	18564	5180	20118	18629

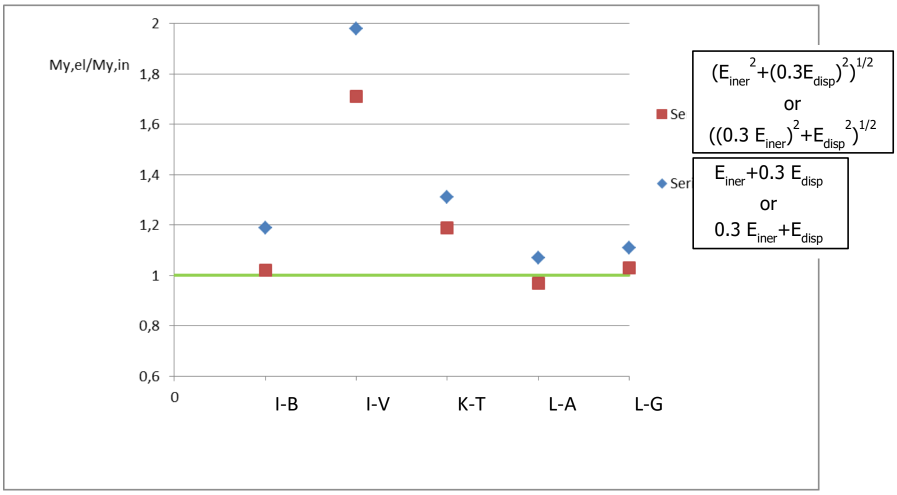

Figure B.4: Ratio of moments Myy at the base of the pier, derived by the elastic versus those derived by the inelastic analyses for the five excitations examined

Σχήμα Β.4 : Λόγος των ροπών Myy που προέκυψαν από την ελαστικές προς αυτές που προέκυψαν από τις μη γραμμικές αναλύσεις για τις πέντε διεγέρσεις που εξετάστηκαν

APPENDIX C

Detailed Bill of Quantities

1. <u>GRAVEL PILES</u>

Methodology

- Volume of improved soil: $V_{impr.}$
- Diameter of gravelpile: $D_{gp.}$
- Length of gravelpile: $H_{gp.}$
- Volume of a gravelpile: $V_{gp}= H_{gp}\ (\pi D_{gp}^2/4)$
- No of gravelpiles: N
- Replacement coefficient: $\alpha_s = (N\cdot V_{gp})/ V_{impr.}$

Total length of gravelpiles: $\mathbf{H_{total}\ (= N\cdot H_{gp}) = \alpha_s\cdot V_{impr}/ (\pi D_{gp}^2/4)}$

CONVENTIONAL DESIGN **(deep foundation with piles)**

α_s=0.196, D_{gp}=0.80m, H_{impr}=24m, dimensions of pilecap L·B=13.55x11.30m^2

Considering an improved soil area equal to pilecap layout increased by a perimetric zone of 1.0m width:

$H_{total}\ (= N\cdot H_{gp}) = \alpha_s\cdot(L+2)(B+2)\cdot H_{impr}/ (\pi D_{gp}^2/4) =$

=9.36(L+2)(B+2)=9.36x(13.55+1.0)x(11.30+1.0)=1675m

Finally, substracking the total length of the 12 foundation piles, it is:

H_{total} = 1675 – 12x24 = 1387m

INNOVATIVE DESIGN **(shallow foundation with footings)**

From Table 10.3, it is:

V_{impr}= 1040m^3, α_s=13.2%

Για D_{gp}=0.80m

$H_{total}\ (= N\cdot H_{gp})$ = 1.99 $\alpha_s\cdot V_{impr}$=1.99x0.132x1040=273m

2. <u>FOUNDATION PILES</u>

CONVENTIONAL DESIGN

<u>Concrete</u>

12 x 25 = 300m

300m x (π x 1.0^2/4) = 236 m^3

<u>Steel</u>

1875Kgr x 12 = 22500 Kgr ≈ 23000 Kgr

3. <u>FOUNDATION SLAB</u>

CONVENTIONAL DESIGN

<u>Concrete:</u> 13.55m x 11.30m x 1.80m = 276 m^3

<u>Steel :</u> 28000 Kgr

INNOVATIVE DESIGN

<u>Concrete:</u> 15.00m x 8.00m x 1.80m = 216 m^3

<u>Steel:</u> 22000 Kgr

4. PIER

CONVENTIONAL DESIGN

Concrete: [6.85m x 1.50m + (π x 1.5^2/4)] X 8.00 = 97 m^3

Steel : 10500 Kgr

INNOVATIVE DESIGN

Concrete: 97 m^3

Steel: 9200 Kgr

5. BEARINGS

CONVENTIONAL DESIGN

- 7 items per abutment 400x500x161 mm^3: 2 x 7 x 40.0 x 50.0 x 16.1 = 450.80 lt
- 2x7=14 items at pier 350x450x131 mm^3: 2 x 7 x 35.0 x 45.0 x 13.1 = 288.86 lt

Total 740 lt

INNOVATIVE DESIGN

- 7 items per abutment 400x500x131 mm^3: 2 x 7 x 40.0 x 50.0 x 13.1 = 366.80 lt
- 2x7=14 items at pier 350x450x116 mm^3: 2 x 7 x 35.0 x 45.0 x 11.6 = 255.78 lt

Total 623 lt

5. EXPANSION JOINTS

CONVENTIONAL DESIGN Joint width: 250mm

- 2 x 13.75m = 27.5m

INNOVATIVE DESIGN Joint width: 200mm

- 2 x 13.75m = 27.5m